Vol.1, No.2, June 2010

Scientific Research

Advances in Bioscience and Biotechnology

www.scirp.org/journal/abb

Journal Editorial Board

http://www.scirp.org/journal/abb

TABLE OF CONTENTS

Volume 1, Number 2, June 2010

Advances in Bioscience and Biotechnology (ABB)

Journal Information

SUBSCRIPTIONS

The *Advances in Bioscience and Biotechnology* (Online at Scientific Research Publishing, www.SciRP.org) is published bimonthly by Scientific Research Publishing, Inc., USA.

Subscription rates:

Print: $50 per issue.
To subscribe, please contact Journals Subscriptions Department, E-mail: sub@scirp.org

SERVICES

Advertisements
Advertisement Sales Department, E-mail: service@scirp.org

Reprints (minimum quantity 100 copies)
Reprints Co-ordinator, Scientific Research Publishing, Inc., USA.
E-mail: sub@scirp.org

COPYRIGHT

PRODUCTION INFORMATION

For manuscripts that have been accepted for publication, please contact:
E-mail: abb@scirp.org

Advances in Bioscience and Biotechnology, 2010, 1, 61-67 **ABB**
doi:10.4236/abb.2010.12010 Published Online June 2010 (http://www.SciRP.org/journal/abb/)

The effect of antibacterial agents on the production of nitric oxide induced by lipopolysaccharide in mice

Hampartsoum Barsoumian, Fadi El-Rami, Alexander M. Abdelnoor

Department of Microbiology & Immunology, Faculty of Medicine, American University of Beirut, Beirut, Lebanon.
Email: aanoor@aub.edu.lb

Received 10 March 2010; revised 20 March 2010; accepted 21 March 2010.

ABSTRACT

Some antibacterial agents have been shown to neutralize the biological properties of bacterial lipopolysaccharide (LPS). The aim of this study was to elucidate the role of gentamicin, tobramycin, imipenem, tigecycline, and isoniazid in affecting the production of nitric oxide (NO) induced by LPS in mice. Groups of mice were injected intraperitoneally with LPS alone, antibacterial agent alone, or LPS in combination with an antibacterial agent. Serum NO levels were determined at 1, 3, 6 and 9 hours post-injection using the Griess reagent method. Thin layer chromatography was performed to determine if antibacterial agent—LPS interaction had occurred. All the antibacterial agents suppressed NO production. Moreover, LPS-induced production of NO was suppressed by all the antibacterial agents, tobramycin and tigecycline being the most effective at 9 hours post-injection. Blocking of any of the stages leading to NO production by the antibacterial agents is suggested. Moreover, thin layer chromatograms obtained are suggestive of LPS-antibacterial agent interactions.

Keywords: Lipopolysaccharide; Antibacterial Agents; Nitric Oxide; Mice

1. INTRODUCTION

Antibacterial agents have been widely used to treat infectious diseases. However, it has become apparent that antibacterial agents may also play a role in the pathophysiological process of septic shock, mainly through their ability to liberate immunologically and inflammatory active components such as lipopolysaccharide (LPS) from the cell wall of Gram negative bacteria [1].

It is well established that septic shock is in part mediated by inflammatory cytokines including tumor necrosis factor alpha (TNF-α), interleukin-1 (IL-1), interleukin-6 (IL-6), and interleukin-12 (IL-12) as well as the excessive production of NO induced by LPS [2]. NO is synthesized by converting L-arginine to L-citrulline. The reaction is catalyzed by a family of nitric oxide synthase (NOS) enzymes. Three different NOS isoforms have been characterized; neuronal NOS (nNOS, NOS I), inducible NOS (iNOS, NOS II) and endothelial NOS (eNOS, NOS III). Among the three, iNOS is expressed in response to various inflammatory stimuli such as LPS and certain pro-inflammatory cytokines which consequently generate a large amount of NO by macrophages, hepatocytes, vascular smooth muscles and cardiac myocytes [2].

A number of LPS-detoxifying agents including some antibacterial agents have been reported. Serum and fractions thereof have been reported to detoxify LPS [3-5]. Hydrogen peroxide [6], lithium aluminum hydride [7], boron trifluoride [8], and sodium deoxycholate [9,10] are some of the agents that have been reported to detoxify LPS. It has been suggested that detoxification could be due to either binding to, or degrading LPS [11,12]. In an earlier study by AL-Shami *et al.* [13], it was shown that there was a decline in interferon-γ and TNF-α levels in mice injected with LPS treated with either tobramycin or vancomycin. David *et al.* [14] reported that lipopolyamines which are essentially nontoxic compounds inhibit, in a dose-dependent manner, LPS-induced activation of the limulus clotting cascade and the production of TNF-α, IL-6, and nitric oxide from LPS-stimulated J774.A1 cells, a murine macrophage-like cell line. Moore *et al.* [15] reported that polymyxin B, gentamicin and streptomycin bind to LPS and lipid A obtained from *Pseudomonas aeruginosa* and possibly sequester their activity. Moreover, various kinds of peptides have been developed that bind to, and neutralize the LPS effect in septic shock. Some of these peptides include α-helical peptides such as magainin and cecropin. Other peptide families include bactenecins, gramicidins, defensins, saposins, and lactoferrins [16]. A more recent study by Zorko and Jerala shows that chlorhexidine and alexidine bind to lipopolysaccharide and lipoteichoic acid preventing their binding to Toll-like receptor 4 (TLR-4) and Toll-like receptor 2 (TLR-2) respectively, hence reducing the NO produced by murine macrophages [17].

The aim of this study was to determine the effects of gentamicin, tobramycin, imipenem, tigecycline and isoniozid on the ability of LPS to induce the production of NO in mice.

2. MATERIALS AND METHODS

2.1. Lipopolysaccharide (LPS) and Antibacterial Agents

LPS from *Salmonella enterica* serovars Minnesota, was obtained from Sigma Chemicals Co., MO, USA. 30 µg/0.5 mL of an LPS suspension in pyrogen-free saline (confirmed by the Limulus Amebocyte Lysate Assay) was prepared.

Gentamicin sulphate, Tobramycin, Imipenem monohydrate and Isoniazid were obtained from Sigma-Aldrich, USA. Tigecycline was obtained from Wyeth Pharmaceuticals Inc., Philadelphia, USA. Dose of each antibacterial agent used alone or in combination with LPS is indicated in **Table 1**.

2.2. Thin Layer Chromatography (TLC)

The procedure described by Buttke and Ingram was followed [18]. Fluka silica plates backed on aluminum, with fluorescence, size: 10 cm × 20 cm (0.2 mm thickness) were used. The solvent (mobile phase) was a mixture of isobutyric acid, concentrated NH_4OH and pyrogen-free water in a ratio of 57:4:39. Ten µL of each of the suspensions/solutions listed in **Table 2** was applied to the plate. The plate was then placed in the vessel containing the solvent (mobile phase). The mobile phase was allowed to ascend the plate for a period of 6 hours. The plate was dried and ultraviolet light was used to observe and mark the bands obtained. Retention Factors (R_f) were calculated by dividing the distance migrated by the band by the distance migrated by the solvent front.

Table 1. Doses of LPS, antibacterial agent, and combination of LPS and antibacterial agent administered intraperitoneally to mice.

Group	Material Injected and Amount
1	pyrogen-free saline, 0.5 mL/mouse
2	LPS, 30 µg/0.5 mL saline/mouse
3	gentamicin, 60 µg/0.5 mL saline/mouse
4	tobramycin, 120/0.5 saline/mouse
5	imipenem, 10 µg/0.5 mL saline/mouse
6	tigecycline, 150 µg/0.5 mL saline/mouse
7	isoniazid, 150 µg/0.5 mL saline/mouse
8	LPS, 30 µg + gentamicin, 60 µg/0.5 mL saline/mouse
9	LPS, 30 µg + tobramycin, 120 µg/0.5 mL saline/mouse
10	LPS, 30 µg + imipenem, 10 µg/0.5 mL saline/mouse
11	LPS, 30 µg + tigecycline, 150 µg/0.5 mL saline/mouse
12	LPS, 30 µg + isoniazid, 150 µg /0.5 mL saline/mouse

Table 2. LPS and Antibacterial Agent Suspensions used in Thin layer Chromatography.

LPS, 20 µg/10 µL saline
Gentamicin; 40 µg/10 µL saline
40 µg Gentamicin + 20 µg LPS/10 µL saline
Isoniazid; 50 µg/10 µL saline
50 µg Isoniazid + 20 µg LPS/10 µL saline
Tigecycline; 100 µg/10 µL saline
100 µg Tigecycline + 20 µg LPS/10 µL saline
Imipenem; 12 µg/10 µL saline
12 µg Imipenem + 20 µg LPS/10 µL saline
Tobramycin; 80 µg/10 µL saline
80 µg Tobramycin + 20 µg LPS/10 µL saline

Plates were loaded with 10 µL of each suspension.

2.3. Mice

Female BALB/c mice aged 6 weeks (weight range: 24-26 g) were obtained from the animal care facility at the American University of Beirut Faculty of Medicine. Mice were treated and sacrificed in accordance to the ethical policies.

Twelve groups, each containing 12 mice were used. They were injected intraperitoneally with pyrogen-free saline, LPS alone, antibacterial agent alone, or a combination of LPS and antibacterial agent (**Table 1**). Three mice from each group were bled by cardiac puncture at 1, 3, 6 and 9 hours post-injection. Timings were deduced from the work of Terao *et al.* [19]. In addition, a group of three mice that received nothing was also sacrificed to measure the basic physiological NO concentration. Prior to bleeding, mice were anesthetized with a 0.5 mL mixture of 0.12 mL ketamine (50 mg/mL), 0.03 mL xylazine (20 mg/mL), and 0.35 mL pyrogen-free water [20]. Blood from each group was collected; serum was separated and used for NO determination.

2.4. Nitric Oxide (NO) Quantification

Griess Reagent system (Fluka Nitrate/Nitrite assay kit, Sigma-Aldrich, USA) was used to measure the amount of NO in the mice sera. The procedure described by the manufacturer was followed. In this method NO is converted to nitrate and nitrite. The nitrate produced is then

converted to nitrite and the total amount of nitrite produced is determined. Each serum specimen was tested in duplicate and the mean and standard deviation reported. Percents change of serum NO levels in the different groups that received antibacterial agent alone were calculated by subtracting the NO level obtained when antibacterial agent alone was given from the basic NO level obtained when nothing was injected. The difference was divided by the basic NO value and multiplied by 100. Percents change of serum NO levels in the different groups that received a combination of LPS and antibacterial agent were calculated by subtracting the concentration of NO obtained when a combination of LPS and antibacterial agent was used from the NO value obtained when LPS alone was injected. The difference was divided by the LPS-alone value and multiplied by 100.

3. RESULTS

3.1. Thin Layer Chromatography

It can be observed in **Table 3** and **Figure 1** that there was a slight change in the R_f value and the appearance of tailing when LPS was treated with gentamicin. Only tailing with no apparent bands was obtained upon treatment of LPS with tobramycin. A single band with slight differences in R_f values were obtained when LPS was treated with the other antibacterial agents. In addition, there were differences in the shape and intensity of the bands.

3.2. Nitric Oxide Levels

The serum nitric oxide levels obtained in the different groups of mice at different time intervals are given in **Table 4**. The percent change in NO levels in mice that received an antibacterial agent or LPS combined with an antibacterial agent are given in **Table 5**. It can be observed that at 1 and 3 hours post-injection, LPS alone caused a decrease in serum NO levels followed by increased levels at 6 and 9 hours post-injection. In all cases where antibacterial agent alone was administered there was a decline in NO levels. In most cases where mice were injected with a combination of antibacterial agent and LPS, there was a decline in serum NO levels when compared to levels obtained in mice that received LPS alone. The most pronounced decline was in the groups that received LPS combined with tobramycin or tigecycline at 9 hours post-injection.

4. DISCUSSION

LPS has a broad spectrum of biological activity. It activates the complement and coagulation systems and interacts with the TLR-4. As a result, a number of biologically active substances are produced in excess, and might lead to disseminated intravascular coagulation, hypotension and shock [2]. It has been suggested that antibacterial agents used to treat Gram negative infections may promote the release of LPS and contribute to transient exacerbation of clinical symptoms [1,21]. On

Table 3. Retention Factors (R_f) of the Different Bands Obtained in Thin Layer Chromatography.

Preparation	R_f
LPS	0.68
Gentamicin	0.63
Gentamicin + LPS	0.60, Tailing
Tobramycin	Tailing, no visible band
Tobramycin + LPS	Tailing, no visible band
Imipenem	0.71
Imipenem + LPS	0.69
Isoniazid	0.79
Isoniazid + LPS	0.79
Tigecycline	0.74
Tigecycline + LPS	0.71

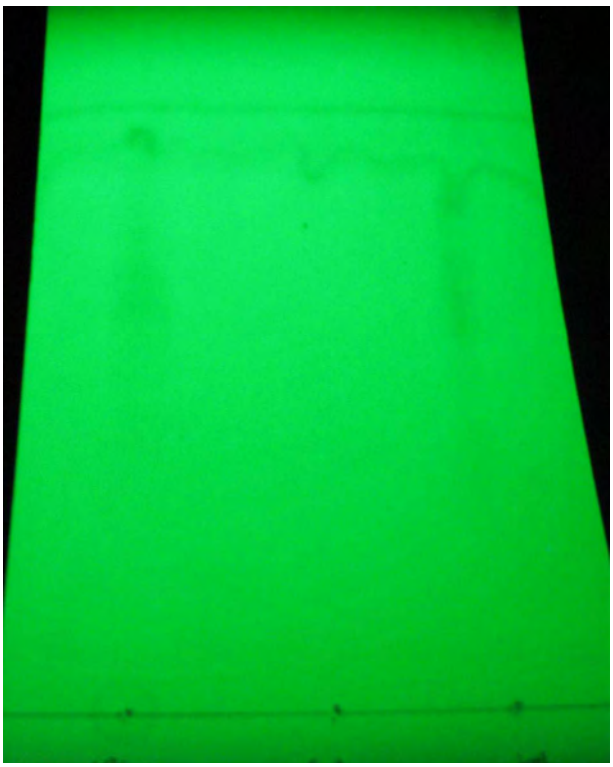

From left to right:
LPS spot: 10 µL containing 20 µg LPS was applied.
Gentamicin spot: 10 µL containing 40µg gentamicin was applied.
LPS + Gentamicin spot: 10µL containing 20 µg LPS + 40 µg getamicin was applied. Note the tailing obtained.
R_f LPS = 0.68; R_f Gentamicin = 0.63; R_f LPS + Gentamicin = 0.6

Figure 1. A representative thin layer chromatogram.

Table 4. Serum Nitric Oxide Levels in Mice Treated with LPS, Antibacterial Agent, or LPS + Antibacterial Agent at Different Time Intervals Post-injection.

Treatment	Nitric Oxide Level (μM) Post-Treatment at			
	1 hour	3 hour	6 hour	9 hour
Saline	198.4 ± 16.8	200.9 ± 16.9	201.9 ± 17.2	202.4 ± 17.1
LPS	106.4 ± 43.6	99.1 ± 23.9	305.1 ± 49.8	454.3 ± 78.6
Gentamicin	58.0 ± 14.7	117.7 ± 20.0	106.7 ± 21.0	58.3 ± 17.2
Imipenem	53.2 ± 34.0	54.1 ± 30.0	69.3 ± 17.6	73.8 ± 21.7
Isoniazid	46.7 ± 10.7	64.1 ± 19.9	44.8 ± 15.0	59.6 ± 19.2
Tigecycline	50.5 ± 10.6	45.8 ± 13.0	61.9 ± 20.8	54.7 ± 21.4
Tobramycin	47.5 ± 5.9	44.7 ± 8.9	32.8 ± 6.4	49.1 ± 6.7
LPS + Gentamicin	69.0 ± 14.0	103.1 ± 19.2	371.4 ± 77.0	261.2 ± 51.1
LPS + Imipenem	63.1 ± 15.6	101.0 ± 21.0	145.1 ± 29.4	275.4 ± 59.1
LPS + Isoniazid	84.2 ± 18.6	78.6 ± 17.4	263.8 ± 53.8	239.6 ± 71.1
LPS + Tigecycline	46.6 ± 5.7	73.4 ± 7.0	194.6 ± 25.0	145.9 ± 13.3
LPS + Tobramycin	53.8 ± 11.9	66.0 ± 19.8	134.6 ± 21.4	107.5 ± 16.6

A group of 3 mice received nothing and the basic NO concentration obtained was 196.4 ± 19.2 μM. comparing this result with values obtained for saline alone, we can deduce that there is almost no difference in the values of both. So injecting saline alone has insignificant or no effect on nitric oxide levels and it can be used safely as a solvent.

Table 5. Percent change in Serum Nitric Oxide Levels in Mice Injected with an Antibacterial Agent or a Combination of LPS and Antibacterial Agent at Different Time Intervals Post-Injection.

Treatment	Percent change Post-treatment at			
	1 hour	3 hour	6 hour	9 hour
Gentamicin	–70.5%	–40.1%	–45.7%	–70.3%
Imipenem	–72.9%	–72.4%	–64.7%	–62.4%
Isoniazid	–76.2%	–67.3%	–77.2%	–69.6%
Tigecycline	–74.3%	–76.7%	–68.5%	–72.2%
Tobramycin	–75.8%	–77.2%	–83.3%	–75.0%
LPS + Gentamicin	–35.2%	0%	0%	–42.5%
LPS + Imipenem	–40.7%	0%	–52.4%	–39.4%
LPS + Isoniazid	–20.9%	–20.7%	–13.5%	–47.3%
LPS + Tigecycline	–56.2%	–26.0%	–36.2%	–67.9%
LPS + Tobramycin	–49.4%	–33.4%	–55.9%	–76.3%

(-) sign represents a decline in NO level

the other hand there are reports indicating that some antibacterial agents have an anti-inflammatory effect, in addition to their anti-bacterial effect [22-27].

In this study the effect of 4 antibacterial agents that are usually used to treat Gram negative infections, and isoniazid used to treat tuberculosis, on the production of NO induced by LPS in mice was investigated. In all cases the antibacterial agent reduced the amount of NO induced by LPS.

LPS is a TLR-4 ligand. LPS first binds to serum Lipid Binding Protein (LBP) which in turn binds to CD14 expressed by dendritic cells, macrophages and other cell

types, and finally the complex interacts with TLR4/MD-2 [28]. Intracellular signals are then transduced through the, MyD88 dependent and independent pathways. In the MyD88 dependant pathway, a series of reactions involving MyD88, interleukin-1 (IL-1) receptor-associated kinase (IRAK) and TNF (tumor necrosis factor)-α receptor-associated factor 6 (TRAF6) will lead to the activation of nuclear factor kappa B (NF-kB). This in turn activates gene expression and causes the production and release of inflammatory mediators including the cytokines TNF-α, IL-1, IL-6 and IL-12 [29].

In the MyD88 independent pathway or TRIF [TIR (Toll/interleukin-1 receptor) domain-containing adaptor protein inducing interferon beta] pathway, the interferon regulatory factor 3 (IRF3) is activated initially, resulting in the production of INF-α, INF-β and NO, later NF-kB is activated as well [30]. On the other hand, antibacterial agents could suppress NO production by suppressing gamma interferon production. LPS induces the production of cytokines such as gamma interferon and tumor necrosis factor. When gamma interferon engages its receptor expressed by cells such as macrophages the signaling pathway results in activation of the transcription factor, IRF-1 and the production of iNOS. In an earlier study by Al-Shami *et al.* it was reported that tobramycin and vancomycin suppressed the production of gamma interferon and tumor necrosis factor induced by LPS [13].

Antibacterial agents might have an anti-inflammatory effect by blocking any one of the stages leading to the production of NO induced by LPS. The fact that all 5 antibacterial agents studied caused a decrease in NO levels and suppressed the NO-producing effect of LPS is in support of their anti-inflammatory property.

Another potential property of antibacterial agents is their ability to bind to LPS and sequester its activity. LPS consists of an O-polysaccharide side chain, a core polysaccharide, and a lipid A which is the main biologically active part of the molecule. Lipid A in itself is a phosphoglycolipid made up of β(1,6) disaccharide glucoseamine backbone that contains α-glycosidic and non-glycosidic phosphoryl groups in the 1 and 4' positions, and (R)-3-hydroxy fatty acids in ester and amide linkages. The disaccharide backbone is believed to be involved in binding to cell receptors and the fatty acid chains are thought to activate the cells following binding [13]. Gentamicin, tobramycin, imipenem, isoniazid, and tigecycline are rich in reactive amide and hydroxyl groups. It could be hypothesized that the antibacterial agents investigated bind to the lipid A portion, possibly to the ester and amide linkages of the fatty acid chains, and alter the bioactivity of LPS, leading to decreased activation of cells expressing TLR-4 and less NO production. The thin layer chromatograms obtained are in support of this hypothesis. Thin layer chromatograms revealed changes in R_f values, appearance of tailing, and differences in the shape and intensity of the bands when LPS alone was compared to LPS treated with antibacterial agent. Tailing could be the result of decomposition, or due to some ionization of the acidic or basic groups in the chemical structure of one or more of the components in the sample [31]. Moreover, Moore *et al.* [15] proved that polycationic aminoglycosides such as gentimicin and streptomycin can displace dansyl polymyxin in binding to LPS and lipid A.

Isoniazid (isonicotinic acid hydrazide) (INH), is usually used to treat tuberculosis, and not Gram negative infections. It prevents the synthesis of mycolic acid, a constituent of the cell wall of *Mycobacterium tuberculosis* [32]. Because of its cationic nature it was assumed that it would bind to LPS and neutralize its effect. The results supported this assumption and it is proposed to use isoniazid in conjunction with other antibacterial agents for treating Gram negative infections in situations where exacerbation of clinical symptoms are anticipated as a result of LPS release.

It is worth noting that LPS when given alone resulted in a decrease in NO production at 1 and 3 hours, followed by an increase at 6 and 9 hours post-injection. Rehan *et al.* [33] reported that LPS affected the production of pro-inflammatory cytokines in a time-dependent manner. At 6 hours post-treatment there was an increase, and at 72 hours a decrease in pro-inflammatory markers. Behling and Nowotny [34] and Haas *et al.* [35] have reported a time-dependent effect related to the adjuvant action of LPS and its derivatives. Depending on the time interval between the administration of antigen and LPS, either immunosuppression or immune enhancement was observed. Reasons for this so-called oscillating effect is not known, but it has been hypothesized that immunosuppression and immune enhancement might be under different genetic control, or the action of LPS on cells in accordance to their stage of development.

In conclusion, the antibacterial agents tested suppressed the production of NO induced by LPS. It appears that two mechanisms might be involved; they bind to LPS and block its action, and/or they interfere with pathways leading to NO production.

5. ACKNOWLEDGEMENTS

This study was supported by funds from the Faculty of Medicine, American University of Beirut.

REFERENCES

[1] Lepper, P.M., Held, T.K., Schneider, E.M., Bolke, E., Gerlach, H. and Trautmann, M. (2002) Clinical implications of antibiotic-induced endotoxin release in septic shock. *Intensive Care Medicine*, **28(7)**, 824-833.

[2] Parratt, J.R. (1998) Nitric oxide in sepsis and endotoxaemia. *Journal of Antimicrobial Chemotherapy*, **41(1)**,

31-39.

[3] Hegemann, F. and Lessmann, H. (1958) Nature of the pyrogen-neutralizing factor in human blood. V. occurrence of the endotoxinneutralizing serum factor in various animal species. *Zeitschrift Für Immunitatsforschung Und Experimentelle Therapie*, **115(5)**, 391-401.

[4] Stauch, J.E. and Johnson, A.G. (1959) The alteration of bacterial endotoxins by human and rabbit serum. *Journal of Immunology*, **82**, 252-263.

[5] Abdelnoor, A.M., Harvie N.R. and Johnson A.G. (1982) Neutralization of bacteria-and endotoxin-induced hypotension by lipoprotein-free human serum. *Infection and Immunity*, **38(1),** 157-161.

[6] Cherkin, A. (1975) Destruction of bacterial endotoxin pyrogenicity by hydrogen peroxide. *Immunochemistry*, **12(6-7)**, 625-627.

[7] Noll, H. and Braude, A.I. (1961) Preparation and biological properties of a chemically modified escherichia coli endotoxin of high immunogenic potency and low toxicity. *Journal of Clinical Investigation*, **40(11)**, 1935-1951.

[8] Nowotny, A. (1963) Endotoxoid preparations. *Nature*, **197(4868)**, 721-722.

[9] Ribi, E., Anacker, R.L., Brown, R., Haskins, W.T., Malmgren, B., Milner, K.C., *et al.* (1966) Reaction of endotoxin and surfactants. I. physical and biological properties of endotoxin treated with sodium deoxycholate. *Journal of Bacteriology*, **92(5)**, 1493-1509.

[10] Tarmina, D.F., Milner, K.C., Ribi, E. and Rudbach, J.A. (1968) Reaction of endotoxin and surfactants. II. Immunologic properties of endotoxins treated with sodium deoxycholate. *Journal of Immunology*, **100(2)**, 444-450.

[11] Keene, W.R., Landy, M. and Shear, M.J. (1961) Inactivation of endotoxin by a humoral component. VII. enzymatic degradation of endotoxin by blood plasma. *Journal of Clinical Investigation*, **40**, 302-310.

[12] Yoshioka, M. and Johnson, A.G. (1962) Characteristics of endotoxin altering fractions derived from normal human serum. *Journal of Immunology*, **89**, 326-335.

[13] Al-Shami, A.K., Itani, L.Y., Skaff, N.N., Haddad, E.K., Abdelnoor, A.M. (1995) Effects of acetyl salicylic acid, tobramycin and vancomycin on some biological activities of endotoxin. *EOS Rivista di Immunologia ed Immunofarmacologia*, **15**, 71-75.

[14] David, S.A., Silverstein, R., Amura, C.R., Kielian, T. and Morrison, D.C. (1999) Lipopolyamines: Novel antiendotoxin compounds that reduce mortality in experimental sepsis caused by gram-negative bacteria. *Antimicrobial Agents & Chemotherapy*, **43(4)**, 912-919.

[15] Moore, R.A., Bates, N.C. and Hancock, R.E. (1986) Interaction of polycationic antibiotics with pseudomonas aeruginosa lipopolysaccharide and lipid A studied by using dansyl-polymyxin. *Antimicrobial Agents & Chemotherapy*, **29(3)**, 496-500.

[16] Jerala, R. and Porro, M. (2004) Endotoxin neutralizing peptides. *Current Topics in Medicinal Chemistry*, **4(11)**, 1173-1184.

[17] Zorko, M. and Jerala, R. (2008) Alexidine and chlorhexidine bind to lipopolysaccharide and lipoteichoic acid and prevent cell activation by antibiotics. *Journal of Antimicrobial Chemotherapy*, **62(4)**, 730-737.

[18] Buttke, T.M. and Ingram, L.O. (1975) Comparison of lipopolysaccharides from agmenellum quadruplicatum to escherichia coli and salmonella typhimurium by using thin-layer chromatography. *Journal of Bacteriology*, **124(3)**, 1566-1573.

[19] Terao, H., Asano, K., Kanai, K., Kyo, Y., Watanabe, S., Hisamitsu, T., *et al.* (2003) Suppressive activity of macrolide antibiotics on nitric oxide production by lipopolysaccharide stimulation in mice. *Mediators of Inflammation*, **12(4)**, 195-202.

[20] Moreira, A.L., Wang, J., Sarno, E.N. and Kaplan, G. (1997) Thalidomide protects mice against LPS-induced shock. *Brazilian Journal of Medical & Biological Research*, **30(10)**, 1199-1207.

[21] Kusser, W.C. and Ishiguro, E.E. (1988) Effects of aminoglycosides and spectinomycin on the synthesis and release of lipopolysaccharide by escherichia coli. *Antimicrobial Agents & Chemotherapy*, **32(8)**, 1247-1250.

[22] Sugiyama, K., Shirai, R., Mukae, H., Ishimoto, H., Nagata, T., Sakamoto, N., *et al.* (2007) Differing effects of clarithromycin and azithromycin on cytokine production by murine dendritic cells. *Clinical & Experimental Immunology*, **147(3)**, 540-546.

[23] Kaushik V., Beduya D., Kalampokis I., Kohlhoff, S., O Joks R., G Durkin H. and Nowakowski M. (2007) Tetracyclines tigecycline and doxycycline inhibit LPS-induced nitric oxide production by RAW 264.7 murine macrophages. *Journal of Immunology*, **178**, (101)1-7.

[24] Cazalis, J., Bodet, C., Gagnon, G. and Grenier, D. (2008) Doxycycline reduces lipopolysaccharide-induced inflammatory mediator secretion in macrophage and ex vivo human whole blood models. *Journal of Periodontology*, **79(9)**, 1762-1768.

[25] Yang, L.P., Zhu, X.A. and Tso, M.O. (2007) Minocycline and sulforaphane inhibited lipopolysaccharide-mediated retinal microglial activation. *Molecular Vision*, **13**, 1083-1093.

[26] Henry, C.J., Huang, Y., Wynne, A., Hanke, M., Himler, J., Bailey, M.T., *et al.* (2008) Minocycline attenuates lipopolysaccharide (LPS)-induced neuroinflammation, sickness behavior, and anhedonia. *Journal of Neuroinflammation*, **5**, (15)1-14.

[27] Eswarappa, S.M., Basu, N., Joy, O. and Chakravortty, D. (2008) Folimycin (concanamycin A) inhibits LPS-induced nitric oxide production and reduces surface localization of TLR4 in murine macrophages. *Innate Immunity*, **14(1)**, 13-24.

[28] He, H., Genovese, K.J., Nisbet, D.J. and Kogut, M.H. (2006) Involvement of phosphatidylinositol-phospholipase C in immune response to salmonella lipopolysacharide in chicken macrophage cells (HD11). *International Immunopharmacology*, **6(12)**, 1780-1787.

[29] Yamamoto, M., Sato, S., Hemmi, H., Sanjo, H., Uematsu, S., Kaisho, T., *et al.* (2002) Essential role for TIRAP in activation of the signalling cascade shared by TLR2 and TLR4. *Nature*, **420**, 324-329.

[30] Bagchi, A., Herrup, E.A., Warren, H.S., Trigilio, J., Shin, H.S., Valentine, C., *et al.* (2007) MyD88-dependent and MyD88-independent pathways in synergy, priming, and tolerance between TLR agonists. *Journal of Immunology*, **178**, 1164-1171.

[31] Rabel, F. (2009) Reviving Thin Layer Chromatography. *Chromatography Techniques*. http://www.laboratoryequipment.com/article-reviving-thi

n-layer-chromatography.aspx

[32] Timmins, G.S. and Deretic, V. (2006) Mechanisms of action of isoniazid. *Molecular Microbiology*, **62(5)**, 1220-1227.

[33] Rehan, V.K., Dargan-Batra, S.K., Wang, Y., Cerny, L., Sakurai, R., Santos, J., *et al.* (2007) A paradoxical temporal response of the PTHrP/PPARgamma signaling pathway to lipopolysaccharide in an in vitro model of the developing rat lung. *American Journal of Physiology. Lung Cellular and Molecular Physiology*, **293(1)**, 182-190.

[34] Behling, U.H. and Nowotny, A. (1977) Immune adjuvancy of lipopolysaccharide and a nontoxic hydrolytic product demonstrating oscillating effects with time. *Journal of Immunology*, **118**, 1905-1907.

[35] Haas, G.P., Johnson, A.G. and Nowotny, A. (1978) Suppression of the immune response in C3H/HeJ mice by protein-free lipopolysaccharides. *Journal of Experimental Medicine*, **148(4)**, 1081-1086.

Advances in Bioscience and Biotechnology, 2010, 1, 68-78 **ABB**
doi:10.4236/abb.2010.12011 Published Online June 2010 (http://www.SciRP.org/journal/abb/)

Relevance of a standard food model in combination with electronic jaw movement recording on human mastication pattern analysis

Gregor Slavicek[1*], Mikhael Soykher[2], Marina Soykher[2], Haymo Gruber[3], Peter Siegl[4]

[1]Steinbeis Transfer Institut Biotechnology in Interdisciplinary Dentistry der Steinbeis Hochschule Berlin, Stuttgart, Germany;
[2]Institute Biotechnology in Interdisciplinary Dentistry, Moscow, Russia;
[3]Dental University of Graz, Austria, and FH Joanneum, Austria, Private Practice, Stallhofen, Austria;
[4]Private Practice, Weiz, Austria.
Email: gregor.slavicek@stw.de

Received 13 February 2010; revised 7 March 2010; accepted 9 March 2010.

ABSTRACT

The aim of this paper is to describe the possibilities of analyzing human mastication. The development of a standardized food model is presented. Based on the findings of a systematic literature search an elastic food model was created with the aim of standardizing size and elastic properties. Three different eatable jellied products were chosen, created by a changing of the amount of gelatin (260 Blooms) related to the total mass of the standard jellied food. The different hardness were classified in soft, medium and hard, flavored identically, but stained with different colors: soft-green, medium-yellow, hard-red. A cylindrical form was chosen with a height of 1 cm and a diameter of 2 cm. A standard protocol for analyzing chewing patterns in men was created. The condylographic data off several patients are described in details to demonstrate the possible clinical implementation. The newly developed standard food model (SFM) showed the capability to serve in experimental settings to analyze human mastication, although only a few patients have been examined. In addition, strength and size of the newly developed SFM load the masticatory system in an extent; it should be possible to disclose subclinical symptoms of patients within a short time of examination. The diagnostic procedure of temporo-mandibular disorder (TMD) should be endorsed by this new method. The condylographic data created by a standardized protocol should have the ability to enhance the clinical functional analysis of patients previous to restorative dental procedures.

Keywords: Human Mastication; Standard Food Model; Mandibular Movement; EMG; Condylography; Biomechanics; Temporo-Mandibular Joint; Swallowing; Chewing; Chewing Muscle Activity; Craniomandibular System; Nutrition; Tooth Loss

1. INTRODUCTION

Mastication is an essential part of the digestive process. The ability of the masticatory organ to mince and process food is directly related to with the individual's vital functions and general state of health. Loss of teeth and the reduced ability to chew have a significant impact on an individual's nutritional condition, health, gastrointestinal disorders, and digestion [1]. However, confirmed evidence of these associations is scarcer than one would expect it to be: key co-factors and variables are yet unknown or only partially identified. In the existing studies, the nutritional habits of the study participants have been poorly or fragmentarily documented. Extrapolation of data from animal experiments is such that the results may be poorly applicable to the human setting [1]. Lifestyle, morbidity and the individual's socioeconomic status are major factors influencing nutrition and oral health.

If one views prosthetic and restorative measures in the light of nutrition and diet, it would be meaningful to explore dental measures critically. In a large and systematic overview about nutrition and its relationship with oral health and systemic disease, the authors showed that the negative impact of edentulism on nutritional habits are inadequately compensated for by dental prostheses and restorative measures [2]. Furthermore, a reduced number of teeth may cause changes in weight; the age and characteristics of the respective population are also involved in this phenomenon. New and well structured studies are needed to evaluate the association between

nutrition, dental status and the individual's state of health. Prospective longitudinal studies taking relevant factors such as mastication and occlusion into account would be consequential [2]. A hypothetical model of the associations between oral health and nutrition is shown in **Figure 1**.

Patients without dementia have twenty-fold more teeth in their mouth than age-matched patients with severe Alzheimer dementia (4.7 vs. 0.2 teeth per patient). The results of the Neuburg dementia study were highly significant. The presence of a large number of teeth in advanced age was identified as a protective factor in respect of Alzheimer dementia. Conversely, edentulism was an independent risk factor for Alzheimer dementia, but not for vascular dementia or ischemic stroke [3].

Occlusion, occlusal interferences, and the severity of craniomandibular disorders (CMD) appear to be associated with mastication: the more numerous the occlusal interferences, the more advanced the CMD, the longer the individual takes to masticate a specific type of food and the more pronounced are the person's atypical masticatory movements [4]. These results may be interpreted as follows: compensatory masticatory patterns occur on a reflex basis, but the effectiveness of such masticatory patterns is doubtful and it may be presumed that these patterns accelerate the progression of a CMD [4].

Human mastication is controlled by the central nervous system. Properties such as the hardness, plasticity, elasticity and size of the ingested food directly influence the feedback control system. Age, gender, and dental status are intrinsic modulators. All of these factors may influence the sequence of mastication. Vertical and lateral amplitudes as well as the velocity of jaw movements during mastication are parameters that can be used for a targeted analysis of determinants that are expressive of the adaptation abilities of healthy individuals and volunteers [5]. On the other hand, the impact of age may not be as significant as was initially assumed. The number of masticatory cycles needed to grind a standardized unit of food increases with age, but the ability to adapt oneself to the properties of food is retained even by elderly individuals [6].

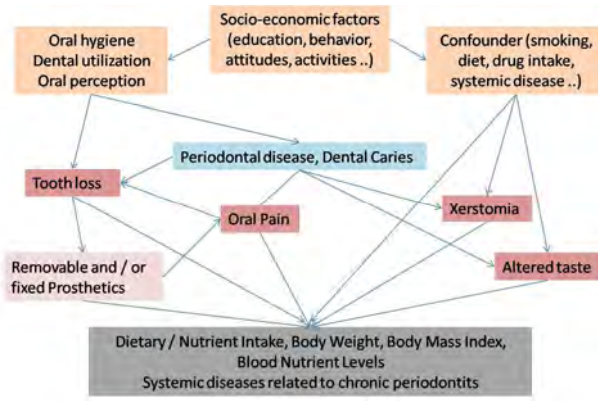

Figure 1. A hypothetical model demonstrating the complex interactions of oral health status, nutrition and systemic diseases (adapted from 17).

Muscular activity and the frequency of masticatory cycles may be influenced by the hardness of food in the initial stage of mastication [7]. Flow properties and the plastic behavior of food influence the entire masticatory cycle. This initial phase is controlled by a programmed pattern steered by the cortex and the brain stem, which adjusts the initial masticatory cycles to the food introduced into the mouth. A mechanism with sensory feedback from the structures of the stomatognathic system is located in the brain stem. This mechanism then takes over the function of modifying the muscle strength of the following masticatory movements to the quality of the ingested food [7].

Food is minced during mastication by a process of selection and breakup. The chances of a component of food being "selected" between the teeth may be viewed in relation to the size of the individual unit of food. The actual breakup of food may be described as a cumulative dividing function. Computer simulations based on these two processes could be used to describe the individual's efficiency of mastication [8]. The efficiency of mincing food may also be determined with the aid of filter methods. A functional model based on a model of human mastication describes the qualitative abilities of the masticatory organ.

Mastication and brain activity are closely interrelated. With the aid of functional magnetic resonance imaging (fMRI) it was shown that mastication involves a bilateral increase in the activity of the sensomotor cortex, the thalamus, the amygdala and the cerebellum [9]. In elderly persons, the magnitude of the increase was less in the first three above mentioned regions, but greater in the cerebellum. Therefore, in the elderly the function of mastication is integrated in the neuronal circuits of the hippocampus and appears to play an important role in preventing age-related disorientation. Mastication may be a useful therapy to prevent senile dementia [9]. Human mastication is supported to a great extent by the tongue. Positioning the food, exploring its consistency and size, as well as aiding the process of changing sides, are essential functions without which mastication would be impossible. Bilateral mastication of chewing gum modulates the activity of the primary sensomotor cortex during tongue movements, as determined on fMRI investigations. This activation appears to differ in the hemispheres, depending on the preferred side of mastication. These data support the postulated existence of short-term memory functions which store the recently executed movement pattern. Stimulation of the brain in the elderly or rehabilitation of injured brains can be supported by controlled mastication activity [9].

Mastication is a concrete load for the mandible and the craniomandibular joint. Loads on the mandible during the closing action reduce the intraarticular distance in the craniomandibular joint [10]. Ipsilateral craniomandibular joints are loaded less during mastication than contra-lateral joints [11].

Forces acting on the jaw during masticatory movement have been investigated. It was found that maximal forces are achieved in the vicinity of the intercuspal position. The forces are lowest when the jaw is opened [12]. The consistency of food is a major factor that modulates muscle strength: harder food reduces closing strength during mastication, but this is not the case when soft food is chewed. The latter causes no significant changes. Persons who wear full prostheses have lost their ability to react adequately to the quality of food [12].

Electromyographic studies are used to analyze the masticatory muscles. A hypothetical model was used: simultaneous activation of the jaw openers during mastication leads to additional activation of the muscles involved in closing the jaw [13]. During mastication, additional and simultaneous activation of the digastric muscle was much more pronounced during closure than it is in isometric tension. However, such activation was mild compared to the maximum possible activation potential of the digastric muscle. Therefore, it may be concluded that simultaneous activation of the openers has no more than a mild impact on the additional activation of masticatory muscles [13]. It was also found that muscle activity measured with EMG does not always permit consistent conclusions about masticatory strength [14]. The higher muscle activity during mastication, as seen on EMG, is not directly associated with an increase in muscle strength-as compared to the activity of bruxism. Additional EMG measurements are needed to analyze the actual masticatory strength. It would not be permissible to draw conclusions about loads on the craniomandibular joints on the basis of muscle activity on EMG [14]. The hardness or consistency of food modulates EMG activity, especially during the initial masticatory movements [15].

Masticatory patterns seem to differ from person to person, and appear to be markedly dependent on intraoral and neuromuscular sensory feedback controls. A high reproducibility may be presumed, provided the chewed object has similar or identical properties [5]. However, it was shown that even healthy probands with class 1 occlusion and no major deviations or missing teeth, and no signs or symptoms of a functional disorder, vary to a certain extent even under standardized conditions [5]. The frequency of mastication, the speed of shift, the amplitude of motions, and the duration of closure were found to differ. Psychological and physical variables such as emotional status, irritation or fatigue may play a role in this context, but an explicit statement in this regard cannot be made yet [5].

Registration of masticatory movements by the use of electronic systems provides deeper insights into the motion and dynamics of the mandible and, at least indirectly, into movements of the craniomandibular joint. Mastication is characterized by gliding of the teeth, a pause in intercuspal position or near-intercuspal position, and wide lateral movements [16]. This is true for children as well as adults. Masticatory movements in the occlusion of milk teeth are marked by a pronounced lateral motion during opening. The extent of lateral movement during opening is typically larger than that during closure. In deciduous teeth, the extent of lateral movement reduces when opening while lateral excursion increases during closure. The adult reveals an entirely different masticatory pattern: medial opening and wide lateral closure characterize the adult masticatory pattern [16]. The properties of food influence masticatory cycles not only in adults but also in children. Hard food enhances the lateral component in the adult, and increases the medial one in children. Neither in the adult nor in the child does one find a pure hinge movement during mastication [16]. Separation of the molars on the working side is closely related to the size of the food bolus. This corroborates the hypothesis that opening does not occur incidentally during mastication, but is controlled by various feedback systems in order to minimize effort during mastication [17].

Swallowing and mastication are closely related to each other. The production of saliva is a basic prerequisite for successful mastication. However, the additional intake of fluid during a masticatory cycle influences mastication positively only when the individual ingests very dry food (for instance, cake); this is not the case when fatty (such as cheese) or watery foods (such as carrots) are ingested [18]. The optimal time point for mastication was investigated, and an optimized mastication and deglutition model was developed [17]. Interestingly, the number of masticatory cycles until the first act of swallowing was very constant in the individual proband, independent of the type of food, such as nuts compared to carrots. In fact, the number of masticatory cycles until the first act of deglutition was strongly correlated with the quantity of produced saliva [17].

Analysis of human mastication is an extremely functional resource of assessing the effectiveness of occlusion and the functional statfus of the stomatognathic system prior to a restorative or prosthetic intervention. For this purpose, it is necessary to standardize the investigation and the registration procedure of mastication. This article describes the use of a standardized model of food in combination with mandibular movement recordings. Principles of standard model food and standard procedures of chewing recording are described elsewhere [19-22].

2. MATERIAL AND METHOD

The model food used to analyze mastication should be elastic, possess different degrees of hardness, and be of a minimum size. Based on a conventional mass of gum for manufacturing commercial fruit gum, a standard cylindrical form (height 1 cm, diameter 2 cm) in three different degrees of hardness (soft, hard, medium) was produced (A. Egger´ Sohn, Süsswaren und Naturmittel GmbH., Mellergasse 4, A-1230 Vienna, Austria). The degrees of hardness were achieved by adding different quantities of gelatin (edible gelatin SPM 5765, Biogel AG Haldenstrasse 11, CH-6006 Lucerne) to the ground mass (soft: 15.5 g per mass; medium: 23 g per mass; hard: 31 g per mass). (**Figure 2(a)** and **2(b)**).

Masticatory movements are visualized by the use of a paraocclusal clutch and joint path registration. The paraocclusal clutch influences the shearing action of the teeth due to its buccal fixation. However, currently we have no other means of fixing the registration arches. The recordings described in this article were made by the use of the CADIAX diagnostic system (®GAMMA med. wiss. FortbildungsGmbH, Josef Brennerstr. 10, A-3400 Klosterneuburg, Austria). All recordings had to be based on a standardized protocol in order to perform an optimal analysis and make inter-individual comparisons.

The analysis is started by performing a conventional visualization of the joint path in three planes (sagittal, frontal, transverse). Initially the extent (quantity) of motion is of interest. The quantity is most easily registered in the sagittal view. This can be determined for the working side (AS) and the non-working side (nAS). AS should be less in terms of quantity than nAS (**Figure 3**). The position of masticatory movements is then analyzed in relation to standard movements (protrusion/retrusion, opening/closing, mediotrusion on the right and the left side). Movements coincident, below or above the standard motions are tolerable (**Figure 4**). In this context one

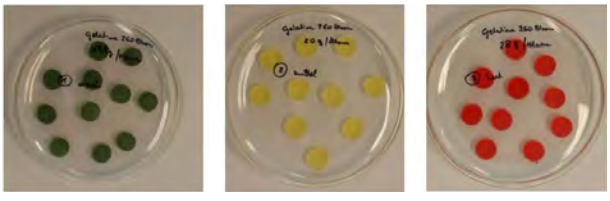

(a)

(b)

Figure 2. (a) Prototypes of the standard food model, green (soft) yellow (medium) and red (hard). The amount of gelatin (260 bloom) per mass was increased for the yellow and hard standard food model, to increase the differences of the elastic qualities; (b) prototypes of the standard food model, green (soft) yellow (medium) and red (hard) with a cylindrical form and the dimensions height 1 cm and diameter 2 cm.

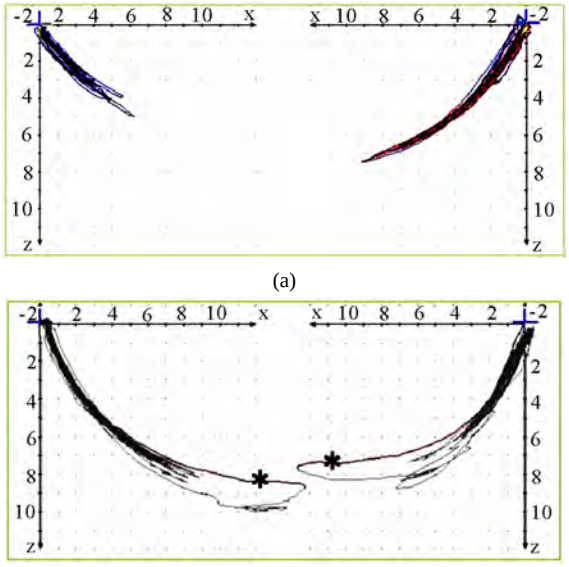

(a)

(b)

Figure 3. Sagittal view of recorded mastication pattern, (a) 21y, ♀, r, s; the right side is the ws and shows clearly a lesser quantity then the nws; (b) 49y, ♂, l, s; the left side (ws) shows a lesser quantity then the nws. The wide movement (*) indicates with the initial first opening for intake of the standard food.

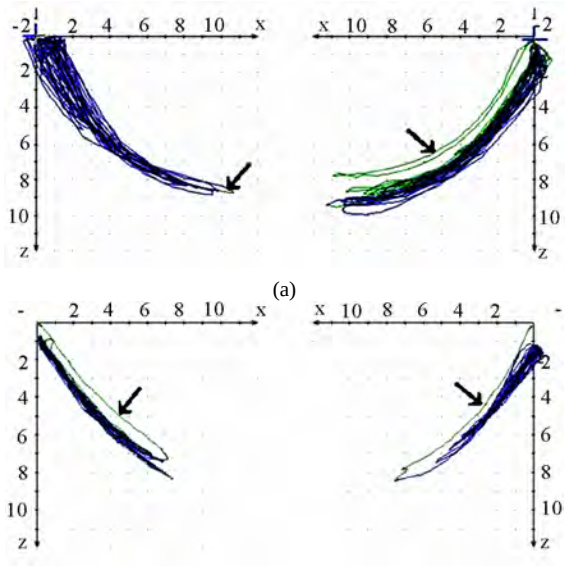

(a)

(b)

Figure 4. Sagittal view of recorded mastication pattern, (a) 18y, ♂, r, h; the right side is the ws, the standard movement (pro-re) is overlaid by the chewing cycles, the left side functions below pro-re; (b) 51y, ♂, r, s; both sides sketches below the pro (↙) and are coincident with re.

should also analyze whether the AS condyle is deviated in a different direction than the nAS condyle during mastication (**Figure 5**). As every movement is started from the reference position (RP) after renewed fixation, the position of masticatory movement can be assessed in relation to RP. Involvement or avoidance of this position may also be included in the analysis. Of course, AS and nAS can and should be assessed as well (**Figure 6**). Assessment of harmony can be achieved by the dynamic movement and by viewing the registered lines during the 18-second recording procedure (**Figure 7**).

Deviations from the points of occlusion (e.g., molar cusps) towards the sides are a physiological phenomenon during mastication and have been described in the published literature [5,6]. One should always consider the fact that the motion is a compound one. The movement of the mandible to the side and the lateral shift of the hinge axis can be analyzed in the frontal view during the motion (**Figure 8**).

Viewing the joint path registration from the cranial aspect (coronary view) provides information about the transverse component of masticatory movement. Movements towards one side or both sides are possible. The extent of motion should be noted. Large individual differences may be found. Associations between the quality of occlusion and the functional state of the ligaments of the stomatognathic system can be derived from these registrations (**Figure 9**).

Visualization of time-pathway diagrams enables the investigator to divide the masticatory cycles of AS and

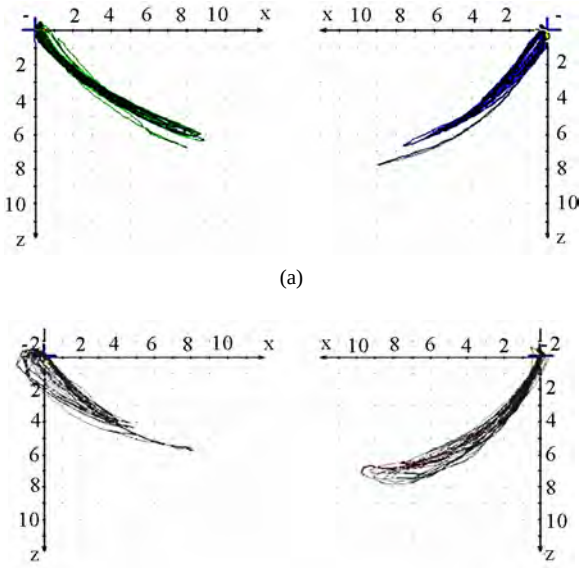

(a)

(b)

Figure 5. Sagittal view of recorded mastication pattern, (a) 21y, ♀, l, s; the right side is the ws, pro-re of both sides are overlaid by the chewing cycles only during the initial phase of the mastication; (b) 17y, ♀, r, h; pro-re is overlaid by the chewing cycles on both sides.

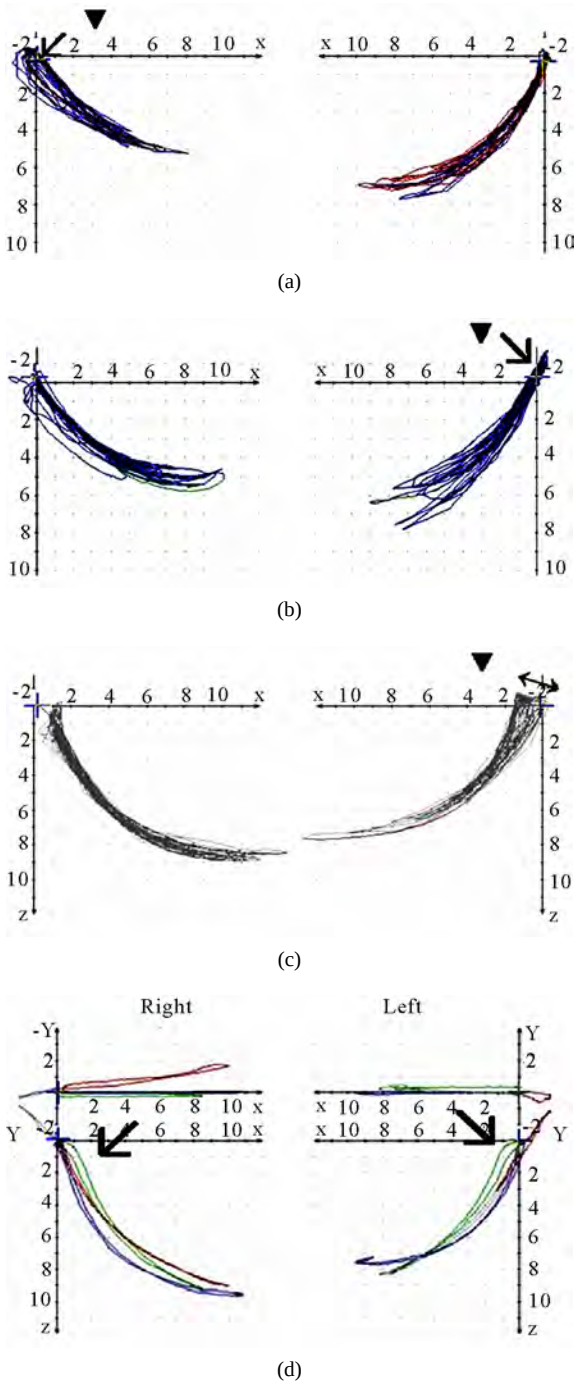

(a)

(b)

(c)

(d)

Figure 6. Sagittal view of recorded mastication pattern, (a) 17y, ♀, r, m; ws (▼) shows a tracing behind RP (↙) and z-axis (vertical axis); (b) same participant as shown in 6(a), l, s; ws (▼) charts a Re-Sur-trusiv tracting (↘); (c) 18y, ♂, l, h; ws (▼) uses the area in front and above RP (←→): participant with dental class II/1 and initial convexity in pro-re recording (see 6(d)); (d) same participant as shown in 6(c); standard tracings: pro-re: green, Open-Close (blue), Mediotrusion right (red), Mediotrusion left (grey). The initial convexity is indicated with arrows (↙).

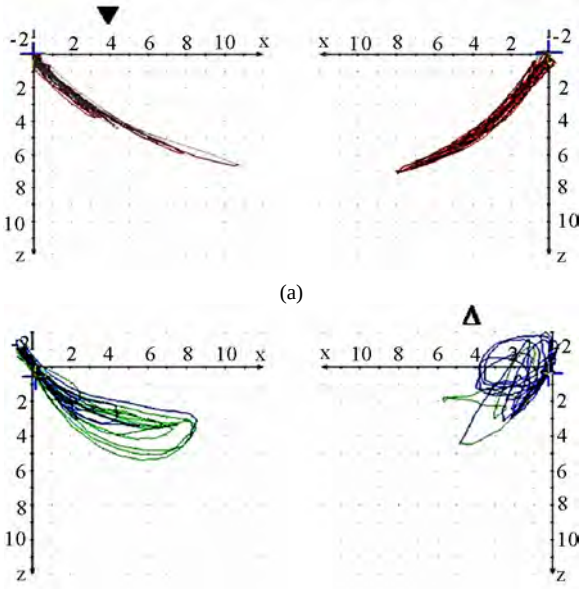

(a)

(b)

Figure 7. Sagittal view of recorded mastication pattern; (a) 21y, ♀, r, s; both sides (ws ▼) demonstrate a appropriate harmony of the chewing strokes; (b) 52y, ♀, r, s; the ws displace a breakup of the harmony, nws (△) plots a non harmonic chewing pattern.

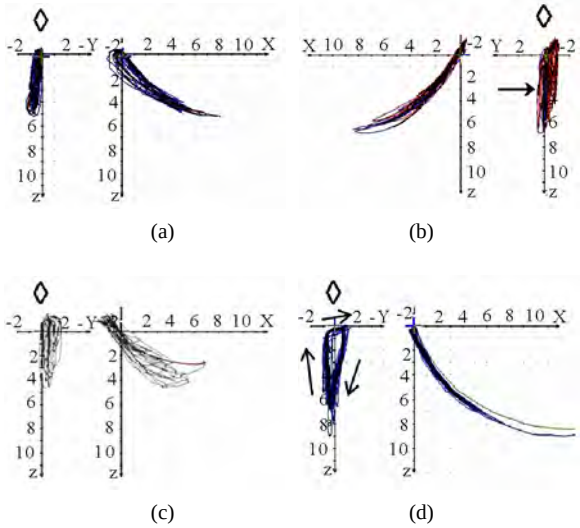

(a) (b)

(c) (d)

Figure 8. Frontal view (◇) of recorded mastication pattern, (a) 17y, ♀, r, m; ws shows a lateral movement to the right; (b) same participant as in 8(a), l, m; ws shows a lateral movement to the left, but also to the right (→); (c) 52y, ♀, r h; ws shows a lateral movement to the left (Class Ⅲ with cross bite); (d) 49y, ♂, r, s, ws with a triangular movement pattern, the arrows indicate the dynamics.

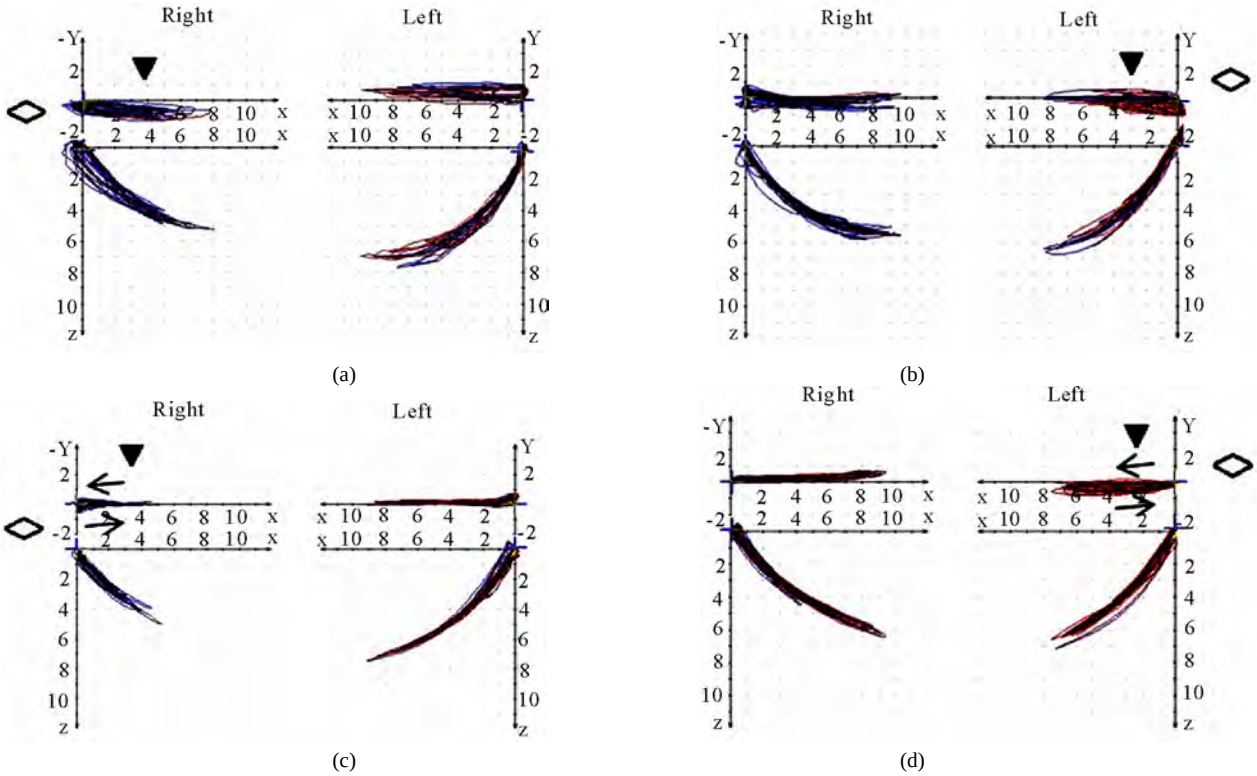

(a) (b)

(c) (d)

Figure 9. Coronar view (◇) of recorded mastication pattern, (a) 17y, ♀, r, m; ws shows (▼) shows a distinct lateral movement to the right; (b) same participant as in 9(a), l, m; ws (▼) plots movements to both sides; (c) 21y, ♀, r, m; ws (▼) charts a movement to the right during opening and to the left during closing (→); (d) same participant as in 9 (c), l, m; ws (▼) shows a straight movement during opening and a shift to the left while closing (→).

nAS and demonstrate these in a similar fashion as an ECG. A single masticatory movement is represented by a peak. The frequency and harmony of a masticatory movement can be viewed separately over an entire mastication process (18 seconds). The height, breadth and symmetry (steepness of the phase before the peak to the steepness of the phase after the peak) of individual peaks can be described. From such visualization one would basically expect a uniform time-pathway diagram with regular peaks, which reduce in height as the model food is minced and broken up. However, this is a speculative assumption and is not confirmed by our perusal of the published literature. Nevertheless, the time-pathway diagram of mastication can be described and analyzed by this method (**Figure 10**).

Interesting data can be derived from the translation-rotation diagram. Movements can be divided into two components, namely translation (horizontal axis) and rotation (vertical axis), and visualized accordingly. Characteristic differences seem to exist between AS and nAS: while AS is associated with greater rotation, nAS is marked by significant translation (**Figure 11**). In this recording, the accuracy of movements close to centric occlusion during mastication can be analyzed well. These sections of movement, which are always accompanied by deceleration, impose great demands on the neuromuscular system. The position and precision of these sections of motion should be included in the investigation procedure. The harmony of motions can be analyzed particularly well in this type of visualization. The direction of rotation of the pathways thus recorded may be significant. Clockwise and anti-clockwise movements are possible; AS and nAS may be oriented in different directions. A change in the direction of rotation may be observed in some cases. However, a conclusive statement about the potential pathological significance of such dynamic features cannot be made at the present time (**Figure 12**).

Gibbs and co-workers as well as other authors have described masticatory movement on the basis of the motion of specific occlusal points such as the points of the mandibular molars or the incisal edge of the lower front teeth [5,6]. Similar visualizations with the aid of CADIAX diagnostic software permit simulation of movements in individual occlusal regions. Sagittal, frontal and coronary views permit spatial analysis. The extent of motion and the direction of motion on the laterotrusion side (*i.e.*, AS) and the mediotrusion side (*i.e.*, nAS) can be analyzed. Notably, the direction of motion of the closing movement is not from the outer lower aspect to the upper inner aspect—in the manner described by Gibbs and co-workers. It was found that the dynamics of some masticatory cycles are changed, and the AS now serves as the mediotrusion side while the food bolus is retained on the same side (**Figure 13**).

Obviously, the above mentioned analyses must always be viewed with regard to the different degrees of hardness of the SFM. The load imposed on the stomatognathic system during mastication of hard food necessarily alters the course of the motion. In a fully functioning masticatory organ, this additional load should be of no major importance. The effects of such loads may be more pronounced in the presence of functional disorders and/or deviations in occlusion (**Figure 14**).

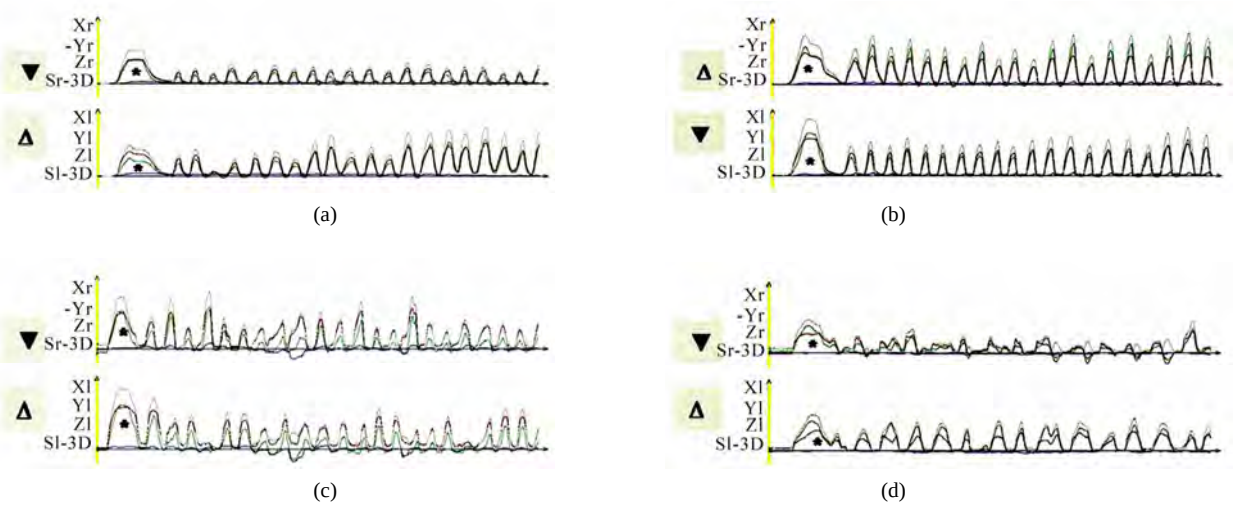

Figure 10. Time-distance diagram of recorded chewing pattern, (a) 21y, ♀, r, s; subsequent to the initial longer and wider mouth opening (*) due to food intake, the ws (▼) plots harmonic and constant chewing cycles. The nws (△) reveals an active positioning of the mandible due to the unequal height of the peaks; (b) same participant as in 9(a), l, s; subsequent to the initial longer and wider mouth opening (*) due to food intake, the ws (▼) plots harmonic and constant chewing cycles. The nws (△) shows an active positioning of the mandible due to the unequal height of the peaks; (c) 51y, ♂, r, h; chewing cycles are irregular; (d) 52y, ♂, r, s; the loss of harmony and constancy of chewing cycles is obvious.

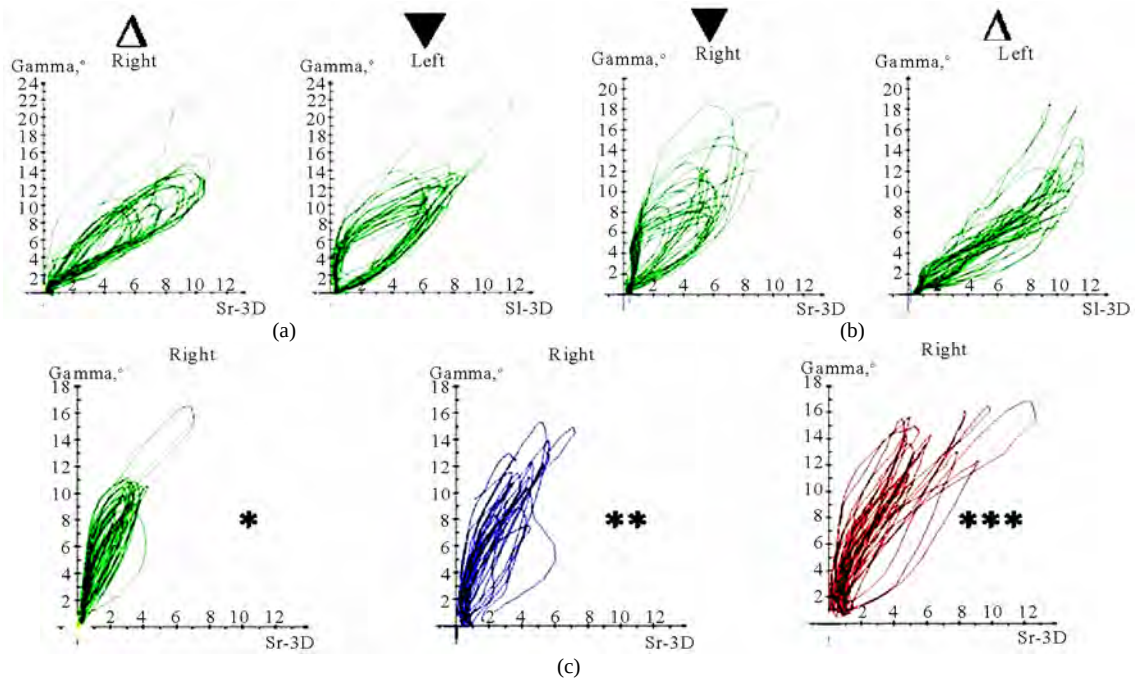

Figure 11. Translation-rotations curves of recorded chewing pattern (rotation is traced vertical, translation horizontal), (a) 21y, ♀, l, s; the rotation on the ws (▼) is larger then on the nws (△); (b) 18y, ♂, r, s; the rotation on the ws (▼) is larger then on the nws (△); the difference is more distinct compared to 11(a); (c) 21y, ♀, r, s (*), m (**), h (***); only the ws is displayed. The load and additional needed movements can be observed when chewing soft (*), medium (**) of hard (***) standard food.

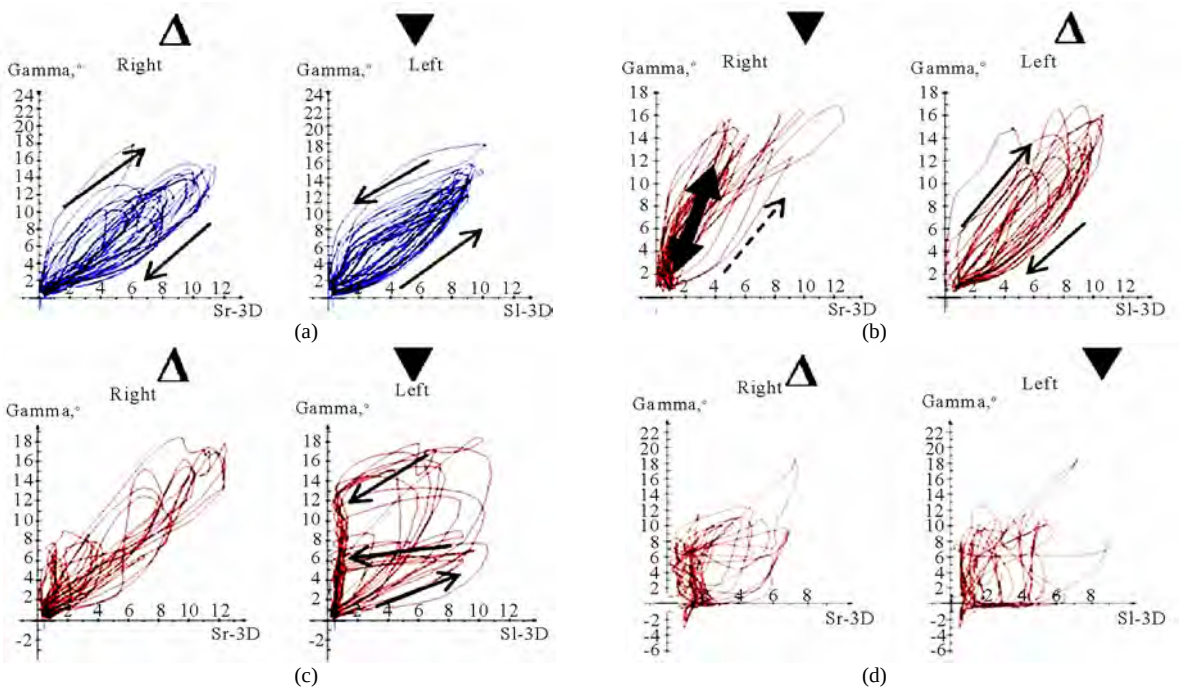

Figure 12. Translation-Rotations curves of recorded chewing pattern, (a) 21a, ♀, l, m; the ws (▼) plots a counterclockwise direction of rotation, while the nws (△) displays a clockwise rotation pattern; (b) same participant as in 12(a), r, h; the ws (▼) do not show a particular rotation pattern (←→), only the final chewing cycles are executed with a counter clockwise rotation (—>). The nws (△) plots a clockwise rotation; (c) 17(a), ♀, l, h; the ws (▼) displays a counterclockwise direction of rotation, but to an unequal extend. The nws (△) plots an indifferent rotation pattern; (d) 52a, ♀, l, h; ws (▼), but also nws (△) shows an undetermined rotation behavior.

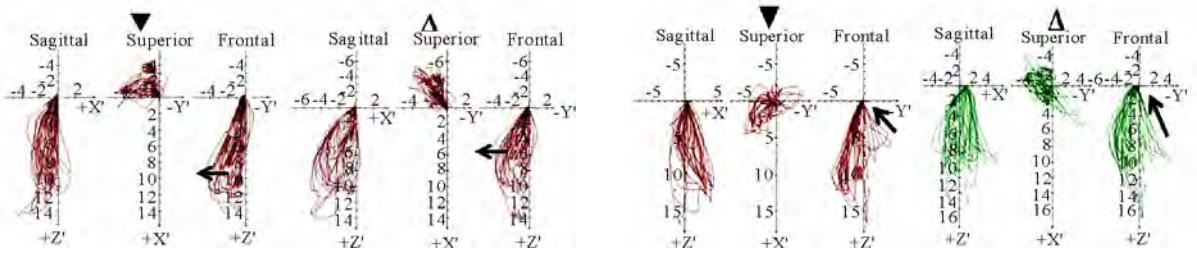

(a) (b)

Figure 13. Tooth movements (Coordinates ws (▼) x = 30, y = 30, z = 30; coordinates nws (△) x = 30, y = -30, z = 30), (a) 18a, ♂, r, h; ws (▼) and nws (△) show a lateral movement in direction to the ws (←). The sagittal view demonstrates the movement back and downward (participant with dental Class l); (b) 18a, ♂, r, m; the frontal view reveals a similar movement, but some chewing strokes are conducted in an atypical manner from down and left (↑). The sagittal movement is more oriented down and anterior (participant with Class ll/1).

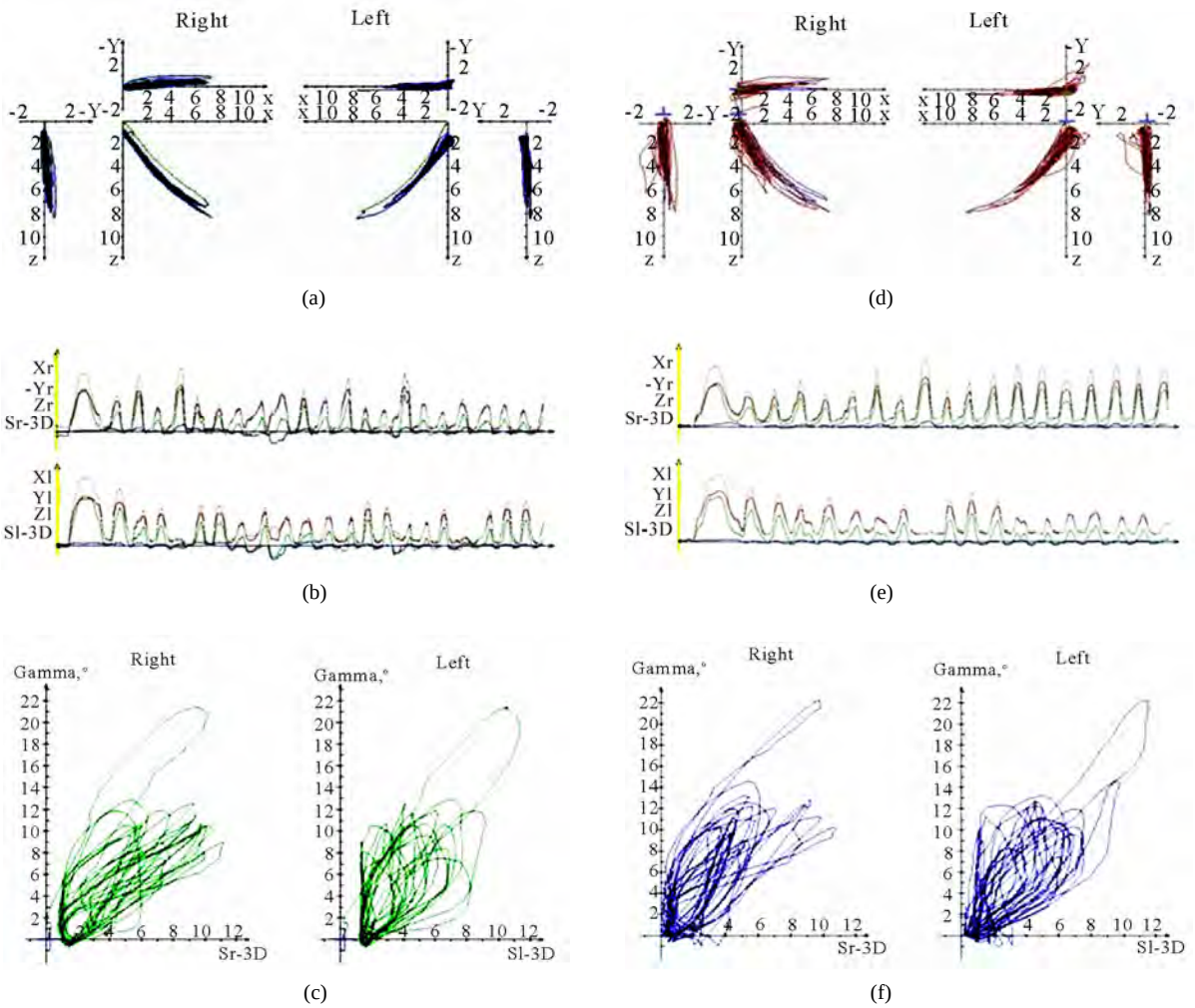

(a) (d)

(b) (e)

(c) (f)

Figure 14. Demonstration of the loading of the chewing organ due to the different hardness of the model food, (a, b, c) 51a, m, r, s; (b, d, f) same participant as in 14(a), r, h.

Bilateral mastication provides no significant additional information for quantitative and qualitative descriptions. However, due to the harmony of changing sides, one may draw conclusions about coordination with other muscle groups such as the floor of the mouth, the suprahyoid muscles, the postural muscles, the tongue, and the mimic muscles (**Figure 15**). One should consider the fact that especially shifting the food bolus from

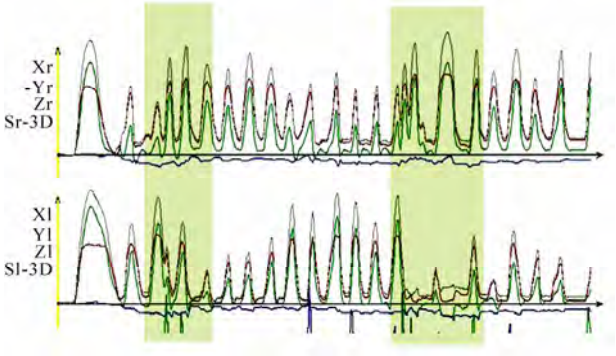

Figure 15. Time-distance diagram of a chewing sequence, up right side, down left side. The participant was asked to change the chewing side twice (shaded areas). The change in the regular chewing cycles can be seen clearly.

the right to the left side or vice versa is rendered much more difficult by the paraocclusal clutch and its handle. The usual physiological processes of the muscles of the cheek, the tongue, and especially the lips are impaired.

During and after the recording of masticatory movements, the proband should always be asked about any sensations or side effects that may have occurred. It was found that the nine recordings of masticatory movements do impose a load on the masticatory muscles and the craniomandibular joints. Even asymptomatic probands notice the loads and also perceive certain muscular sensations (general fatigue of muscles, individual sites of pain in muscles, pain in the craniomandibular joint either spontaneously or on palpation).

3. SUMMARY AND CONCLUSIONS

This article highlights the significance of a standardized procedure for analysis of human mastication. A database consequently created should, in the future, enable the dentist to comprehend and describe the physiological masticatory pattern and all of its conceivable individual variations. Based on the physiological processes thus identified, it will be possible to determine parameters that influence mastication and utilize these for the individual analysis. The discovery of deviations from the physiological masticatory pattern, and especially the identification of pathophysiological masticatory movements by this process, might pave the way for new strategic approaches in the diagnosis and treatment of the stomatognathic system. However, dynamic processes can only be analyzed on the basis of standardization of the data thus obtained. Therefore, this article is intended to serve as a contribution to the discussion and may initiate new research approaches in the clinical as well as experimental setting.

4. ACKNOWLEDGEMENTS

The authors declare no conflict of interest.

REFERENCES

[1] Geissler, C.A. and Bates, J.F. (1984) The nutritional effects of tooth loss. *American Society for Clinical Nutrition*, **39(3)**, 478-489.

[2] Ritchie, C.S., Joshipura, K., Hung, H.-C. and Douglass, C.W. (2002) Nutrition as a mediator in the relation between oral and systemic disease: Associations between specific measures of adult oral health and nutrition outcomes. *Critical Reviews in Oral Biology and Medicine*, **13(3)**, 291-300.

[3] Dienel, M. (2006) Ein neu entdeckter Schutzfaktor vor Alzheimer-Demenz: Zahlreiche noch erhaltene Zähne-die Neuburger Demenzstudie. *European Journal of Geriatrics*, **8(3)**, 166-170.

[4] Felicio, C.M., De Melchior, M.O., Da Silva, M.A. and Celeghini, R.M.S. (2007) Masticatory performance in adults related to temporo-mandibular disorder and dental occlusion. *Pró-Fono Revista de Atualização Cientifica*, **19(2)**, 151-158.

[5] Lassauzay, C., Peyron, M.A., Albuisson, E., Dransfield, E. and Woda, A. (2000) Variability of the masticatory process during chewing of elastic model foods. *European Journal of Oral Sciences*, **108(6)**, 484-492.

[6] Peyron, M.A., Blanc, O., Lund, J.P. and Woda, A. (2003) Influence of Age on adaptability of human mastication. *Journal of Neurophysiology*, **92(2)**, 773-779.

[7] Foster, K.D., Woda, A. and Peyron, M.A. (2006) Effect of texture of plastic and elastic model foods on the parameters of mastication. *Journal of Neurophysiology*, **95(6)**, 3469-3479.

[8] Schneider, G. and Sender, B. (2002) Clinical relevance of a simple fragmentation model to evaluate human masticatory performance. *Journal of Oral Rehabilitation*, **29(8)**, 731-736.

[9] Sasaguri, K., Sato, S., Hirano, Y., *et al.* (2004) Involvement of chewing in memory processes in humans: an approach using fMRI. *International Congress Series*, **1270**, 111-116.

[10] Huddleston Slater, J.J., Visscher, C.M., Lobbezoo, F. and Naeije, M. (1999) The intra-articular distance within the TMJ during free and loaded closing movements. *Journal of Dental Research*, **78(12)**, 1815-1820.

[11] Naeije, M. and Hofman, N. (2003) Biomechanics of the human Temporomandibular Joint during chewing. *Journal of Dental Research*, **82(7)**, 528-531.

[12] Gibbs, C.H., Mahan, P.E., Lundeen, H.C., *et al.* (1981) Occlusal forces during chewing—Influences of biting strength and food consistency. *Journal of Prosthetic Dentistry*, **46(5)**, 561-567.

[13] Proeschel, P.A. and Raum, J. (2003) Task-dependence of jaw elevator and depressor co-activation. *Journal of Dental Research*, **82(8)**, 617-620.

[14] Proeschel, P.A. and Morneburg, T. (2002) Task-dependence of activity/bite force relations and its impact on estimation of chewing force from EMG. *Journal of Dental Research*, **81(7)**, 464-468.

[15] Peyron, M.A., Lassauzay, C. and Woda, A. (2002) Effects of increased hardness on jaw movement and muscle ac-

tivity during chewing of visco-elastic model foods. *Experimental Brain Research*, **142(1)**, 41-51.

[16] Gibbs, C.H., Wickwire, N.A., Jacobson, A.P., Lundeen, H.C., Mahan, P.E. and Lupkiewicz, S.M. (1982) Comparison of typical chewing patterns in normal children and adults. *Journal of American Dental Association*, **105(1)**, 33-42.

[17] Miyawaki, S., Ohkochi, N., Kawakami, T. and Sugimura, M. (2000) Effect of food size on the movement of the mandibular first molars and condyles during deliberate unilateral mastication in humans. *Journal of Dental Research*, **79(7)**, 1525-1531.

[18] Pereira, L.J., Gavião, M.B., Engelen, L. and Van der Bilt, A. (2007) Mastication and swallowing: Influence of fluid addition to foods. *Journal of Applied Oral Science*, **15(1)**, 55-60.

[19] Slavicek, G., Soiher, M., Gruber, H., Siegl, P. and Oxtoby, M. (2009) A novel standard food model to analyze the individual parameters of human mastication. *International Journal of Stomatology and Occlusion Medicine*, **2(4)**, 163-174.

[20] Slavicek, G., Soiher, M., Gruber, H., Siegl, P. and Oxtoby, M. (2009) Fallstudien zur analyse des Kauens Teil 1: Die standardanalyse. *Stomatologie*, **106(7)**, 119-129.

[21] Slavicek, G., Soiher, M., Gruber, H., Siegl, P. and Oxtoby, M. (2009) Fallstudien zur analyse des Kauens Teil 2: Spezielle analysemöglichkeiten. *Stomatologie*, **106(8)**, 137-148.

[22] Slavicek, G., Soiher, M., Gruber, H., Siegl, P. and Oxtoby, M. (2010) Fallstudien zur analyse des Kauens Teil 3: Analyse von Höckerbewegungen. *Stomatologie*, **107(1)**, 1-7.

Advances in Bioscience and Biotechnology, 2010, 1, 79-90 **ABB**
doi:10.4236/abb.2010.12012 Published Online June 2010 (http://www.SciRP.org/journal/abb/)

Isolation, purification and characterization of an N-acetyl-D-lactosamine binding mitogenic and anti-proliferative lectin from tubers of a cobra lily *Arisaema utile* Schott

Vikram Dhuna[1], Kshitija Dhuna[1], Jatinder Singh[1], Ajit Kumar Saxena[2], Satyam Kumar Agrawal[1], Sukhdev Singh Kamboj[1]

[1]Department of Molecular Biology and Biochemistry, Guru Nanak Dev University, Amritsar, India;
[2]Department of Pharmacology, Indian Institute of Integrative medicine, Jammu Tawi, India.
Email: vikramdhuna@gmail.com

Received 18 April 2010; revised 7 May 2010; accepted 8 May 2010.

ABSTRACT

Lectins are the carbohydrate-binding proteins of non-immune origin which have been the subject of intense investigation over the last few decades owing to the variety of interesting biological properties. Most of the lectins which have been purified and characterized from plants have been obtained from dicotyledons. In the present study a lectin was purified from tubers of a monocot plant Arisaema utile (AUL) Schott by affinity chromatography on asialofetuin-linked amino activated silica beads. AUL gave a single band in SDS-PAGE at pH 8.3 corresponding to subunit Mr 13.5 kDa. The native molecular mass of AUL was 54 kDa suggesting a homotetrameric structure. AUL gave multiple bands in isoelectric focusing and in native PAGE at pH 8.3. AUL was inhibited by N-acetyl-D-lactosamine (Lac NAc), a disaccharide and asialofetuin, a complex desialylated serum glycoprotein. When treated with denaturing agents, the lectin was stable in the presence of urea (3 M), thiourea (4 M) and guanidine HCl (4 M). AUL was a glycoprotein with a carbohydrate content of 1.2%. Complete loss of activity was observed upon modification of tryptophan residues of the lectin. The activity was reduced to 25% after modification of tyrosine. Chemical modification of arginine, histidine, serine and cysteine residues of AUL did not affect its activity. Using Far UV CD spectra the estimated secondary structure was 37% α-helix, 25% β-sheet and 38% random contributions. The lectin showed potent mitogenic response towards human lymphocytes. In vitro anti-proliferative assay using 11 human cancer cell lines resulted in 50% inhibition of six cell lines viz. SW-620, HCT-15, SK-N-SH, IMR-32, Colo-205 and HT-29 at 38, 42, 43, 49, 50 and 89 µg/ml, respectively.

Keywords: *N*-acetyl-D-lactosamine; *Arisaema Utile*; Affinity Purification; Anti-Proliferative; Asialofetuin; Chemical Modification; Lectin; Mitogenicity

1. INTRODUCTION

Lectins are proteins or glycoproteins of non-immune origin that bind specifically to carbohydrates [1]. Most lectins are usually multivalent and able to agglutinate erythrocytes and other cells [1,2]. They have been proved excellent and versatile macromolecular tools for the study of normal or transformed cell surfaces, for the isolation of glycoconjugates and for use in other areas of biomedical science [3]. One of the most exiting properties resulting out of the interaction of lectins with lymphocytes is mitogenicity, *i.e.* the triggering of quiescent, non-dividing lymphocytes into a state of growth and proliferation. The discovery of first mitogenic lectin Nowell [4] led to the detection of many other such lectins, most notably concanavalin A [5], Wheat germ agglutinin [6] and Pokeweed mitogen [7]. However, every new lectin may have slight differences in the ligand binding specificity to serve as a diagnostic tool to find immunocompetence of patients suffering from a variety of diseases with immunological abnormalities [8]. Thus, such mitogenic lectins are invaluable tools to study the proliferation of various immune cells and biochemical changes associated with lymphocyte activation.

Very few lectins have been investigated for their use in cancer research and therapy. Preliminary investigations suggest that some lectins but not all can detect alterations of malignant cells as well as reduce the cancer cell tumorigenicity by immunomodulation and thus may be helpful for prognosis of the immune status of the pa-

tients [9]. The lectin from *Viscum album* (mistletoe), for instance, increases the reactivity of the lymphocytes of tumor-bearing mice *in vitro*, indicating its immune stimulating effects on the cancer-immunosuppressed lymphocytes. It also inhibits the protein synthesis in various malignant cell lines [10]. Some lectins inhibit cell proliferation while others stimulate it [11,12]. A few plant lectins have been identified which induce apoptosis in tumor cells, as for example, *Viscum album* L. [13,14]. Lectins interact with specific carbohydrate structures on the tumor cell surface and may be used to differentiate malignant from normal cells [15]. We report herein purification, characterization and amino acid modifications of a new monocot plant lectin from Himalayan cobra lily *Arisaema utile* Schott belonging to family Araceae which has shown significant proliferation inhibition towards six human cancer cell-lines and potent mitogenic response towards human lymphocytes.

2. MATERIALS AND METHODS

2.1. Materials and Chemicals

Underground tubers of Himalayan cobra lily *A. utile* were collected from Khajjiar, Dalhousie, India. Fetal calf serum from Sera Lab (GB) and RPMI-1640 from GIBCO-BRL (New York, USA) were procured and stored at 4℃. Carbohydrates, diethylpyrocarbonate (DEP), *N*-acetylimidazole, (NAI), *N*-bromosuccinimide (NBS), 2-hydroxy-5-nitrobenzyl bromide (HNB-Br), bis-dithionitrobenzoic acid, (DTNB), bovine serum albumin, sodium azide, Con A, 5-fluorouracil, adriamycin, mitomycin-C and other general chemicals were obtained from Sigma Chemical Co. (St. Louis, USA). Standard molecular weight markers, gel filtration markers and ampholine (pH 3.0-10.0) were procured from Amersham Pharmacia (New Jersey, USA). Amino activated silica beads used were from Clifmar, UK. The Cell-lines viz. MCF-7 (Breast), SK-N-SH (CNS), 502713 (Colon), Colo-205 (Colon), HCT-15 (Colon), HT-29 (Colon), SW-620 (Colon), Hep-2 (Liver), IMR-32 (Neuroblastoma), DU-145 (Prostate) and PC-3 (Prostate) were procured from National Center for Cell Sciences, Pune, India. These cell lines were maintained in RPMI 1640 medium with 10% FCS, 10 U/ml penicillin and 100 μg/ml streptomycin at 37℃, in humidified atmosphere (90% air and 10% CO_2) in CO_2 incubator (Heracell, Heraeus).

2.2. Isolation and Purification of AUL

Lectin from homogenized *A. utile* tubers was extracted overnight at 4℃ with 10 mM phosphate-buffered saline (PBS), pH 7.2 (1:5 w/v). After centrifugation at 20,000 x*g* for 30 min, the supernatant was chromatographed on asialofetuin-linked amino activated silica beads (1000Å; pore size, 100 μ; diameter) as described by Shangary *et al.* [16]. The bound lectin was eluted with 100 mM glycine-HCl buffer, pH 2.5. The fractions were neutralized immediately with 2 M Tris-HCl buffer, pH 8.3. The protein rich fractions were dialyzed against PBS and stored at 4℃ for further analysis.

2.3. Lectin-Activity Assay and Sugar Inhibition of Lectin

To 30 μl (1 mg/ml) of serial two fold dilution of the lectin in microtitre plate, an equal volume of 2% (v/v) suspension of rabbit erythrocytes (3.5×10^8 cells/ml) was added [17]. Agglutination was assessed after 1h at 37℃ when the RBCs in the control well had fully settled to form buttons. Agglutination activity was expressed as the reciprocal of the highest dilution that gave a positive result and was reckoned as one hemagglutination unit. To find the carbohydrate specificity of AUL, sugar inhibition was performed in a manner analogous to the hemagglutination test [17]. For this purpose, a series of 42 sugars/derivatives were used which included 4 pentoses: D-Arabinose, L-arabinose, D-ribose, D-xylose; 18 hexoses or their derivatives: D-fructose, D-galactose, D-glucose, D-mannose, L-sorbose, L-fucose, L-rhamnose, *N*-acetyl-D-galactosamine, *N*-acetyl-D-glucosamine, *N*-acetyl-β-D-mannosamine, phenyl-D-glucosamine, α-methyl-D-glucopyranoside, α-methyl-D-mannopyranoside, β-methyl-D-glucopyranoside, β-phenyl-D-glucopyranoside, sialic acid, adonitol, myo-inositol; 10 disaccharides: β-gentiobiose, D-lactose, α-maltose, D-melibiose, D-trehalose, α-D-man (1,2)-D-man, α-D-man (1,3)-D-man, α-D-man (1,6)-D-man, *N*-acetyl-D-lactosamine and *N*-acetyl neuraminic acid; 3 trisaccharides: melezitose, raffinose and N,N',N"-triacetylchitotriose; 3 polysaccharides: chitin, inulin and yeast mannan. Four glycoproteins, *i.e.*, asialofetuin, fetuin, mucin and thyroglobulin were also used. Sugars or their derivatives were tested at a concentration of 100 mM while polysaccharides and glycoproteins at a concentration of 4 mg/ml. Lectin was used at twice the lowest concentration causing agglutination of rabbit RBCs as determined through double dilution technique. The minimum concentration of the sugar in the final mixture that completely inhibited the lectin induced hemagglutination was taken as minimal inhibitory sugar concentration (MISC). To ascertain the biological specificity of AUL, the hemagglutination activity was tested against both normal as well as neuraminidase treated erythrocytes from rabbit, goat, sheep, guinea pig, rat, and human (ABO) blood and human lymphocytes [17].

3. BIOCHEMICAL AND BIOPHYSICAL CHARACTERIZATION

3.1. Protein and Neutral Sugar Content Analysis

Protein concentration in the crude and purified lectin was determined by the method of Lowry *et al.* [18] using

bovine serum albumin as standard while neutral sugar content of the purified lectin preparation was estimated by anthrone method [19] using D-glucose as standard.

3.2. Polyacrylamide Gel Electrophoresis of Native and Denatured Lectin

Native polyacrylamide gel electrophoresis (PAGE) was carried out using 7.5% (w/v) gel at pH 4.5 [20] and 10% (w/v) gel at pH 8.3 [21,22]. SDS–PAGE was performed according to Laemmli [23] using 11% (w/v) separating gel. The lectin sample was heated in the presence/ absence of 2-mercaptoethanol for 10min in boiling water bath. The gels were stained with Coomassie Brilliant Blue. The subunit molecular mass of the purified lectin was determined by comparing its electrophoretic mobility with those of molecular weight markers (14.4-94 kDa).

3.3. Isoelectric Focusing

It was carried out in 5% polyacrylamide tube gels containing 5% ampholine of pI range 3.0-9.5 according to Robertson *et al.* [24]. A set of pI markers was also loaded on a separate tube gel. Before staining, ampholine were eluted from the gel by incubation in 10% trichloroacetic acid (TCA) for 10 min followed by 1% TCA for 30 min at room temperature. The gels were stained with Coomassie brilliant blue. Isoelectric point was calculated by comparing the mobility of lectin with that of pI markers.

3.4. Gel-Exclusion Chromatography

The molecular mass of the native lectin was determined by gel filtration chromatography on Biogel P-200 column (1.6 × 62 cm) calibrated with molecular weight markers in the range of 12.4-66 kDa according to the method of Andrews [25]. The column was equilibrated and eluted with 10mM PBS, pH 7.2.

3.5. Effect of Temperature, PH, Denaturants, and Chelating Agents on Lectin Activity

To determine thermal stability of affinity purified AUL, 100 µl of it was heated for 15min at a defined temperature ranging from 20 to 100℃ and cooled to room temperature. As the bound lectin was desorbed from the affinity matrix by employing glycine-HCl buffer, pH 2.5, the effect of such a low pH on lectin-induced hemagglutination was ascertained before standardizing the purification protocol. The lectin sample was incubated with the above-mentioned buffer for time intervals ranging from 15 min to 6 h, followed by neutralization with Tris-HCl buffer, pH 8.3. Thereafter, titer of each treated sample was compared with that of controls *i.e.* lectin sample mixed with glycine-HCl followed by immediate neutralization and lectin sample in PBS alone. The effect of three denaturing agents *i.e.* urea, thiourea, and guanidine-HCl, at a concentration range of 1.0-8.0 M was tested on lectin activity by incubating 100 µl of each denaturant solution with equal volume of AUL at 37℃ for 1h. To examine divalent cation requirement of AUL for hemagglutination, demetallization of purified lectin was carried out by the method of Paulova *et al.* [26] by using EDTA followed by dialysis of sample with 0.1M $CaCl_2$ and $MnCl_2$. Following these treatments hemagglutination assay was performed with each sample and titer was compared with that of respective untreated samples.

4. SPECTROSCOPIC MEASUREMENTS

4.1. Fluorescence Studies

Fluorescence measurements were performed on a Shimadzu RF-1501 Spectrofluorophotometer. Samples were excited at 295 nm and emission spectra were recorded between 250 nm to 500 nm. Excitation and emission slit widths were 5 nm. Measurements were made using lectin at a concentration of 0.1 mg/ml protein in deionized water. Base-line corrections were carried out with deionized water without protein in all cases. The fluorescence spectra of native and NBS modified lectin samples were recorded.

4.2. Circular Dichroism Studies

Circular dichroism spectra of AUL were recorded using a Jasco J-715 spectropolarimeter over a wavelength of 200-250 nm at a scan speed of 50 nm/min, under constant N_2 purging according to the manufacturer's instructions (Jasco). The lectin was used at a concentration of 0.15 mg/ml in deionized water, in quartz cuvettes of 0.1 mm path length. The accumulated average of five protein spectra was corrected by subtraction of the spectra measured from deionized water blank. Analysis of CD spectra in terms of secondary structure content was performed using K2D programme.

4.3. Chemical Modification Studies of Amino Acids

The modification of tryptophan residues was carried out using NBS [27] and HNB-Br [28] Modification of tyrosine residues was carried out using NAI [29]. Arginine, histidine, serine and cysteine residues of AUL were modified as per defined conditions in **Table 1**. Both modified and unmodified lectin samples were dialyzed and residual activity was determined after appropriate dilution. Percentage residual activities were calculated using the native lectin as control possessing 100% activity. For ligand protection, AUL was pre-incubated for 30 minutes with N-acetyl-D-lactosamine and then modification was done.

Table 1. Condition for the chemical modification studies of amino acids of AUL.

Residue modified	Reagent	Concentration (mM)	Buffer used	Solvent	Reagent	Temperature in ℃	Time (min)
Tryptophan	NBS	10	50 mM acetate buffer, pH 6.0	Water	NBS	30	60
Tryptophan	HNB-Br	10	50 mM acetate buffer, pH 3.0	Dry Acetone	HNB-Br	30	60
Tyrosine	NAI	10	50 mM Tris-HCl buffer, pH 8.0	Water	NAI	30	60
Arginine	Phenylglyoxal	10	100 mM Sodium bicarbonate, pH 8.0	Water	Phenylglyoxal	30	60
Histidine	DEPC	10	100 mM PBS, pH 7.2	Absolute alcohol	DEPC	30	60
Serine	PMSF	10	50 mM PBS, pH 7.2	Water	PMSF	30	60
Cysteine	DTNB	10	100 mM Phosphate buffer, pH 8.0	Water	DTNB	30	60

NBS- *N*-bromosuccinimide; HNB-Br- 2-hydroxy-5-nitrobenzyl bromide; NAI- N-acetylimidazole; DEPC- Diethylpyrocarbonate; PMSF- Phenylmethylsulphonyl fluoride; DTNB- 5, 5'-dithiobis 2-nitrobenzioc acid.

5. BIOLOGICAL CHARACTERIZATION

5.1. Serological Studies

Antiserum against Purified AUL was raised by immunizing healthy rabbits with one mg/ml of the lectin and 1 mL of Freund's complete adjuvant (Sigma). Three doses were given at one-week interval each. After a weak of the last dose, the blood was collected by puncturing the ear pinna vein of the animal. Antiserum separated was preserved at –20℃ in aliquots containing 0.01% sodium azide. Double immunodiffusion (Ouchterlony) was performed to study serological cross-reactions. The gels stained for 30 minutes with 0.1% amido black and destained with 7% glacial acetic acid to visualize the stained precipitin lines.

5.2. Assay of Anti-Fungal Activity

Anti-fungal activity of AUL against selected plant pathogenic fungi, *i.e., Fusarium oxysporum, Fusarium graminearum, Trichoderma reesei, Colletotrichum lindemuthianum, Alternaria solani, Rhizoctonia solani and Botrytis cinerea* was performed as described by Wang *et al.* [30].

5.3. MTT (3, 4, 5-Dimethylthiazol-2yl-2, 5-Diphenyltetrazolium Bromide) Assay

A non-radioactive method [31] was employed to test the mitogenic potential of lectin on human peripheral blood mononuclear cells (HPBMC) separated by the method of Boyum [32]. The assay was carried out in quadruplicates in microtitre plate having 96 U-shaped wells (Nunc, Denmark). The test lectin and standard mitogen con A were filtered through 0.22 µ membrane filters (13 mm diameter, Schleicher and Schull, Germany) and stored at 4℃ in aliquots of 1 ml each. The protein content was estimated for all the lectin samples after filtration. The lectins were diluted in RPMI-1640 medium supplemented with 10% FCS to obtain the desirable concentration required for the experiment. A volume of 50 µl of each affinity purified lectin at concentrations ranging between 1.25-80.0 µg/ml along with standard Con A (1 mg/ml) was dispensed into 96 well microtitre plate. Now, 50 µl of lymphocyte suspension containing 2×10^6 cells/ml was added to each well of the microtitre plate and incubated for 72 hours. Four hours before the termination of cultures, 25 µl of MTT having a concentration of 2 mg/ml was added to each well. After 4 hours, 100 µl of acidified isopropanol was added. The blue colour of formazan formed was read at 492 nm with Labsystems Multiskan EX ELISA reader against a reagent blank.

5.4. Proliferation Inhibition Assay

To check that the lectin receptors for mitogenicity are glyco-components in nature, the inhibitors revealed by sugar inhibition assay AUL was used to analyze their effect on the proliferation by MTT assay. AUL had been were inhibited by a complex desialylated glycoprotein *i.e.* asialofetuin. Therefore, asialofetuin (Sigma, USA) was dissolved in RPMI-1640 medium supplemented with 10% FCS at a final concentration of 2 mg/ml. In the wells of a microtitre plate, asialofetuin from its stock solution was serially double diluted in a total volume of 25 µl. To this an equal volume of each lectin at double the optimum concentration was added and the plate was incubated at 37℃ for one hour. For the positive controls, 25 µl each of test lectin and ConA at their optimum concentrations with an equal volume of supplemented medium, were set in quarduplicates, thus constituting a total volume of 50 µl/well. After the incubation step, 50 µl of lymphocyte suspension at a concentration of 2×10^6 cells/ml was added to each well.

5.5. *In Vitro* Anti-Proliferative Potential of AUL on Human Cancer Cell Lines

Inhibitory potential of the lectin was tested against eleven human cancer cell lines viz. MCF-7 (Breast), SK-N-SH (CNS), 502713 (Colon), Colo-205 (Colon), HCT-15 (Colon), HT-29 (Colon), SW-620 (Colon), Hep-2 (Liver), IMR-32 (Neuroblastoma), DU-145 (Prostate) and PC-3 (Prostate) according to the method of Monks *et al.* [33] known as SRB assay. Cells were seeded at 10^4 cells/well in 100 µl RPMI medium containing 10% FCS in 96-well tissue culture plate and incubated for 24 h in CO_2 incubator. Subsequently, 100 µl of lectin solution (100 µg/ml), prepared in RPMI 1640 medium, was added to cells and the cultures were incubated for 48 h. After incubation period, adherent cell cultures were fixed *in situ* by adding 50 µl of 50% (v/v) trichloroacetic acid (final concentration 10% TCA) and incubated for 1h at 4℃. The supernatant was discarded and plates were washed five times with deionized water and dried. Hundred microliters of sulforhodamine B (SRB, 0.4% w/v in acetic acid) was added to each well and the cultures were incubated for 30min at room temperature. The unbound SRB was removed by washing with 1% acetic acid and plates were air-dried. The dye bound to basic amino acids of the cell membranes was solubilized with Tris buffer (10 mM, pH 10.5) and the absorption was measured at 540 nm using ELISA reader to determine the relative cell growth viability in the treated and untreated cells. Anti-cancer agents 5-flurouracil at a concentration of 1×10^{-5} M and mytomycin C and adriamycin at a concentration of 1×10^{-6} M were used as positive controls.

6. RESULTS AND DISCUSSION

6.1. Lectin Purification, Activity and Sugar Inhibition

In the present study, a plant lectin having mitogenic and antiproliferative activity has been purified from tubers of *Arisaema utile* Schott by affinity chromatography using asialofetuin as affinity ligand. The results of isolation of the lectin are summarized in **Table 2**. The lectin was eluted with 0.1 M glycine-HCl buffer, pH 2.5 (**Figure 1**). In a separate experiment, AUL was found to be stable at pH 2.0-9 for 1 hour. The efficiency of single step affinity purification protocol is apparent from the fact that there was 76% recovery of the lectin activity. It is also noteworthy that lectin constitutes a sizable (21%) proportion of the total extractable tuber protein and may serve as a major storage protein in the tubers as also reported for *Arum maculatum* [34].

Out of the 42 sugars/derivatives tested, N-acetyl-D-lactosamine (LacNAc) and asialofetuin inhibited lectin-induced hemagglutination. Earlier reports on monocot lectins from the family araceae have shown their inhibition by, N-acetyl-D-lactosamine [16,17] and mannose [35]. It is noteworthy that monocot lectins from families amaryllidaceae and alliaceae bind mannose with high affinity [36] but lectins from family araceae are refractory towards mannose except in *Acorus* lectins [35]. The specific inhibitor of AUL *i.e.* LacNAc is one of the important cancer markers [37]. In this context the AUL specific for this disaccharide may serve as a marker for the detection of various types of cancers. Minimal inhibitory sugar concentration with LacNAc was 25.0 mM, while for asialofetuin was 250 µg/ml. Inhibition of hemagglutination with asialofetuin and not with fetuin may suggest that sialic acid hinders the binding of the lectin to the recognition sites on fetuin. The structure of asialofetuin reveals that it consists of 80% Asn-linked oligosaccharides terminating in LacNAc (Gal-β-1, 4 GlcNAc) and 20% Ser/Thr-linked oligosaccharides having T-Disa-ccharide (Gal-β-1, 3-GalNAc) [38]. In the sugar inhibition assay lectin showed binding with LacNAc but not to T-Disaccharide and similar may be the case of asialofetuin which has both disaccharides in its structure.

AUL was reactive towards erythrocytes from rabbit, rat, goat, sheep, and guinea pig and human lymphocytes but non-reactive towards human ABO blood group erythrocytes even after neuraminidase treatment (**Table 3**). In this regard AUL has broad biological specificity as

Table 2. Affinity purification of *Arisaema utile* lectin on asialofetuin-linked amino activated silica beads.

Step	Total Protein (mg)	Total activity (HU)	Specific activity (HU/mg)	Purification fold	Recovery (%)	MEAPC (µg/ml)
Crude	890	12800	14.38	1.0	100.0	69.53
PBS fractions	230	--	--	--	--	--
Glycine-HCl fractions	188	9760	51.91	3.60	76.25	19.26

Data are for 100 g tubers.
HU = Hemagglutination unit. MEAPC = Minimal erythrocyte agglutinating protein concentration
HU- One hemagglutination unit (HU) is defined as the reciprocal of the highest dilution still causing a visible agglutination.

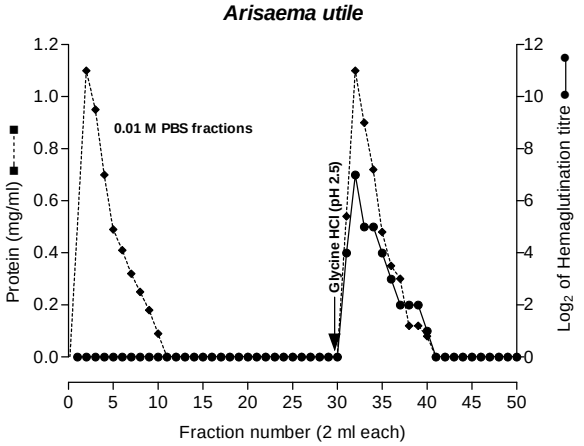

Figure 1. Affinity purification of AUL from tuber extract on asialofetuin-linked amino activated silica beads. Crude dialyzed tuber extract of *A. utile* was applied to the column (0.8 × 6.0cm), pre-equilibrated with 10mM PBS, pH 7.2. Bound lectin was eluted with 100mM glycine-HCl, pH 2.5 at flow rate 30 ml/h. [● ●] Absorbance of the complex formed, in protein estimation by Lowry *et al.* (1951), was taken at 540 nm. [♦----♦] Log_2 hemagglutination titre was determined using 2% suspension of rabbit erythrocytes.

Table 3. Reactivity of AUL towards different types of erythrocytes and human lymphocytes.

Erythrocytes	MEAPC/MLAPC (µg/ml)	
	Untreated	Neuraminidase treated
Rabbit	14.0	14.0
Rat	56.2	14.0
Guinea pig	28.1	7.0
Sheep	28.1	28.1
Goat	NA	135
Lymphocytes		
Human	14.0	7.0

reported earlier for other araceous lectins [11,12,16]. The preferential agglutination of rabbit RBCs over other animal blood cells may suggest easy availability of AUL receptors on these cells, their scanty presence on RBCs of rat, sheep and guinea pig and complete absence on human red blood cells. Further, increase in reactivity of rat and guinea pig erythrocytes and human lymphocytes following neuraminidase treatment supports the fact that sialic acid hinders access of lectin to their receptors.

6.2. Biochemical and Biophysical Characterization

Purified AUL was subjected to various tests to check the purity of the preparation. In SDS-PAGE at pH 8.3, under both reducing and non-reducing conditions, AUL migrated as a single band of 13.5 kDa (**Figure 2(a)**). Similarly, in native PAGE at pH 4.5 it moved as single band (**Figure 2(b)**). The native molecular mass of AUL was 54 kDa, as determined by gel filtration chromatography on calibrated Biogel P-200 column (**Figure 2(c)**). The results of SDS-PAGE under reducing and non-reducing conditions and gel filtration chromatography revealed that the lectin exists as a homotetramer of four identical subunits which are not held together by disulphide linkages [12,35]. However, AUL gave two bands when subjected to native PAGE at pH 8.3 (**Figure 2(d)**). These results indicate the presence of isolectins in the affinity purified AUL. Similarly, when subjected to isoelectric focusing, multiple bands were seen representing a mixture of isolectins, mostly in acidic range (**Figure 2(e)**) as reported in many lectins. These findings for AUL corroborate with earlier observations on various monocot as well as dicot lectins [39-41]. The lectin isomers may be due to variations in oligosaccharide chains [42] or it may stem from few altered amino acids in the lectins [43]. The carbohydrate content of the lectin was 1.2% indicating the lectin to be a glycoprotein. Lectin remained stable up to 55℃ for 15 minutes beyond which activity was gradually decreased and completely lost at 80℃ (data not shown) indicating high thermal stability of AUL as reported earlier for other araceous lectins [16]. AUL was stable in 3M Urea, 4M thiourea and 4M Guanidine-HCl. The activity declined at higher concentrations of denaturants but was not completely lost even at 8 M concentration of urea, thiourea and guanidine hydrochloride (data not shown). The denaturation by these agents indicates the globular nature of lectins, stabilized mainly by hydrophobic interactions (Nelson and Cox, 2001). EDTA treatment cations showed no effect on lectin activity suggesting that either the lectin activity was not dependent on metal cations or these metal ions are too strongly held in lectin structure and cannot be removed by dialysis (data not shown).

6.3. Spectroscopic Measurements and Amino Acid Modifications

Native AUL upon excitation at 295 nm exhibited a fluorescence emission maximum (λmax) at 340 nm. When compared with emission maximum of free tryptophan (348 nm), the emission peak of the tryptophan residue in AUL blue-shifted by about 8 nm to 340 nm, which showed that tryptophan residue of AUL is located in hydrophobic areas [44]. As shown above, the modification of tryptophan residues in AUL were essential groups and the hydrophobic areas where they were located help in lectin-sugar binding. The decline in fluorescence spectrum on modification of tryptophan residues of AUL was caused by modification of Trp (**Figure 3**).

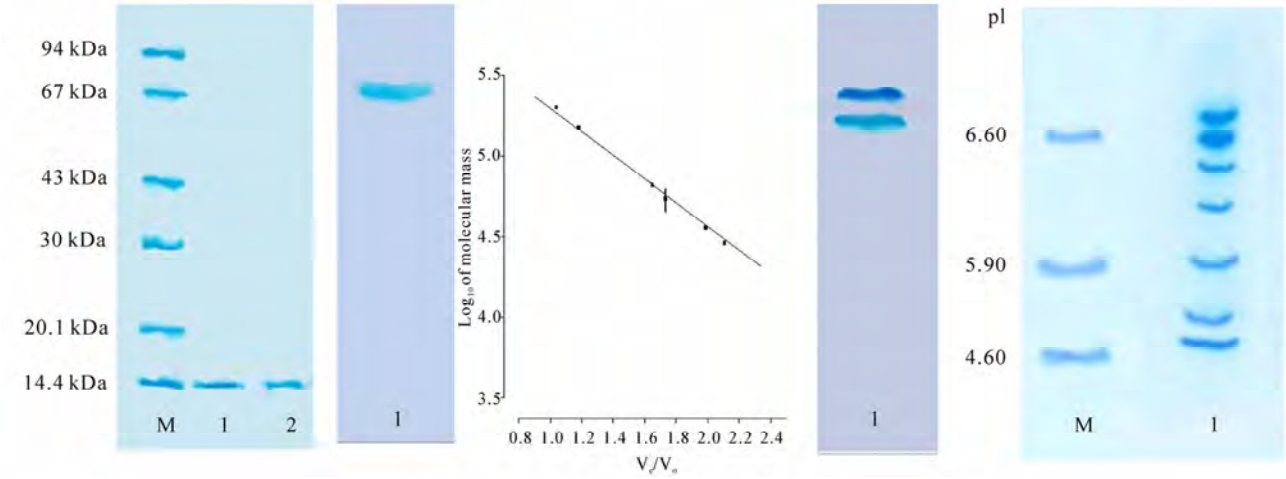

Figure 2. (a) SDS–PAGE, pH 8.3, patterns of purified AUL (lane 1) using 12% gel with (lanes 1) and without (lanes 2) 2% 2-mercaptoethanol (running time 3 h at a constant 100 V). The amount of purified lectin loaded is 20 µg. 40 µg of marker mixture loaded in Lane M, (from top to bottom): phosphorylase b (94 kDa); albumin bovine (67 kDa); ovalbumin (43 kDa); and carbonic anhydrase (30 kDa); trypsin inhibitor (20.1 kDa); and a-lactalbumin (14.4 kDa). The gel was stained with Coomassie brilliant blue. (b) Discontinuous-PAGE, pH 4.5, using 7.5% gel (running time 6 h at a constant 100 V); protein load, 30 µg; lane 1, AUL. (c) Native molecular mass estimation by standard plot of AUL on Biogel P-200 superfine gel filtration chromatography column. Standards used for gel filtration analysis were 1) β-amylase 2) Alcohol dehydrogenase 3) Albumin bovine serum 4) Carbonic anhydrase 5) Cytochrome C (d) Discontinuous-PAGE, pH 8.3, using 10% gel (running time 6 h at a constant 100 V); amount of protein loaded, 30 µg; lane 1, AUL. (e) Isoelectric focussing of non-denatured AUL lectin on 7.5% polyacrylamide gel using carrier ampholine of pH range 3.5-10.0 (running time 12 h at a constant 200 V); protein load, 30 µg; lane M, position of pI marker proteins; 1) carbonic anhydrase I, human erythrocytes (pI 6.6); 2) carbonic anhydrase II, bovine erythrocytes (pI 5.9); and 3) trypsin inhibitor, soybean (pI 4.6); lane (1) AUL.

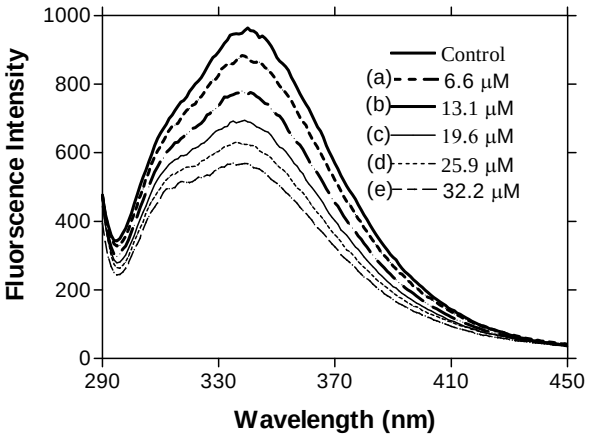

Figure 3. The decline of fluorescence intensity of AUL during tryptophan modification (with NBS) of AUL (100 µg/ml) was excited at 295 nm, and spectra were recorded between 250 and 500 nm. Control is without NBS and rest values (a, b, c, d and e) indicate the concentration of NBS in protein solution.

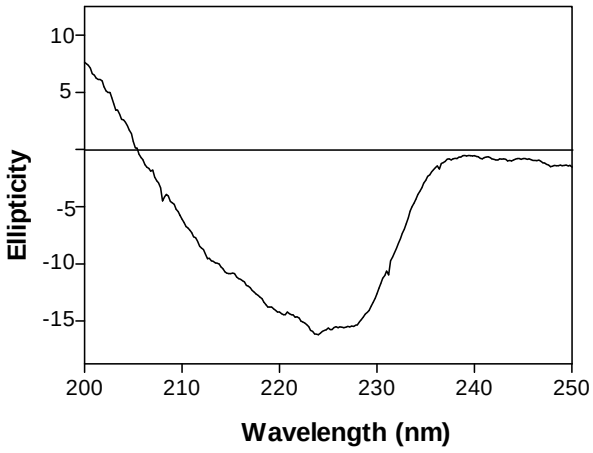

Figure 4. Far-UV CD spectrum of AUL in water.

Far UV CD spectra of AUL were recorded (**Figure 4**). The spectrum is characterized by two negative minima at around 224 and 228 nm and a positive to negative crossover at around 205 nm. Using K2D software the estimated secondary structures are 37% α-helix, 25% β-sheet and 38% random contributions. The secondary structure of AUL is comparable with Con A [45] and *Arisaema helliborifolium* [46].

Upon chemical modification of tryptophan with *N*-bromosuccinimide (NBS) as well as 2-hydroxy-5-nitrobenzyl bromide (HNB-Br), AUL completely lost its activity. Ligand protection with N-acetyl-D-lactosamine did not protect the lectin from losing activity suggesting that tryptophan may not be present within the sugar binding site but is essential in maintaining the functional

three dimensional structure of the lectin. Tyrosine modification with N-acetylimidazole (NAI) led to 50% inactivation of AUL lectin-sugar interaction. Ligand protection assay before tyrosine modification completely protected its activity which further supported the presence of tyrosine in the sugar binding site of the lectin. On the contrary, modification of arginine, histidine, serine and cysteine residues with pyridoxal, diethylpyrocarbonate (DEPC), phenylmethylsulphonyl fluoride (PMSF) and bis-dithionitrobenzoic acid (DTNB) respectively did not affect hemagglutinating activity of AUL suggesting that these amino acids may not play any important role in lectin-sugar interactions. Earlier, tryptophan modification studies on *Glycine max* [47], *Erythrina indica* [48] and *Erythrina speciosa* [49] have been shown to have deleterious effect on the lectin activity. In *Trichosanthes dioica* lectin [50], tyrosine residues are essential in carbohydrate binding and hemagglutination activities. Both tryptophan and tyrosine seem to play an important role in AUL activity in the present study.

6.4. Biological Characterization

In Oucterlony's double immunodiffusion, AUL antisera gave lines of identity with lectins from other araceous species (**Figure 5**), thus indicating evolutionary conservation of antigenic determinants on lectins from these species. In case of Amaryllidaceae and Alliaceae, serological relationship has been reported, as lectins from them resemble each other in their molecular structure and carbohydrate-binding properties. When the purified lectins from *Allium moly, A. sativum, A. vineale* and *A. ursinum* were loaded against antiserum raised against *Narcissus* cv Carlton lectins, single precipitin lines of identity were observed between the Alliaceae and Amaryllidaceae lectins thus indicating the evolutionary conservation of these monocot mannose-binding lectins [36]. When tested for anti-fungal activity against plant pathogenic fungi, AUL was found non-inhibitory.

In MTT assay, AUL gave potent mitogenic response towards human peripheral blood mononuclear cells. The relative mitogenic stimulation of AUL towards human lymphocytes was almost equal to that of Con A, a well-known standard plant mitogen (**Figure 6**). The optimum proliferation dose of AUL was 20 μg/ml. The mitogenic response of AUL was inhibited in a concentration dependent manner in the presence of asialofetuin that has been found inhibitory towards *A. utile* (**Figure 7**). The inhibition of hemagglutination and mitogenicity induced by AUL in the presence of asialofetuin confirms that lectin is producing mitogenic effect.

The *in vitro* anti-proliferative activity of AUL was carried out on eleven human cancer cell lines viz. MCF-7 (Breast), SK-N-SH (CNS), 502713 (Colon), Colo-205 (Colon), HCT-15 (Colon), HT-29 (Colon), SW-620 (Colon), Hep-2 (Liver), IMR-32 (Neuroblastoma), DU-145 (Prostate) and PC-3 (Prostate) (**Table 4**). AUL produced

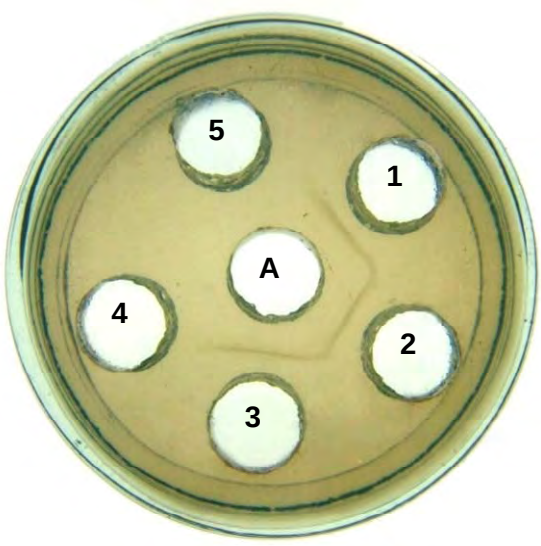

Figure 5. Double immunodiffusion. AUL antiserum was loaded in the central well (A), 15 mg of the purified AUL was loaded in the peripheral (well 1) and the same amount of purified lectin from *Sauromatum guttatum* (well 2), *Gonatanthus pumilus* (well 3). The wells 4 and 5 were without lectin.

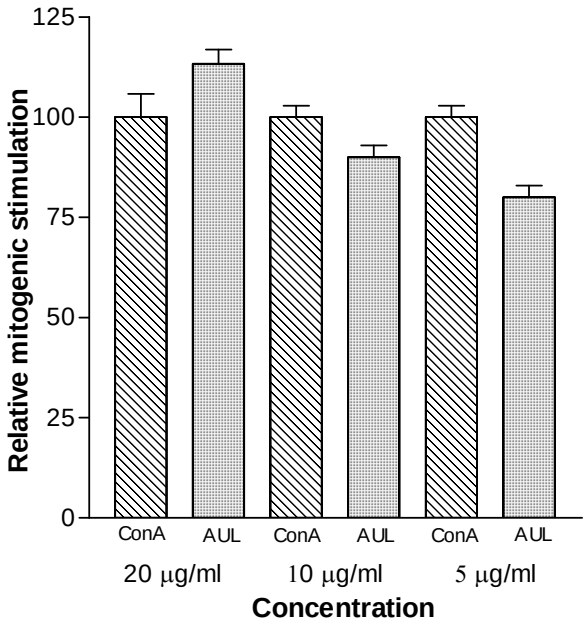

Figure 6. Relative mitogenic index of AUL. Human peripheral blood lymphocytes (1×10^5 cells/well) were cultured with AUL at different concentrations. A positive control is also shown using Con A at different concentrations. In the control wells, cells were cultured with medium alone (no lectin). The proliferation of lymphocytes was measured by MTT assay and the mitogenic index was calculated by dividing absorbance of AUL-stimulated lymphocytes with absorbance of lymphocytes without lectin. The relative mitogenic index of AUL is its mitogenic index relative to mitogenic index of Con A (taken as 100). (Data represent means ± SD, n = 4.)

Table 4. *In vitro* antiproliferative activity of AUL against human cancer cell lines.

Test Sample	Conc. µg/ml	Percentage inhibition										
		Human Cancer Cell Lines (source)										
		MCF-7 (Breast)	SK-N-SH (CNS)	502713 (Colon)	Colo-205 (Colon)	HCT-15 (Colon)	HT-29 (Colon)	SW-620 (Colon)	Hep-2 (Liver)	IMR-32 (Neu-robl-asto ma)	DU-145 (Prostate)	PC-3 (Prostate)
AUL	100	42 ± 6.1	73 ± 5.6	36 ± 5.3	63 ± 4.8	77 ± 7.2	56 ± 5.1	81 ± 5.6	43 ± 6.6	72 ± 4.8	23 ± 4.4	45 ± 4.6
AUL	50	30 ± 2.5	54 ± 5.1	24 ± 4.0	50 ± 6.5	52 ± 6.6	30 ± 5.2	62 ± 5.5	37 ± 6.8	50 ± 5.3	17 ± 2.8	35 ± 4.6
AUL	30	17 ± 3.7	42 ± 4.5	17 ± 3.2	39 ± 4.8	45 ± 5.6	22 ± 4.6	41 ± 5.8	30 ± 4.8	33 ± 4.2	10 ± 3.5	27 ± 3.5
AUL	10	10 ± 2.5	33 ± 3.6	11 ± 2.2	27 ± 4.5	31 ± 4.1	12 ± 3.2	30 ± 4.2	22 ± 5.6	20 ± 5.2	8 ± 4.2	22 ± 4.5
5-Fluorouracil	1×10^{-5} M	45 ± 5.4	39 ± 4.3	41 ± 4.5	29 ± 6.4	44 ± 4.6	30 ± 4.2	28 ± 4.9	14 ± 4.3	22 ± 4.2	39 ± 5.4	10 ± 4.2
Adriamycin	1×10^{-6} M	73 ± 6.4	68 ± 6.2	54 ± 5.2	38 ± 5.1	60 ± 5.2	15 ± 4.4	65 ± 6.4	50 ± 5.6	82 ± 5.9	81 ± 5.4	11 ± 5.1
Mitomycin C	1×10^{-6} M	41 ± 5.8	48 ± 4.8	65 ± 4.5	20 ± 4.5	26 ± 5.1	17 ± 3.6	34 ± 5.5	28 ± 3.8	25 ± 4.6	58 ± 5.2	10 ± 4

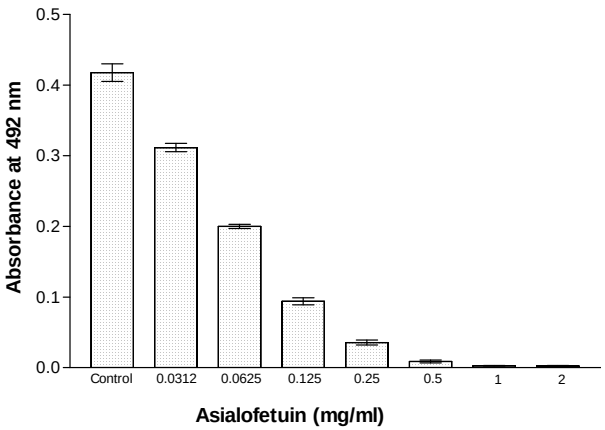

Figure 7. Inhibition of lectin-induced mitogenic stimulation of Human peripheral blood lymphocytes with asialofetuin at a concentration ranging between 2 and 0.0312 mg/ml. Bars represents the percentage inhibition of proliferation. (Data represent means ± SD, n = 4).

50% inhibition (IC_{50}) of cancer cell lines viz. SW-620, HCT-15, SK-N-SH, IMR-32, Colo-205 and HT-29 at 38, 42, 43, 49, 50 and 89 µg/ml respectively as calculated from graph plotted between percentage inhibition and concentration of AUL (**Figure 8**). However, IC_{50} was not achieved in MCF-7, 502713, Hep-2, DU-145 and PC-3 cell lines even at 100 µg/ml. The difference in proliferation inhibition of various cell-lines may be due to slight differences in the glycoconjugates expressed on the surface of cancer cells. In the present study, AUL was found specific for LacNAc which has been reported as one of the important cancer markers [37]. It is possible that LacNAc may be one of the components expressed on the tumor cells under investigation and responsible for in teraction with AUL. As every lectin has unique fine sugar specificity, there is a need to investigate a range of lectins against a number of cancer cell-lines to generate a battery of anti-cancer reagents. There are a few reports of mitogenic lectins which also possess anti-proliferative

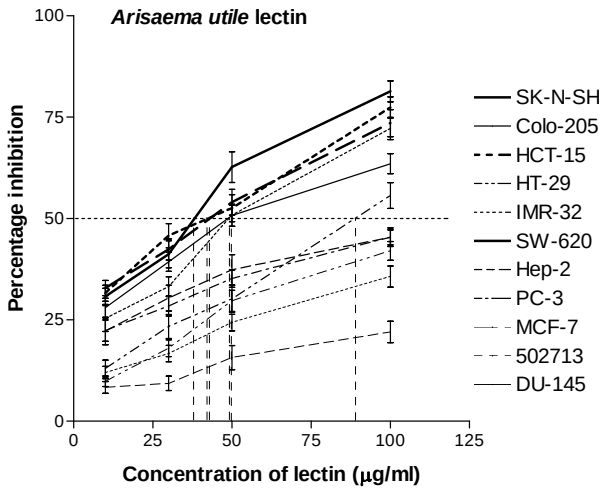

Figure 8. *In vitro* anti-proliferative effect of *Arisaema utile* lectin. Inhibitory effect of AUL was tested on human cancer cell lines MCF-7 (Breast), SK-N-SH (CNS), 502713 (Colon), Colo-205 (Colon), HCT-15 (Colon), HT-29 (Colon), SW-620 (Colon), Hep-2 (Liver), IMR-32 (Neuroblastoma), DU-145 (Prostate) and PC-3 (Prostate). Anticancer drugs 5-Fluorouracil, Adriamycin, Mitomycin C were used as positive control. Four different concentrations of lectin *i.e.* 10, 30, 50 and 100 µg/ml lectin were used for each cancer cell line. Plot between percentage inhibition of cancer cell lines and concentration of AUL was used to calculate the lectin concentration required for 50% inhibition. In the control wells cells were cultured with medium alone (no lectin added). Growth inhibition of cancer cell lines was measured by sulphorhodamine B dye staining assay (Data represent means ± SD, n = 4).

activity. In this aspect AUL is similar to the lectins isolated from mushrooms having potent mitogenic activity as well as anti-proliferative activity [51-53]. Although several hypotheses have been put forward which suggests that this effect is associated with the ability of lectins to modulate the growth, differentiation, proliferation and apoptosis of premature cells *in vivo* and *in vitro* yet the exact molecular mechanism(s) of the anti-proliferative effect of plant lectins is not clear at present.

7. CONCLUSIONS

A lectin with mitogenic as well as anti-proliferative activities have been purified and characterized from *Arisaema utile* Schott in the present study. The lectin was inhibited by N-acetyl-D-lactosamine and asialofetuin. Pure lectin is a homotetrameric molecule of 54 kDa with subunit molecular mass of 13.5 kDa. The lectin is as mitogenic as con A so it could also be used for mitogenic studies to explore the mechanism of lymphocyte activation as lectin bind to sugars of their specificity. Anti-proliferative property of AUL suggests the binding of lectin to certain receptor on the cell surface which are responsible for cancerous growth. Therefore this lectin may also be detected as histochemical marker in these type of cancers. The information from clinical studies using pure lectins is promising therefore additional research, including clinical trials, mechanisms of action at the molecular level, and structure-function relationships, should help researchers continue to examine and elucidate the therapeutic effects of lectins Although there is still more to know about the effects of lectins on cancer detection and treatment, this area of research holds great potential.

REFERENCES

[1] Goldstein, I.J., Hughes, R.C., Monsigny, M., Osawa, T. and Sharon, N. (1980) What should be called a lectin? *Nature*, **285(5760)**, 66.

[2] Sharon, N. and Lis, H. (1989) Lectins as cell recognition molecules. *Science*, **246(4927)**, 227-234.

[3] Sharon, N. and Lis, H. (2003) Lectins. 2nd Edition, Kluwer Academic Publishers, Dordrecht.

[4] Nowell, P.C. (1960) Phytohemagglutinin: An initiator of mitosis in cultures of normal human leucocytes. *Cancer research*, **20**, 462-464.

[5] Harris, H. and Robson, E.B. (1963) Precipitin reactions between extracts of seeds of *Canavalia ensiformis* (jack bean) and normal and pathological serum proteins. *Vox Sanguinis*, **8(3)**, 348-355.

[6] Aub, J.C., Sanford, B.H. and Wang, L.H. (1965) Reactions of normal and leukemic cell surfaces to a wheat germ agglutinin. *Proceedings of the National Academy of Sciences, USA*, **54(2)**, 400-402.

[7] Brittinger, G. and Konig, E. (1969) Lymphocyte stimulation by pokeweed mitogen (pwm). *Klin Wochenschr*, **47(24)**, 1307-1313.

[8] Krickeberg, H., Mauff, G., Mertens, T., Plum, G. and Heitmann, K. (1990) Lymphocyte proliferation in aids-related complex/walter-reed 5 patients: Response to herpes simplex virus and tuberculin antigen and mitogen during intravenous immunoglobulin treatment. *Vox Sanguinis*, **59(Suppl 1)**, 38-43.

[9] Gabius, H.J. (1987) Endogenous lectins in tumors and the immune system. *Cancer investigations*, **5(1)**, 39-46.

[10] Zarkovic, N., Vukovic, T., Loncaric, I., Miletic, M., Zarkovic, K. and Borovic, S. (2001) An overview on anticancer activities of the *Viscum album* extract isorel. *Cancer Biotherapy and Radiopharmaceuticals*, **16(1)**, 55-62.

[11] Singh, J., Singh, J. and Kamboj, S.S. (2004) A novel mitogenic and antiproliferative lectin from a wild cobra lily. *Arisaema flavum*. *Biochemical and Biophysical Research Communications*, **318(4)**, 1057-1065.

[12] Kaur, A., Kamboj, S.S., Singh, J., Saxena, A.K. and Dhuna, V. (2005) Isolation of a novel N-acetyl-D-lactosamine specific lectin from *Alocasia cucullata*. *Biotechnology Letters*, **27**, 1815-1820.

[13] Bantel, H., Engels, I.H., Voelter, W., Schulze-osthoff, K. and Wesselborg, S. (1999) Mistletoe lectin activates caspase-8/flice independently of death receptor signaling and enhances anticancer drug-induced apoptosis. *Cancer Research*, **59(9)**, 2083-2090.

[14] Park, R., Kim, M.S., So, H.S., Jung, B.H., Moon, S.R. and Chung, S.Y. (2000) Activation of cJun N-terminal kinase 1 (JNK1) in mistletoe lectin II-induced apoptosis of human myeloleukemic U937 cells. *Biochemical Pharmacology*, **60(11)**, 1685-1691.

[15] Ohba, H., Bakalova, R., Moriwaki, S. and Nakamura, O. (2002) Fractionation of normal and leukemic t-cells by lectin affinity column chromatography. *Cancer letters*, **184(2)**, 207-214.

[16] Shangary, S., Singh, J., Kamboj, S.S., Kamboj, K.K. and R. S. Sandhu (1995) Purification and properties of four monocot lectins from the family araceae. *Phytochemistry*, **40(2)**, 449-455.

[17] Dhuna, V., Singh, J., Kamboj, S.S., Singh, J., Shanmugavel and Saxena, A.K. (2005) Purification and characterization of a lectin from A*risaema tortuosum* schott having *in-vitro* anticancer activity against human cancer cell lines. *Journal of Biochemistry and Molecular Biology*, **38(5)**, 526-532.

[18] Lowry, O.H., Rosebrough, N.J., Farr, A.R. and Randall, R.J. (1951) Protein measurements with folin-phenol reagent. *The Journal of Biological Chemistry*, **193(1)**, 265-275.

[19] Spiro, R.G. (1966) Analysis of sugars found in glycoproteins. *Methods in Enzymology*, **8**, 3-26.

[20] Reisfeld, R.A., Lewis, O.J. and Williams, D.E. (1962) Disc electrophoresis of basic proteins and peptides on polyacrylamide gels. *Nature*, **145**, 281-283.

[21] Davis, B.J. (1964) Disc electrophoresis: Methods and applications to human serum proteins. *Annals of the New York Academy of Sciences*, **121**, 404-427.

[22] Bryan, J.K. (1977) Molecular weights of proteins multimers from polyacrylamide gel electrophoresis. *Analytical Biochemistry*, **78(2)**, 513-519.

[23] Laemmli, U.K. (1970) Cleavage of structural proteins during the assembly of the head of bacteriophage T4.

Nature, **277(5259)**, 680-685.

[24] Robertson, E.F., Dannelly, H.K., Malloy, P.J. and Reeve, H.C. (1987) Rapid isoelectric focusing in a vertical polyacrylamide minigel system. *Analytical Biochemistry*, **167(2)**, 290-294.

[25] Andrews, P. (1964) Estimation of the molecular weights of proteins by sephadex gel-filtration. *Biochemical Journal*, **91(2)**, 222-233.

[26] Paulova, M., Entlicher, G., Ticha, M., Kostir, J.V. and Kocourek, J. (1971) Studies of phytohemagglutinins. Vii. Effect of Mn^{2+} and Ca^{2+} on hemagglutinin of phytohemagglutinin of P*isum sativum* l. *Biochimica et Biophysica Acta*, **237**, 513-518.

[27] Spande, T.F. and Witkop, B. (1967) Determination of tryptophan content of protein with N-bromosuccinimide. *Methods in Enzymology*, **11**, 498-532.

[28] Horton, H.R. and Koshland, Jr., D.E. (1972) Modification of proteins with active benzyl halides. *Methods in Enzymology*, **25**, 468-477.

[29] Riordan, J.F., Wacker, W.E.C. and Vallee, B.L. (1965) N-acetyl imidazole: A reagent for determination of free tyrosyl residues of proteins. *Biochemistry*, **4**, 1758-1765.

[30] Wang, H., Ye, X.Y. and Ng, T.B. (2001) Purification of chrysancorin, a novel antifungal protein with mitogenic activity from garland chrysanthemum seeds. *Biological Chemistry*, **382(6)**, 947-951.

[31] Mosmann, T. (1983) Rapid colorimetric assay for cellular growth and survival: Application to proliferation and cytotoxicity assays. *Journal of Immunological Methods*, **65(1-2)**, 55-63.

[32] Böyum, A. (1968) Separation of leukocytes from blood and bone marrow. *Scandinavian Journal of Clinical and Laboratory Investigation*, **97(7)**, 77-89.

[33] Monks, A., Scudiero, D., Skehan, P., Shoemaker, R., Paul, K. and Vistica, D. (1991) Feasibility of a high-flux anticancer drug screen using a diverse panel of cultured human tumor cell lines. *Journal of the National Cancer Institute*, **83(11)**, 757-766.

[34] van Damme, E.J., Goossens, K., Smeets, K., van Leuven, F., Verhaert, P. and Peumans, W.J. (1995) The major tuber storage protein of araceae species is a lectin. Characterization and molecular cloning of the lectin from *Arum maculatum*. *Plant Physiology*, **107(4)**, 1147-1158.

[35] Bains, J.S., Dhuna, V., Singh, J., Kamboj, S.S., Nijjar, K. K. and Agrewala, J.N. (2005) Novel lectins from rhizomes of two acorus species with mitogenic activity and inhibitory potential towards murine cancer cell lines. *International Immunopharmacology*, **5(9)**, 1470-1478.

[36] Van Damme, E.J.M., Goldstein, I.J. and Peumans, W.J. (1991) A comparative study of mannose-binding lectins from amaryllidaceae and alliaceae. *Photochemistry*, **30 (2)**, 509-514.

[37] Ito, N., Imai, S., Haga, S., Nagaike, C., Morimura, Y. and Hatake, K. (1996) Localization of binding sites of U*lex europaeus*, H*elix pomatia* and G*riffonia simplicifolia* i-b4 lectins and analysis of their backbone structures by several glycosidases and poly-n-acetyllactosamine-specific lectins in human breast carcinoma. *Histochemistry and Cell Biology*, **106(3)**, 331-339.

[38] Green, E.D., Adelt, G., Baenziger, J.U., Wilson, S. and van Halbeek, H. (1988) The asparagine-linked oligosaccharides on bovine fetuin. Structural analysis of n-glycanase-released oligosaccharides by 500-megahertz 1h nmr spectroscopy. *The Journal of Biological Chemistry*, **263**, 18253-18268.

[39] van Damme, E.J.M., Allen, A.K. and Peumans, W.J. (1988) Related mannose-specific lectins from different species of the family amaryllidaceae. *Plant Physiology*, **73(1)**, 52-57.

[40] Chandra, N.R., Prabu, M.M., Suguna, K. and Vijayan, M. (2001) Structural similarity and functional diversity in proteins containing the legume lectin fold. *Protein Engineering*, **14(11)**, 857-866.

[41] Pang, Y., Shen, G.A., Liao, Z.H., Yao, J.H., Fei, J., Sun, X.F. and Tang, X. (2003) Molecular cloning and characterization of a novel lectin gene from Z*ephyranthes candida*. *DNA Sequence*, **14(3)**, 163-167.

[42] Hayes, C.E. and Goldstein, I.J. (1974) An alpha-d-galactosyl-binding lectin from bandeiraea simplicifolia seeds. Isolation by affinity chromatography and characterization. *The Journal of Biological Chemistry*, **249(6)**, 1904-1914.

[43] van Damme, E.J., Smeets, K., Torrekens, S., van Leuven, F., Goldstein, I.J. and Peumans, W.J. (1992) The closely related homomeric and heterodimeric mannose-binding lectins from garlic are encoded by one-domain and two-domain lectin genes, respectively. *European Jou nal of Biochemistry*, **206(2)**, 413-420.

[44] Devyani, N. and Mala, R. (1998) Structural and functional role of tryptophan in xylanase from an extremophilic *bacillus*: Assessment of the active site. *Biochemical and Biophysical Research Communications*, **249(1)**, 207-212.

[45] Zand, R., Agrawal, B.B.L. and Goldstein, I.J. (1971) pH-dependent conformational changes of concanavalin A. *Proceedings of the National Academy of Sciences, USA*, **68**, 2173-2376.

[46] Kaur, M., Singh, K., Rup, P.J., Saxena, A.K., Khan, R.H., Ashraf, M.T., Kamboj, S.S. and Singh, J. (2006) A tuber lectin from A*risaema Helleborifolium* schott with anti-insect activity against melon fruit fly *Bactrocera Cucurbitae* (coquillett) and anti-cancer effect on human cancer cell lines. *Archives of Biochemistry and Biophysics*, **445(1)**, 156-165.

[47] Desai, N.N., Allen, A.K. and Neuberger, A. (1983) The properties of potato (*Solanum tuberosum*) lectin after deglycosylation by triflouromethanesulphonic acid. *Biochemical Journal*, **211(1)**, 273-276.

[48] Konozy, E.H.E., Mulay, R., Faca, V., Aard, R.J., Greene, L.J., Roque-barriera, M.C., Sabharwal, S. and Bhide, S.V. (2002) Purification, some properties of a d-galactose-binding leaf lectin from *Erythrina indica* and further characterization of seed lectin. *Biochimie*, **84(10)**, 1035-1043.

[49] Konozy, E.H.E., Bernardes, E.S., Rosa, C., Faca, V. Greene, L.J. and Ward, R.J. (2003) Isolation, purification, and physicochemical characterization of a d-galactose-binding lectin from seeds of *Erythrina speciosa*. *Archives of Biochemistry and Biophysics*, **410(2)**, 222-229.

[50] Sultan, N.A.M., Kenoth, R. and Swamy, M.J. (2004) Purification, physicochemical characterization, saccharide specificity, and chemical modification of a gal/galnac specific lectin from the seeds of *Trichosanthes dioica*. *Archives of Biochemistry and Biophysics*, **432(2)**, 212-

221.

[51] Yu, L.G., Fernig, D.G., White, M.R., Spiller, D.G., Appleton, P. and Evans, R.C. (1999) Edible mushroom (A*garicus bisporus*) lectin, which reversibly inhibits epithelial cell proliferation, blocks nuclear localization sequence-dependent nuclear protein import. *The Journal of Biological Chemistry*, **274(8)**, 4890-4899.

[52] Wang, H.X., Ng, T.B., Liu, W.K., Ooi, V.E. and Chang, S.T. (1995) Isolation and characterization of two distinct lectins with antiproliferative activity from the cultured mycelium of the edible mushroom *Tricholoma mongolicum*. *International Journal of Peptide and Protein Research*, **46(6)**, 508-513.

[53] Ngai, P.H. and Ng, T.B. (2004) A mushroom (*Ganoderma capense*) lectin with spectacular thermostability, potent mitogenic activity on splenocytes, and antiproliferative activity toward tumor cells. *Biochemical and Biophysical Research Communications*, **314(4)**, 988-993.

Advances in Bioscience and Biotechnology, 2010, 1, 91-96 **ABB**
doi:10.4236/abb.2010.12013 Published Online June 2010 (http://www.SciRP.org/journal/abb/)

A new fibrinogenase from *Echis multisquamatis* venom is a perspective agent for limited proteolysis and defibrinogenation

Volodymyr O. Chernyshenko[1,2*], Olha V. Gornytska[2], Tetyana M. Platonova[2], Liudmyla I. Sokolovska[2]

[1]Kyiv National Shevchenko University, Kyiv, Ukraine;
[2]Palladin Institute of biochemistry, Kyiv, Ukraine.
Email: bio.cherv@gmail.com

Received 17 February 2010; revised 8 March 2010; accepted 24 March 2010.

ABSTRACT

A serine proteinase with a fibrinogenase activity was isolated from the venom of viper *Echis multisquamatis*. Isolation was performed by the combination of Q-sepharose and Heparine-agarose chromatography. The enzyme has apparent molecular weight 35 ± 1 kDa. It posesses strong fibrinogen *β*-chain, moderate *α*-chain proteolytic activity, arginine-amidase activity as the majority of serine fibrinogenases. The Km value was determined for *β*-chain fibrinogenolytic activity: Km = 8.3 μM. Kinetic parameters for amidase activity were also determined. Amino-acid composition was revealed. Limited hydrolysis of fibrinogen by the obtained fibrinogenase allowed us to detemine stable hydrolytic subproducts with definite molecular weights. The manner of the proteolytic processes suggests possible use of this fibrinogenase in probing fibrinogen structure dinamics by limited proteolysis. Applicability of the obtained fibrinogenase in therapeutic practice is speculative, but presented data about its nature are encouraging and require additional investigation.

Keywords: Fibrinogenase; Serine Proteinase; Snake Venom; Fibrinogen

1. INTRODUCTION

Snake venoms are mixtures of high-reactive enzymes which can influence the haemostasis components. The enzymes affect coagulation factors and proteins of endothelial cells' and platelets' membranes. They influence the system both non-selectively (through nonspecific hydrolysis) and selectively. The latter way is activation or inhibition of enzymes of coagulation, fibrinolysis and platelets activation. They also often are resistant to physiological inhibitors [1,2].

There is a group of fibrinogenases among snake venom enzymes. These direct-acting endopeptidases do not cleave off fibrinogen fibrinopeptides and therefore do not induce polymerization [3,4]. These enzymes are either serine- or metalloproteinases.

They are classified according to their action on the *α*- or *β*-chains of fibrinogen. Fibrinogenases slow down blood coagulation, because truncated fibrinogen does not form as strong a fibrin clot as the native one. This action is more evident for *α*-fibrinogenases [5].

As a rule, *α*-fibrinogenases contain Zink and have molecular weights of 20-26 kDa on an average. Disulfide bonds are often found in their structures. Most of them are inhibited by blood serum proteins and have affinity both to fibrinogen and to stabilized fibrin [3,4].

On the other hand, serine proteinases are mostly β-fibrinogenases and cleave the α-chain but moderately (there are some *α*-specific ones, though) [6,7]. Apart from fibrinogenase and arginine-esterase activities common for all of serine fibrinogenases, some can degrade fibrin, too. Average molecular weights vary between 23-32 kDa. Serine fibrinogenases unlike metalloproteinases are more heat-stable and less dependent on pH changes. Most of them are glycoproteins [4,6,8].

There is extensive sequence homology between the fibrin(ogen)olytic serine proteinases and the plasminogen activators and thrombin-like venom serine proteinases. However they do not have thrombin-like activity, and β-chain hydrolysis takes part in different non-thrombin sites [4,8].

Serine proteinases, including fibrinogenolytic enzymes are very abundant in Viperidae venoms in which they may account for 20% of their total protein content [9]. The unique specifity of snake venom proteinases makes them potentially useful in research of fibrinogen-depletion [10,11] and limited proteolysis.

The aim of our work was to obtain and characterize the fibrinogenase from *Echis multisquamatis* venom.

2. MATERIALS AND METHODS

2.1. Materials

Q-sepharose, acrylamide, Bis, SDS, TEMED were pur-

chased from GE Healthcare. Heparin-agarose type II was from Sigma. Chromogenic substrates were purchased from Chromogenix.

2.2. Chromatography

The crude venom was dissolved in 0.05 M Tris-HCl buffer of pH 8.9 and was applied onto an Q-sepharose column pre-equilibrated with the same buffer. The column volume was 3 ml, a flow rate of 2.55 ml/min/cm^2. The solution was eluted with step gradient of NaCl, the fraction with fibrinogenase activity was taken at the ionic strength of 0.125 M (**Figure 1**). The active fraction was further purified by Heparin-agarose type II, (Sigma) equilibrated with 0.05 M Tris-HCl buffer of pH 7.4, column volume 2 ml, flow rate of 1.27 ml/min/cm^2. The fraction with fibrinogenase activity was taken at the ionic strength of 0.3 M NaCl (**Figure 2**). Three chromatographycal cycles were required due to the volume obtained after Q-sepharose process.

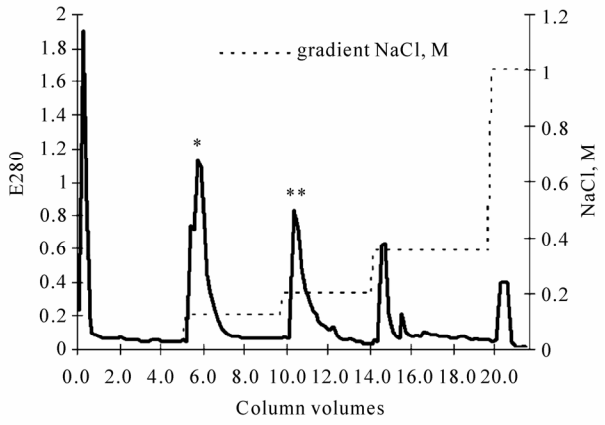

Figure 1. Chromatogram of fibrinogenase (*) and prothrombin activator (**) fraction of crude *E. multisquamatis* venom on Q-sepharose.

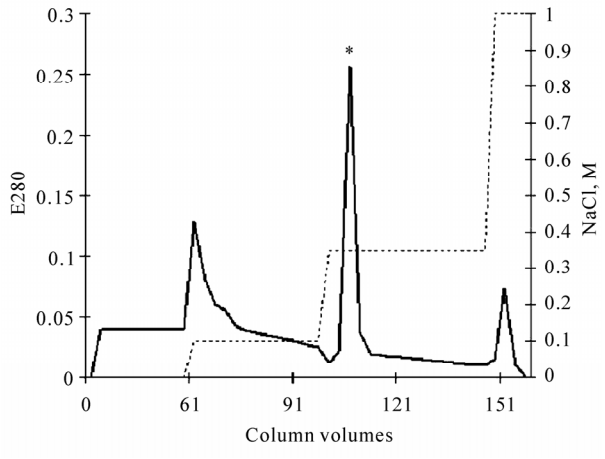

Figure 2. Chromatogram of fibrinogenase (*) of the fibrinogenase fraction of crude *E.multisquamatis* venom on Heparin-agarose type II.

2.3. Electrophoretic Analysis

Protein fractions were analysed in SDS-PAGE Laemli system [12], the proteins are identified using coomassie brilliant blue (R-250). Molecular weight markers "Fermentas" #0671 (170, 130, 100, 72, 55, 40, 33, 24 kDa).

2.4. Absorbance Coefficient Estimation

To determine the absorbance coefficient we estimated adsorption at 280 nm and carried on the Bradford analysis [13].

2.5. Amino-Acid Composition Analysis

Amino-acid composition was revealed using automatic amino-acid analyzer T-339 "Mikrotekno". Hydrolysis of protein was performed in the presence of 6 M NaCl, 120°C [14].

2.6. Amidase Activity Assay

Hydrolysis of chromogenic substrates (S2238 – H-D-Phe-Pip-Arg-pNA, S2251 – D-Val-Leu-Lys-pNA, S2765 – Z-D-Arg-Gly-Arg-pNA, S236 – pyro-Glu-L-Pro-L-Arg-pNA, S2302 – H-D-Pro-Phe-Arg-pNa) under the influence of fibrinogenase was studied using the reader (Titerteck-multiscan), E405 – E492. The analysis was done in 0.05M Tris-HCl buffer of pH 7.4 solution, 37°C. Chromogenic substrates concentration – 30 mM, that of fibrinogenase – 0.010 mg/ml.

2.7. Inhibitory Assay

The fibrinogenase was verified for inhibition by serine proteinases (DFF, PMSF, benzamidine), metalloproteinases (EDTA) and cystein proteinases (PCMB) inhibitors. PMSF – phenylmethylsulphonyl fluoride; DFP – Diisopropyl-fluorophosphate; PCMB – p-chloromercuribenzoate; EDTA – ethylenediaminetetraacetic acid. For the assay we used the thrombin-specific chromogenic substrate S2238 (H-D-Phe-Pip-Arg-pNA) using the reader (Titerteck-multiscan), E405 – E492. The analysis was done in 0.05M Tris-HCl buffer of pH 7.4 solution, 37°C. S2238 concentration was 40-120 mM, that of fibrinogenase – 0.010 mg/ml, and that of an inhibitor 0.8 mM.

2.8. Fibrinogenase Activity

1.5 mg/ml fibrinogen had been incubated with 0.050 mg/ml protein fractions in 0.05M Tris-HCl buffer of pH 7.4, 37°C for 10 minutes before being treated with 1 NIH/ml thrombin. The prolongation of clot formation time comparing to the control (native fibrinogen) was then determined.

2.9. Kinetic Parameters

To evaluate the Michaelis constants we studied hydrolysis of chromogenic substrates and native fibrinogen.

Hydrolysis of chromogenic substrates was studied using the reader (Titerteck-multiscan), E405 – E492. The analysis was done in 0.05 M Tris-HCl buffer of pH 7.4, 25°C. Chromogenic substrates concentration – 40-120 mM, that of fibrinogenase – 0.010 mg/ml.

Plasminogen-free fibrinogen (0.5-2.5 mg/ml) was incubated with the fibrinogenase (0.008 mg/ml) under similar conditions. The hydrolyzates were analyzed using SDS-PAGE Laemmli electrophoresis in the presence of 0.2% β-mercaptoethanol and quantitatively evaluated by Totallab TL100.

2.10 Fibrin(ogen) Fragments Obtaining

Obtaining of fibrin(ogen) degradation products was performed according to the method [15].

2.11. Fibrinogenase Treatment of Fibrin(ogen) Fragments

Fibrinogen fragments (1.3 mg/ml) were incubated with the fibrinogenase (0.08 mg/ml) during 60 minutes in 0.05 M Tris-HCl buffer of pH 7.4 solution, 25°C. Analyzed with electrophoresis as described above.

3. RESULTS

To achieve determined goal we fractionated crude venom, purified the fibrinogenase and analyzed it electrophoretically, determined substrate specificity and conducted an inhibitory assay.

Fractioning the *Echis multisquamatis* venom on Q-sepharose revealed two fractions of enzymes able to act on haemostasis components. The one eluted at ionic strength 0.2 M NaCl contained a prothrombin activator (**Figures 1** and **2**).

Therefore, 50 mg of crude venom yielded 2.5 mg of electrophoretically pure fibrinogenase. Its molecular weight is 35 ± 1 kDa. According to densitometry assay using Totallab TL100 (**Figure 3**) the content of the enzyme in crude venom was 5.83%, so the yield was 85.6%.

Amino-acid composition was revealed (**Table 1**). It was comparable with amino-acid compositions of some snake venom serine proteinases: bothrops protease A (β-fibrinogenase), shedaoenase (α-fibrinogenase) and afaacytin ($\alpha\beta$-fibrinogenase).

The enzyme was characterized under pH 7.4 as consistent with its evaluated pH optimum. It degraded chromogenic substrates. To qualitative determine the amidase activity of fibrinogenase we evaluated Michaelis constant for degradation of every substrate (**Table 2**). The affinities to kallikrein, plasmin, and thrombin chromogenic substrates highest exceeded affinities to others.

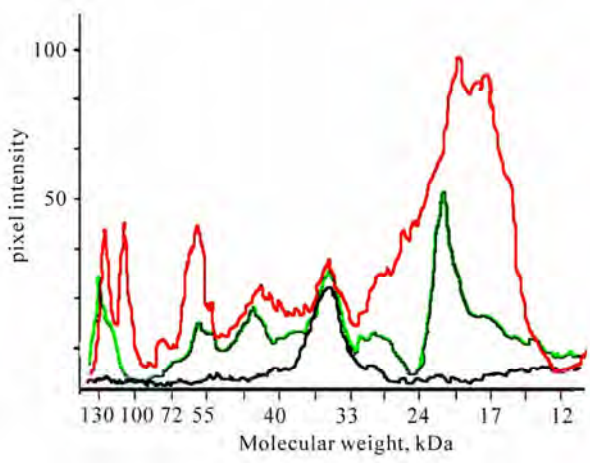

Figure 3. Densitogram of crude *E. multisquamatis* venom (red), fibrinogenase fraction after Q-sepharose (green) and purified fibrinogenase after Heparin-Sepharose (black), calculated in Totallab TL100.

Inhibitory assay was performed. Of the used inhibitors of different types of proteinases, PMSF, benzamidine and DFP had inhibitory effect on amidase activity of the enzyme. It means that it belongs to the serine proteinases. Degree of inhibitory effect was evaluated by Michaelis constant calculation (**Table 3**).

The target of proteolytic action of the fibrinogenase on fibrinogen was found to be the β-chain of the molecule that loses 3.3 ± 0.2 kDa of its weight at the early stages of hydrolysis (**Figure 4**) already, while the α-chain begins degradation after 40 minutes of incubation losing 9 kDa. Further hydrolysis results in more profound degradation.

To evaluate Michaelis constant we analysed the serie of electrophoregrams with densitometry soft Totallab TL100. Evaluated Michaelis constants for β-chain is 8.3 μM.

To localize the initial sites of β-chains cleavage we compared the abilities of fibrinogenase to hydrolyze fibrinogen, fibrin DD-fragment, fibrinogen E_2- and D-fragments [18]. Studied fragments are representing different sequences of fibrinogen. D and DD – distal C-terminal parts of molecule, E_2-fragment – central N terminal parts, except of Aα 1-17 Bβ 1-54 sequences [19]. The concentration of fibrinogenase was enough for profound Bβ-chain and initial α-chain degradation. Hydrolysis was not observed for all fragments (**Figures 5(a)**, **(b)** and **(c)**) but was evident for fibrinogen (**Figure 5(d)**). Thus we concluded that target of initial fibrinogen proteolysis by fibrinogenase is contained in N-terminal part of fibrinogen Bβ-chain.

4. DISCUSSION

We purified a new fibrinogenase of the *E. multisquamatis* venom by the two-step chromatographical protocol. It is

Table 1. Amino acid composition of fibrinogenase from the venom of *Echis multisquamatis* compared with that of other fibrinogenases.

	Echis multisquamatis venom fibrinogenase		Bothrops protease A [16]		Shedaeonase [6]		Afaacytin [17]	
Lys	12	4.24	7	2.713	13	5.485	24	6.575
His	7	2.66	8	3.101	7	2.954	12	3.288
Arg	11	4.18	13	5.039	12	5.063	17	4.658
Asx	29	10.48	27	10.47	26	10.97	45	12.33
Thr	18	6.55	15	5.814	15	6.329	nd	nd
Ser	19	7.01	18	6.977	17	7.173	28	7.671
Glx	23	6.63	19	7.364	16	6.751	21	5.753
Pro	16	5.88	16	6.202	19	8.017	22	6.027
Gly	29	10.6	25	9.69	19	8.017	33	9.041
Ala	20	7.3	17	6.589	12	5.063	21	5.753
Cys	10	3.55	12	4.651	12	5.063	20	5.479
Val	10	3.77	15	5.814	12	5.063	18	4.932
Met	2	0.69	6	2.326	3	1.266	4	1.096
Ile	20	7.45	20	7.752	16	6.751	28	7.671
Leu	25	9.25	23	8.915	18	7.595	30	8.219
Tyr	14	5.04	5	1.938	6	2.532	12	3.288
Phe	8	2.84	8	3.101	9	3.797	6	1.644
Trp	nd	nd	4	1.55	5	2.11	nd	nd
Total	273		258		237		365	
	amount	Ratio, %	amount	Ratio, %	amount	Ratio, %	amount	Ratio, %

Table 2. Cinetics of amidase activity of *E. multisquamatis* venom fibrinogenase.

Substrate	Sequence	Km, mM
S2302	*H-D-Pro-Phe-Arg-pNa*	0.016
S2765	*N-α-Cbo-D-Arg-Gly-Arg-pNa*	0.026
S236	*Pyro-Glu-Pro-Arg-pNa*	0.124
S2238	*H-D-Phe-Pip-Arg-pNa*	0.095
S2251	*H-D-Val-Leu-Lys-pNa*	0.231

Table 3. The influence of some inhibitors on amidase activity of *E. multisquamatis* venom fibrinogenase.

inhibitor	inhibition	Ki, mM
EDTA	–	–
PCMB	–	–
PMSF	+	0.841
DFP	+	1.958
benzamidine	+	1.129

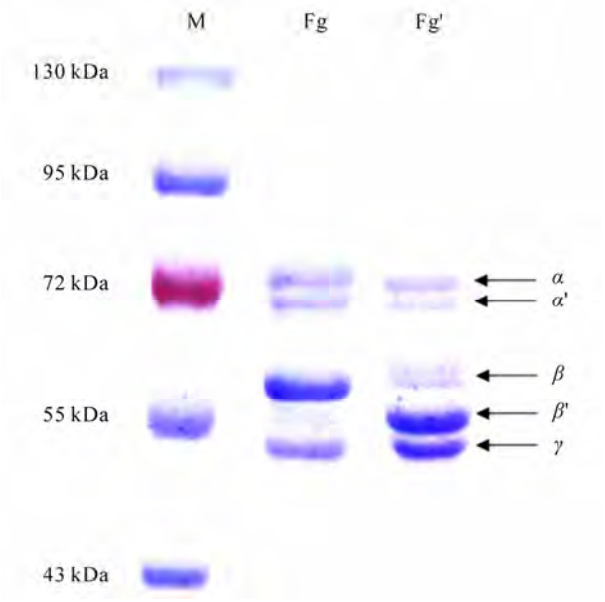

Figure 4. Electrophoregram of fibrinogen hydrolyzed by fibrinogenase from the venom of *E.multisquamatis.* Fg – native fibrinogen; Fg' – early stages hydrolytic product (incubation 7,5 min). Samples were prepared in the presence of 0.2% *β*-mercaptoethanol. M – molecular weight markers.

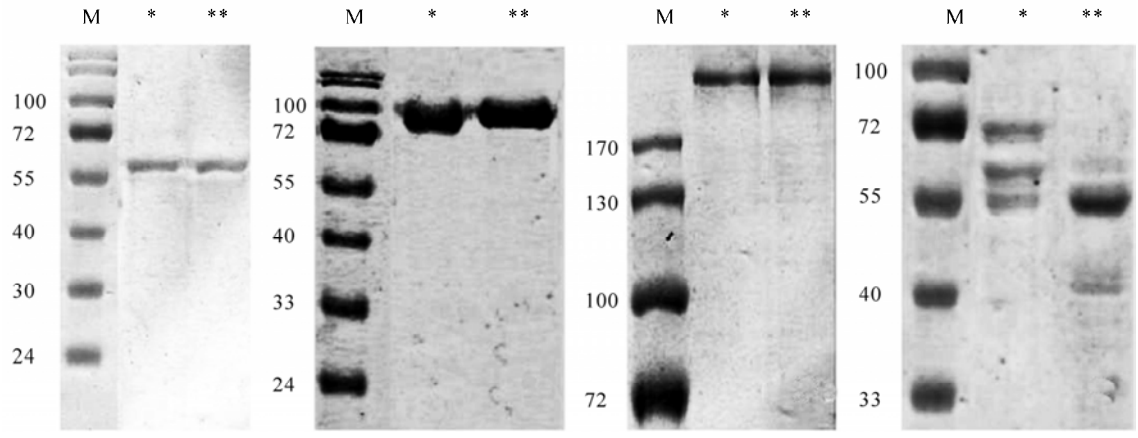

Figure 5. Electrophoregram of fibrinogen E_2-fragment (a), D-fragment (b), fibrin DD-fragment (c) and fibrinogen (d) treated by fibrinogenase. * - before treatment, ** - after treatment. Samples D were prepared in the presence of 0,2% β-mercaptoethanol.

N-terminal specific serine *β*-fibrinogenase with molecular weight of 35 ± 1 kDa. It has amidase activity of a wide range and no fibrinolytic one (data not shown).

The course of fibrinogenolysis suggests its possible usefulness in limited proteolysis fibrinogen study. The limited proteolysis technique gives information about structure, conformation and irregular sections of proteins consistent with spectroscopic data. It also may be applicable to obtain fragments of proteins that would preserve to an extent both tertial structure and functional active sites of the native molecules [20-22].

According to the dynamics of hydrolysis, one can assume that fibrinogenolysis leads to conformational changes in the molecule which in turn reveal sites of further degradation [23]. The structure-functional properties of truncated fibrinogen are of interest for studies of fibrin polymerization and of all types protein-protein and protein- blood cells interaction concerning fibrin(ogen). The partly degraded form of fibrinogen can be a useful tool for study of fibrinogen structure and functions [24].

The properties of the fibrinogenase from the venom of *E. multisquamatis* suggest that it should reasonably be studied as a potential fibrinogen-depleting agent [25]. Hyperfibrinogenemia is known to be not only a symptom but also a cause of thrombotic complications in case of inflammatory processes and cardiovascular diseases [26]. Fibrinogen depletion through hydrolysis by a fibrinogenase may be promising for intravascular coagulation prevention [27].

It is known that serine fibrinogenases have no hemorrhagic activity, do not influence protein C and fibrinolytic systems and do not hydrolyze PAR-receptors. It is therefore possible that they can provide fibrinogen depletion without at least the known side effects [11].

A new fibrinogenase was characterized and peculiarities of its functional activity determined. The obtained results encourage further investigations that may contribute both to science and medicine.

REFERENCES

[1] Braud, S., Bon, C. and Wisner, A. (2000) Snake venom proteins acting on hemostasis. *Biochimie*, **82(9-10)**, 851-859.

[2] Segers, W.H. and Ouyang, C. (1991) Snake venoms and blood coagulation. Snake venoms. In: Lee, C.-Y., Ed., *Handbook of Experimental Pathology*, **52**, 703-711.

[3] Markland, F.S. (1988) Fibrin(ogen)olytic enzymes from snake venoms. In: Pirkle, H. and Markland, F.S., Jr., Ed., *Haemostasis and Animal Venoms*, 149-165.

[4] Swenson, S. and Markland, F.S. (2005) Snake venom fibrin(ogen)olytic enzymes. *Toxicon*, **45(8)**, 1021-1039.

[5] Kini, R.M. (2006) Anticoagulant proteins from snake venoms: Structure, function and mechanism. *Biochemical Journal*, **397(3)**, 377-387.

[6] Jiao, H.M., Yang, L.X., Lu, B., *et al.* (2005) Shedaoenase, a novel fibrinogenase from the venom of Agkistrodon shedaoenthesis Zhao. *Acta Biochimica et Biophysica Sinica*, **37(12)**, 835-842.

[7] Samel, M., Subban, J., Siigur, J. and Siigur, E. (2002) Biochemical characterization of fibrinogenolytic serine proteinases from vipera lebetina snake venom. *Toxicon*, **40(1)**, 51-54.

[8] Matsui, T., Sakurai, Y., Fujimura, Y., *et al.* (1998) Purification and amino acid sequence of halystase from snake venom of Agkistrodon halys blomhoffii, a serine protease that cleaves specifically fibrinogen and kininogen. *European Journal of Biochemistry*, **252(3)**, 569-575.

[9] Wisner, A., Braud, S. and Bon, C. (2001) Snake venom proteinases as tools in hemostasis studies: structure-function relationship of a plasminogen activator purified from Trimeresurus stejnegeri venom. *Haemostasis*, **31(3-6)**, 133-140.

[10] Koh, D.C.I., Armugam, A. and Jeyaseelan, K. (2006) Snake venom components and their applications in biomedicine. *Cellular and Molecular Life Sciences*, **63(24)**, 3030-3041.

[11] Gardiner, E.E. and Andrews, R.K. (2008) The cut of the clot(h): Snake venom fibrinogenases as therapeutic agents. *Journal of Thrombosis and Haemostasis*, **6(8)**, 1360-1362.

[12] Laemli, R.V. (1970) Cleavage of structural poteteins during the assembly of the head of bacteriophage T4. *Nature*, **227(5259)**, 680-685.

[13] Bradford, M.M. (1976) A rapid and sensitive method for the quantitation of microgram quantities of protein utilizing the principle of protein-dye binding. *Analytical Biochemistry*, **72**, 248-254.

[14] Speckmann, D., Stein, W. and Moore, S. (1958) Automatic recording apparatus for use in the chromatography of amino acids. *Analytical Chemistry*, **30**, 1190-1196.

[15] Platonova, T.M., Chernyshenko, T.M. and Sokolovska, L.I. (2006) Effect peculiarities of D-domain-containing specific inhibitors of polymerization on the fibrin self-assembly process. *Ukrainian Biochemical Journal*, **78(3)**, 124-129.

[16] Murayama, N., Saguchi, K. and Mentele, R. (2003) The unusual high molecular mass of *Bothrops* protease A, a trypsin-like serine peptidase from the venom of *Bothrops jararaca*, is due to its high carbohydrate content. *Biochimica et Biophysica Acta* (*BBA*) – *Proteins* & *Proteomics*, **1652(1)**, 1-6.

[17] Lababa-Djebari, F., Martin-Eauclaire, M.-F.I., Mauco, G. and Marchot, P. (1995) Afaacytin, an *αβ*-fibrinogenase from Cerastes cerastes (Horned Viper) venom, activates purified factor X and induces serotonin release from human blood platelets. *European Journal of Biochemistry*, **233**, 756-765.

[18] Collen, D., Kudryk, B., Hessel, B. and Blomback, B. (1975) Primary structure of human fibrinogen and fibrin. Isolation and partial characterization of chains of fragment D. *Journal of Biological Chemistry*, **250(15)**, 5808-5817.

[19] Gãrdlund, B. (1977) Human fibrinogen amino acid sequence of fragment E and of adjacent structures in the A*α*- and B*β*-chains. *Thrombosis Research*, **10(5)**, 689-702.

[20] Fontana, A., Fassina, G., Vita, C., *et al.* (1986) Correlation between sites of limited proteolysis and segmental mobility in thermolysin. *Biochemistry*, **25(8)**, 1847-1851.

[21] Fontana, A., de Laureto, P.P., Spolaore, B., *et al.* (2004) Probing protein structure by limited proteolysis. *Acta Biochimica Polonica*, **51(2)**, 299-321.

[22] Zappacosta, F., Pessi, A., Bianchi, E., *et al.* (1996) Probing the tertiary structure of proteins by limited proteolysis and mass spectrometry: the case of minibody. *Protein Science*, **5(5)**, 802-813.

[23] Chernyshenko, V.O. and Korolova D.S. (2008) Echis multisquamatis venom enzymes acting on haemostasis. *Bridges in Life Sciences Annual Scientific Review Meeting*, Zagreb, 4 October 2008.

[24] Cooley, B.C. and Isermann, B.H. (2004) Cause-effect relation between hyperfibrinogenemia and vascular disease. *Blood*, **103(5)**, 1728-1734.

[25] Chernyshenko, V.O. and Maksymovych, I.S. (2009) Echis multisquamatis venom fibrinogenase is a prospective fibrinogen-depletive agent. 1*st World Conference on Physico-Chemical Methods in Drug Discovery and Development*, Rovinj, 27 September-1 October 2009, 40.

[26] Siebenlist, K.R., DiOrio, J.P., Budzynski, A.Z. and Mosesson, M.W. (1990) The polymerization and thrombin-binding properties of des-(Bbeta 1-42)-fibrin. *Journal of Biological Chemistry*, **265(30)**, 18650-18655.

[27] Liu, M., Counsell, C., Zhao, X.L. and Wardlaw, J. (2005) Fibrinogen-depleting agents for acute ischemic stroke. *Stroke*, **36(1)**, 173-174.

Advances in Bioscience and Biotechnology, 2010, 1, 97-109 **ABB**
doi:10.4236/abb.2010.12014 Published Online June 2010 (http://www.SciRP.org/journal/abb/)

Mitochondria: transportation, distribution and function during spermiogenesis*

Xiao Sun, Wan-Xi Yang

The Sperm Laboratory, Institute of Cell Biology and Genetics, College of Life Sciences, Zhejiang University, Hangzhou, China.
Email: wxyang@spermlab.org

Received 19 March 2010; revised 29 March 2010; accepted 30 March 2010.

ABSTRACT

Spermiogenesis is a dynamic process which includes organelle reorganization and new structure formation. The morphology and distribution of the mitochondria in germ cells change to accommodate the cellular requirement. Multiple molecular motors and related proteins participate in carrying and anchoring mitochondria to the midpiece during spermiogenesis and this process is regulated precisely. Energetic metabolism provides energy for cellular activity and influences sperm survival and motility directly. Ubiquitination of mitochondria takes place during spermiogenesis, which has been implicated in sperm quality control and mitochondrial inheritance. In light of the essential roles of mitochondria in energy production, calcium homeostasis and apoptosis, mitochondria dysfunction cause severe human diseases, such as male infertility. The present study paves a way for a more detailed exploration of the biology of mitochondria during spermiogenesis.

Keywords: Spermiogenesis; Mitochondria; Molecular Motors; Sperm Motility; Ubiquitination; Infertility

1. INTRODUCTION

Spermiogenesis is the last phase of spermatogenesis, where spherical spermatids differentiate into elongated spermatozoa in mammals [1,2]. Dynamic and pronounced changes occur in the process of spermiogenesis, including the formation of a condensed and elongated nucleus in the head, a well shaped acrosome flattened along the large portion of the nucleus, as well as a long flagellum. The flagellum is composed of cytoskeletal components and mitochondria provide the motors for sperm motility.

Mitochondria have a significant role in energy production, calcium homeostasis and apoptosis. Both sperm biosynthesis and motility require ATP. Recent findings indicate that two metabolic pathways are providing ATP for normal sperm function: oxidative phosphorylation in the midpiece and glycolysis in the principal piece [3-7]. Mitochondria are dynamic both in their morphological transitions and distribution. Several kinds of molecular motors have been indentified to be responsible for transporting mitochondria, including microtubule-dependent kinesins and dyneins, and microfilament-dependent myosins [8-14]. Several related proteins also function in transporting and docking of mitochondria [15]. Mitochondria provide maternal inheritance, and ubiquitination of mitochondria takes place to facilitate their degradation after fertilization [15]. Due to the indispensable role of mitochondria during fertilization, defect of sperm mitochondria or associated proteins can lead to male infertility.

In this review we mainly focus on the morphology and distribution of mitochondria, as well as the functions of this organelle during spermiogenesis. Furthermore, based on the transporting mechanisms within somatic cells, we attempt to define how mitochondria migrate to the midpiece, and to describe some related proteins that have been revealed in the mitochondria anchoring in the midpiece. Then, we review briefly about two energetic metabolisms that provide ATP for sperm motility, the ubiquitin modification during spermiogenesis, and finally talk about some mitochondria-related male infertility.

2. DISTRIBUTION AND MORPHOLOGICAL CHANGES OF MITOCHONDRIA DURING SPERMIOGENESIS

Spermiogenesis is a complicated morphogenesis occurring in the seminiferous epithelium of the testis during which the haploid spermatid is transformed into the finely shaped spermatozoon. Spermiogenesis has been divided into four phases in mammals: Golgi phase, cap phase, acrosome phase and maturation phase [1,16-19].

*Grant sponsor: National Natural Science Foundation of China, Grant number: No. 30671606 and 40776079; National Basic Research Program of China (973 Program), Grant number: No 2007CB948104.

The different stages show their own features. At the early stages of spermiogenesis (Golgi and acrosome phase), the spermatids are round; vesicles originated from the Golgi apparatus migrate towards the pole where the pre-acrosomal vesicle locates; the axoneme emerges from the distal centriole and grows actively. At the acrosome phase, the nucleus initiates to elongate and condense, the mitochondria begin to migrate to the opposite pole of the pre-acrosome. During the maturation phase, the ODFs (outer dense fibers) grow rapidly outside of the axoneme, the mitochondria begin to elongate and condense to form the mitochondrial sheath; at the same time, the acrosome is well developed, the spermatids discard most of the cytoplasm defined as the residual body to become mature spermatozoa.

The flagellum of the mammalian spermatozoon consists of four distinct regions: the connecting piece, the mid piece, the principal piece, and the short end piece. In the central part of the mid piece, the axoneme is composed of a "9 + 2" array of microtubules, nine ODFs surround the axoneme, and mitochondria are positioned in four helices along the ODFs [19-21]. The axoneme and seven ODFs surrounded by the fibrous sheath designate as the principal piece, while the end piece only includes the axoneme. During spermiogenesis, the mitochondria undergo dramatic changes both in morphology and location. In rat, the normal mitochondria with lamellar cristae are oval in shape. We observed the main events that happened during spermiogenesis in rat which supported the conclusion by De Martino *et al.* (1979) [22]. Our data show that, during the Golgi phase, cap phase and the early acrosome phase of spermiogenesis, the small, round or oval condensed mitochondria are distributed at the cell periphery, with its inner space flattened (**Figures 1** and **2**). The number of the mitochondria increases considerably. Therefore, the mitochondria are efficient to produce sufficient energy for exchanging metabolites between the adjacent Sertoli cells and spermatids or between the nucleus and the cytoplasm. The mitochondria exhibit convoluted cristae at the late acrosome phase and early maturation phase. We found that part of them move to the flagellum, whereas the remaining start to aggregate (**Figure 3**). These aggregated mitochondria are discarded within the residual bodies which are disposed by phagocytosis through the Sertoli cells or by autolysis in the mature spermatids [23]. Our data show that, at the late maturation phase, the mitochondria begin to condense and to elongate, and finally show a crescent shape along the ODFs in the mid piece (**Figures 4** and **5**). Mitochondria are supposed to generate ATP efficiently and rapidly. The length of the midpiece is similar in the same species, whereas it is obviously different among different species [24]. Possibly

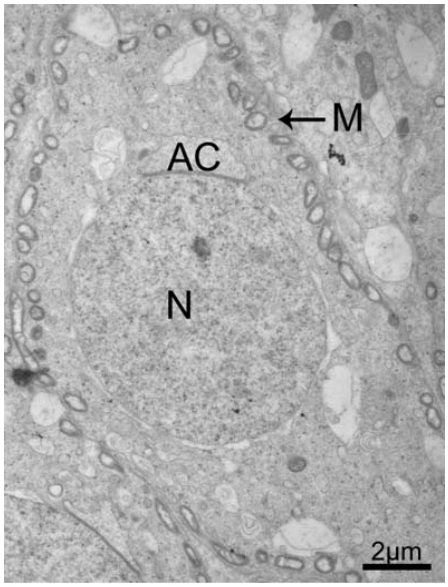

Figure 1. Mitochondria distribute at the cell periphery at the cap phase during rat spermiogenesis (black arrows in 1). M *mitochondria*, AC *acrosome*, N *nucleus*.

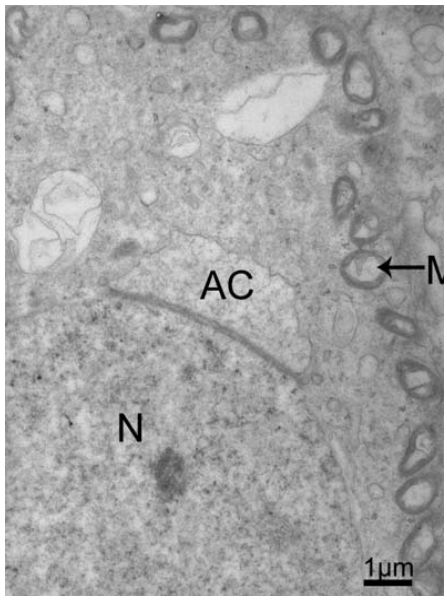

Figure 2. The magnification of partial **Figure 1**.

the whole length of the midpiece is responsible for energy supply when the fertilization process begins. A recent work by Ho *et al.* (2007) proposed a new three dimensional model to illustrate the mitochondrial arrangement in the mid piece in mouse. Initially, four dextral mitochondrial helices surround the outer dense fibers at stage 1. Subsequently, two mitochondria of the opposing arrays form circular structures at stage 2. Then, staggered mitochondria form the sinistral double helix at

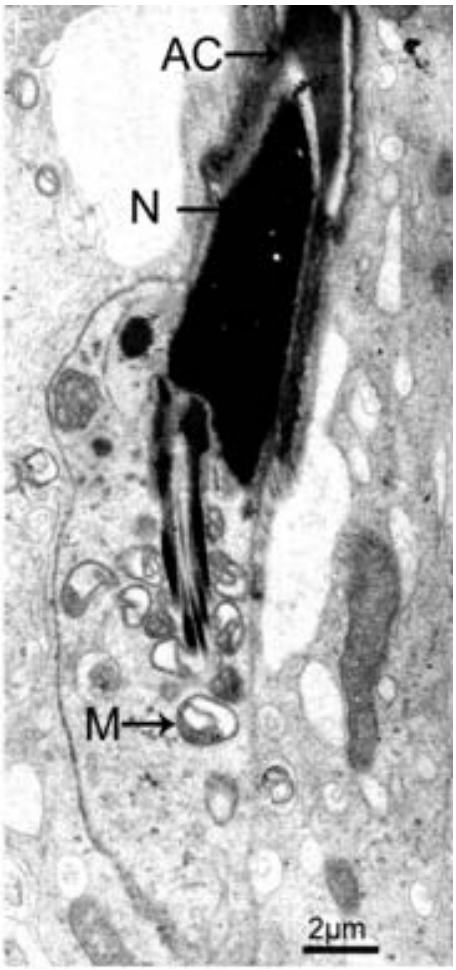

Figure 3. Part of mitochondria has been transported to the midpiece at the maturation phase.

stage 3. At the last stage, the crescent-shaped mitochondria transform to a rod-shaped form [25]. These observations provoke the question how the number, morphology and distribution of the mitochondria are controlled during spermatid differentiation.

Ultrastructure of the spermatozoa displays special features to adapt to the particular environment where fertilization takes place. In marine and freshwater animals, the spermatozoa morphology is different from mammals, exemplified by mollusk and fish.

Most of the marine bivalve mollusk spermatozoa are aquasperm, with a slightly curved or round or short-rodnucleus, a kind of species special acrosome (usually of conical shape), the midpiece consisting of one to six spherical mitochondria (four to five generally, such as *Scapharca broughtoni*, **Figures 6** and **7**) arranged in a circle that are surrounding a pair of centriole or a single large mitochondrion derived from fusion of several mitochondria, and a classical "9 + 2" flagellum [24,26-31]. Some cephalopod spermatozoa have a characteristic

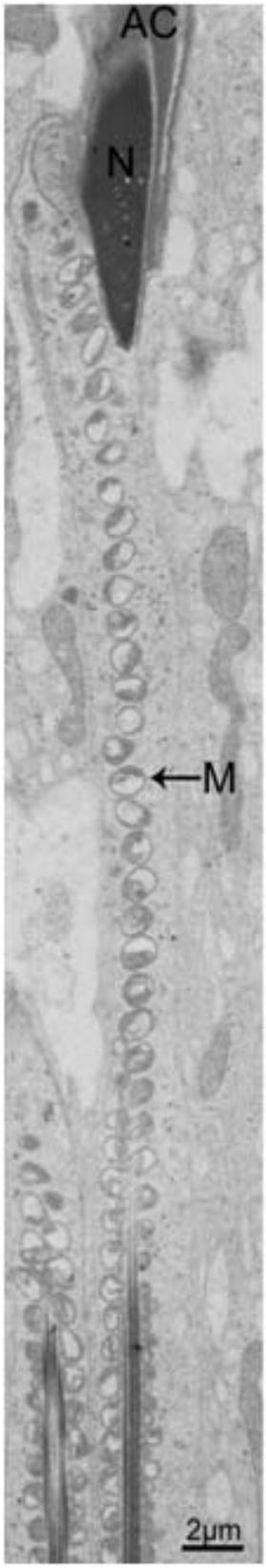

Figure 4. The mature spermatozoon of rat through head and midpiece.

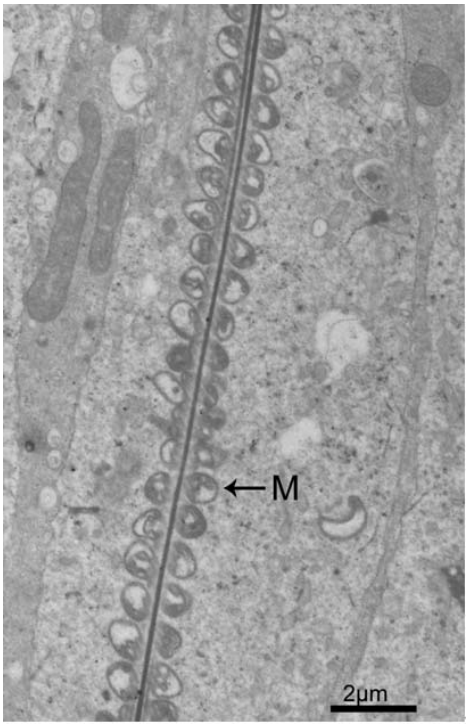

Figure 5. Mitochondrial localization in midpiece.

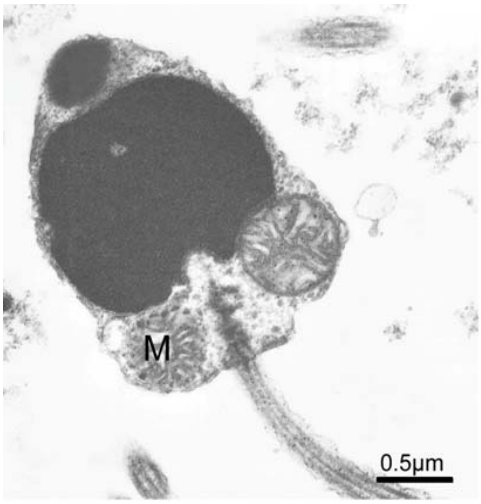

Figure 6. Typical spermatozoon of *Scapharca broughtoni*, two mitochondria visible.

acrosome with periodic and conical bands, and the mitochondrial number ranges from 9 to 11 in the midpiece, exemplified by *Octopus tankahkeei* [32-35] (**Figures 8** and **9**). Some kinds of teleostean spermatozoa belong to the aquasperm. Taking bony fish of the Perciformes as an example, their spermatozoa have a round head with a spherical nucleus, showing no acrosome, but a short midpiece with a cytoplasmic channel, and a flagellum-with typical axonemes [29,36,37]. Gusmão-Pompiani *et al.* (2005) found that in the marine teleost family Sciae-

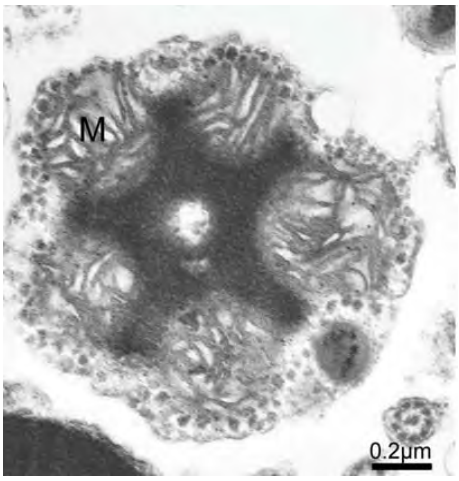

Figure 7. Cross section of midpiece in spermatozoon of *Scapharca broughtoni*, five mitochondria visible.

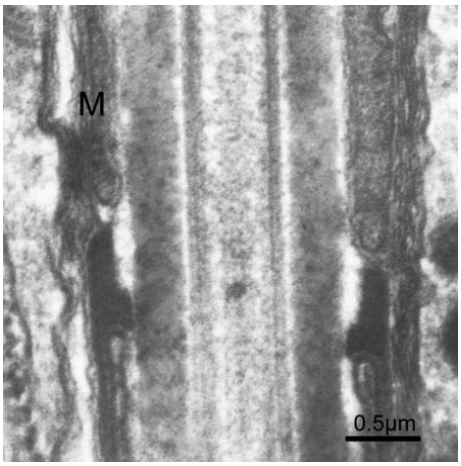

Figure 8. Joint between the midpiece and principal piece of the spermatozoon in *Octopus tankahkeei*.

nidae, there are less than ten spherical or elongate mitochondria which are located close to the nucleus and are arranged in one or two layers at the basal part of the mid piece [37]. Some exceptions exist in the Polynemidae, which are characterized by an arched nucleus surrounded by a large ring of mitochondria with a "C" shape in cross section [37]. The number of mitochondria in the midpiece in mollusks and teleostei is less prominent than in mammals.

Gage (1998) demonstrated that the flagellum length and the head length show a positive association with the mid piece length, these components may have co-evolved to provide effective fertilization [38]. The sperm swimming speed shows a positive ratio with sperm length, males with high sperm motility have higher fertilization success in mammals [39]. Mollusk and teleost employ external or internal fertilization. Sperm competition in the

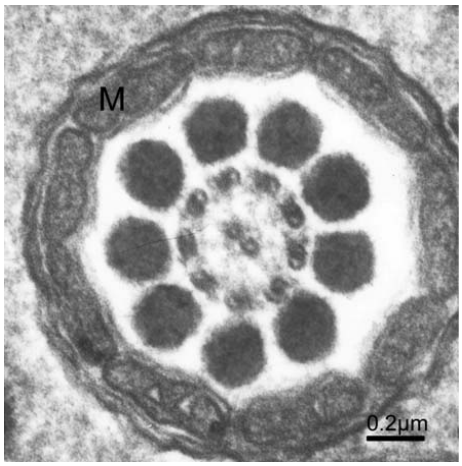

Figure 9. Cross section of the spermatozoon at the midpiece of the tail, showing 9 mitochondria.

course of external fertilization is mainly provided through the sperm number. Sperm longevity is negatively related to sperm length. Mean sperm length is shorter in free spawners compared to teleost with internal fertilization [40].

Sperm ultrastructure also reflects an adaption of the fertilization pattern to the environment. The flagellum becomes a longer mid piece containing a higher number of mitochondria and a fibrous sheath as an adaptation to internal fertilization. Such structural differences will enhance sperm motility which is necessary for successful fertilization.

3. THE TRANSPORT OF MITOCHONDRIA

The interaction between mitochondria and the cytoskeleton is essential for mitochondrial movement within cells. It was demonstrated that mitochondria move along the cytoskeleton depending on various molecular motors [12]. Different motors associate with mitochondria by docking intermediates such as adaptor proteins. Microtubule-dependent motors and actin-dependent motors are responsible for mitochondrial movement and docking. The head domain of two kinds of motors consists of a track binding site and an ATP catalytic site, on the other hand, the tail domain is responsible for recognizing and binding to diverse cargoes.

The microtubules show polarity within cells, with the minus end pointing to the centrosome and the plus end pointing to the cell periphery. Mitochondria move along the microtubule in a bidirectional manner, they usually stop and change directions under regulation to satisfy the cell metabolism. Kinesins and dyneins are microtubule dependent motors. The kinesin superfamily includes three classes of kinesins: N-terminus (KIN-N), C-terminus (KIN-C) and M-terminus (KIN-M). KIN-N moves toward the plus end of the microtubules and is responsible for anterograde transport in axons, whereas the cytoplasmic dyneins and KIN-C move to the minus end and are in charge of retrograde transport [41,42]. KIF1B and KIF5B belonging to KIN-N have been proposed to be involved in mitochondrial anterograde transport in axons [11]. KIF1B belonging to the kinesin 3 family is a monomeric motor participating in mitochondrial transport [10]. KBP (KIF1 binding protein) can regulate mitochondrial movement by increasing the motility of KIF1Bα by a mechanism that remains unknown as yet, which is clear that it does not serve as an adaptor [43]. Mitochondria aggregate around the nucleus when kif5B (a member of kinesin-1) is knocked out, which implicates that kif5B takes part in anterograde transport [9]. Various adaptors have been indentified in coupling kinesins to mitochondria, including the kinesin light chain (KLC), miro and milton complex, syntabulin, APLIP1, Miro and Grif-1 complex [44-48]. Different KLC isoforms target kinesins to different cargoes, and one type of KLC functions as an adaptor between mitochondria and kinesin-1 [44]. However, it was recently suggested that KLC is not necessary for kinesin-1 to transport mitochondria when miro-milton complexes are present in cultured cells [47]. It is therefore possible that KLC and miro-milton function together to transport mitochondria, each can substitute another when it is defective in a functional compensation mechanism. Miro anchors the mitochondria outer membrane by its tail domain, recruiting kinesin to form a functional complex in an indirect or direct manner. Glater *et al.* (2006) found that miro and milton form a complex linking mitochondria to kineisn-1 in *Drosophila*. In addition, milton also has a role in regulating the transport through diverse splicing patterns, by providing various modifications or by changing the state of miro [47]. In mammalian neurons, miro associates with Grif-1 to mediate mitochondrial motility in a signaling dependent way [48]. There are other findings in support of this. Miro contains GTP and Ca^{2+} binding domains and it functions as a linker. Miro also serves as a signal integrator and Ca^{2+} sensor, which has a role in regulating mitochondrial shape and transportation through interaction with cell signal transduction [49-51]. On the other hand, miro can bind kinesin independently [50]. Moreover, miro can prolong the process of kinesin and dynein on microtubules, by which it facilitates the mitochondria anterograde and retrograde transport [51]. Syntabulin, a membrane associated protein, acts as a kinesin-1 adaptor involved in mitochondria transport in mammalian neurons [45]. Whether syntabulin targets to mitochondria membranes directly or through other proteins requires further research. APLIP1, a kind of c-Jun N-terminal kinase (JNK) interacting protein (JIP1), has been demonstrated to affect both kinesin and dynein based mitochondria transport, maybe acting as both kinesin and

dynein linkers [46]. JNK signaling pathway possibly influences mitochondria transport by dissociating kinesin and APLIP1 or other related proteins [52].

Whether these different kinds of kinesin-adaptors work collectively to transport mitochondria, or in an individual manner by responding to different signaling pathways remain to be studied. The same holds for the molecular mechanisms that regulate motors to perform their action in the right sequence and the right place.

The main molecular motor responsible for minus-end transport along the microtubule is cytoplasmic dynein. It is involved in retrograde mitochondrial movement in axons. Dynein and dynactin form a complex to facilitate mitochondria transport [8]. In addition to control the distribution of mitochondria, dynein/dynactin complex also influence the Drp 1 recruitment to mitochondria. It takes part in the maintenance of normal mitochondrial morphology [53]. When Arp1 (a subunit of dynactin) is silent in *Drosophila* axons, the level of the kinesin heavy chain associating with the mitochondria is reduced which impair the anterograde and retrograde movement severely [54]. Conspicuously, similar to miro, dynactin has a role in coordinating bi-directional transport. However, the mechanism of dynactin function is not well understood. More interestingly, the retrograde movement of mitochondria is limited with kinesin-1 inhibition. Further experiments demonstrate that kinesin-1, dynein and dynactin form a complex to associate with the mitochondria [55]. There is also evidence that KIF5 interacts with dynein directly and specifically with KLCs. It also interacts with the dynein intermediate chain [56]. Based on these observations, it is speculated that KIF5 and dynein may serve as each other's cargo. Another possibility is that kinesin and dynein may form a complex to coordinate the bi-directional transport. It is still unknown whether they function independently to facilitate the transport in two opposite direction, or there exist other mechanisms to regulate the transport along the microtubules.

The activity of many proteins can be regulated by phosphorylation and dephosphorylation through protein kinases. Some signal pathways have been involved in mitochondria movement. Kinesins can bind to cargoes through kinesin light chains (KLC). KLC are hyperphosphorylated in the TNF signal pathway, then the phosphorylated KLC represses the activation of kinesin and leads to clusters of mitochondria around the nucleus [57]. NGF and PI3-kinase pathways also influence the mitochondrial distribution. NGF serves as a stop signal in neurons [58]. When the axons are stimulated by NGF, only the mitochondria begin to aggregate at the stimulated place [58]. Further experiments demonstrated that this process is regulated through PI 3-kinase by affecting the membrane receptors, a NGF downstream pathway [59]. The JNK pathway has been demonstrated to influence mitochondrial transport by segregating the linkers and the cargoes [46,52].

However, whether different kinesin motors are walking in the same direction and binding to the cargoes simultaneously? What is the molecular mechanism to regulate the motors activities preciously? All these remain to be studied further.

While cargoes make long range transport on microtubules, actin filaments and myosins are responsible for short range transport within cells. Myosins are actin-based molecular motors, which are fundamental in cellular transport. Their motor domain is responsible for actin binding, and the tail domain for cargo binding. In budding yeast, myo2, a member of the myosin V family, plays a major role in mitochondrial motility and morphology, the transporting and docking of mitochondria on the actin filaments without myo2 are abolished [13]. Ypt11p, a small rab GTPase, may serve as an adaptor for myo2 to bind to mitochondrial membranes [60]. Recently, a novel class myosin, myo19 has been proposed to associate with mitochondria in human [14]. It is the first myosin discovered to be involved in the transportation of mitochondria in vertebrate cells. Further characterization of more myosin candidates and linking proteins may help us to understand mitochondria transport on the microfilaments. Considering all these results, it is reasonable to assume that molecular motors work together to dispatch the mitochondria in a way that their function can optimally be performed. We propose a model for mitochondria transport in somatic cells based on the available evidence (**Figure 10**). Several aspects need to get refined. These include the interaction and regulatory mechanism among multiple adaptors, molecular motors and the mitochondria. How various motors coordinate to facilitate the transport, and how the motors are transported to the location where they become functional remain unknown.

3. TRANSPORT AND ANCHORING OF MITOCHONDRIA DURING SPERMIOGENESIS

Similar to somatic cells, mitochondria transport during spermiogenesis has not been investigated in detail. How the mitochondria are delivered to the developing sperm tail is not clear as yet. Intramanchette transport (IMT) and intraflagellar transport (IFT) are involved in the sperm head and tail development, both of which are related to molecular motors associating with cargoes that are walking along the cystoskeletal elements [61]. The manchette, a transient structure, appears when the nucleus begins to elongate and disappears when the spermatid is well formed. IMT consists of both microtubule based and F-actin based transport. Kinesin II, dynein, myosin

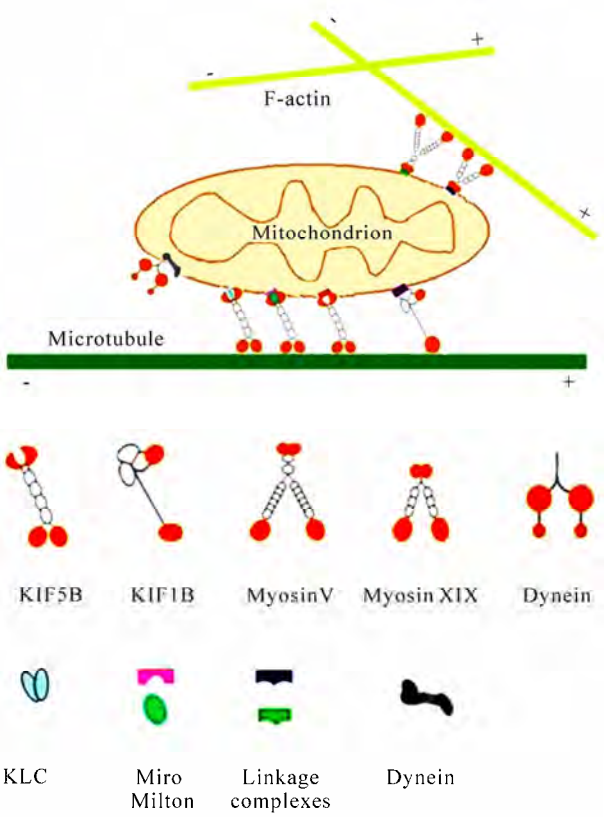

Figure 10. Diagrammatic representation of mitochondrial transport along the cystoskeletal elements in mammalian somatic cells. Motor proteins target mitochondria through special linkage complex. For instance, KIF5B associated mitochondria by KLC, Miro and Grif-1; Dynein and Dynactin form a complex to carry mitochondria. Myosin V and Myosin XIX transport mitochondria walk along the F-actin.

Va have been indentified to localize on the manchette, kinesin II is also involved in intraflagellar transport [62-66]. Further evidence supports that motors cooperate to facilitate intraflagellar transport in *Caenorhabditis elegans* [67,68]. IMT and IFT deliver materials for the tail development during spermiogenesis, thus, it is plausible to speculate that mitochondria migrate to the midpiece by IMT and IFT (**Figure 11**).

Some proteins take part in mediating mitochondria morphology and their localization has been uncovered. Nectin-2, Spergen-1 and KLC are three identified proteins that associate mitochondria to ODFs [69,70]. Nectin-2, a kind of cell adhesion molecule, localizes in the middle piece in mature spermatozoa. In nectin-2 depleted mice, the mitochondria exhibit abnormal distribution: some spermatozoa have disorganized mitochondrial sheaths, and some mitochondria dislocalize on the head [69]. Spergen-1 is only expressed in late spermiogenesis from the elongating spermatid to the mature spermatozoon. It is localized at the mitochondrial surface in the

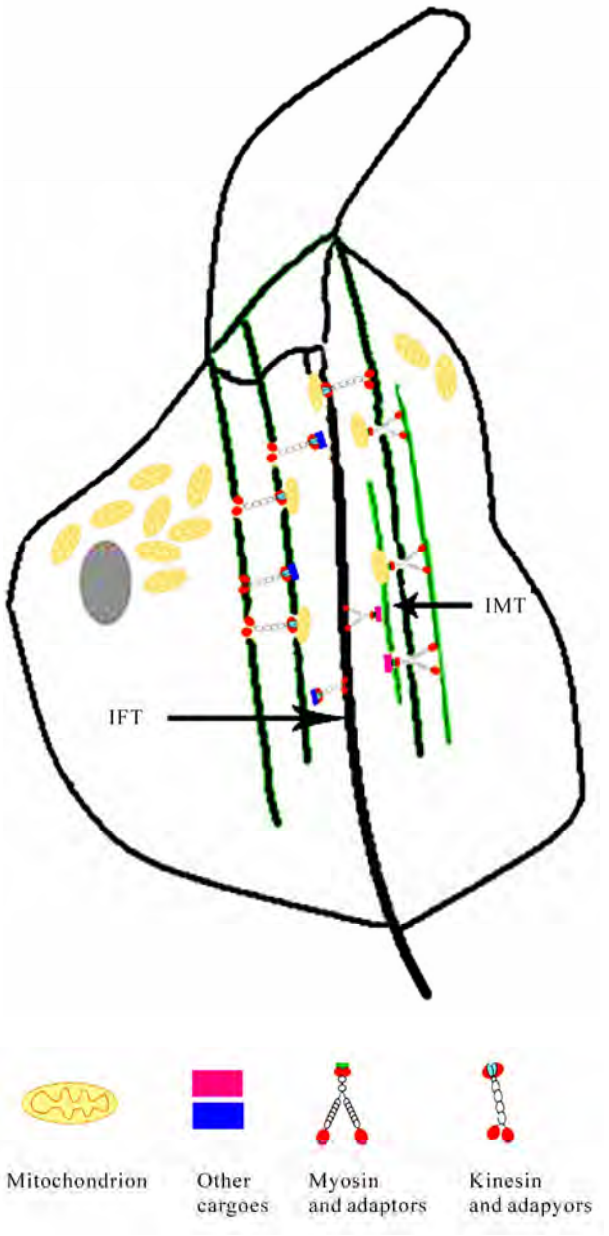

Figure 11. Diagrammatic representation about mitochondria transport at the early maturation phase in rat spermiogenesis. Kinesins and myosins work together to transport mitochondria and other cargoes to the tail through IMT and IFT.

mitochondria in cultured cells, it also contributes to couple mitochondria to ODFs during spermiogenesis [70-73]. Another spermatid specific protein is Kinesin Light Chain 3 (KLC3) and it has been found to connect to mitochondria through its TPR domain in the process of midpiece formation, more interestingly, KLC3 binds to ODFs using the HR domain in mature spermatozoa [72,73]. It is therefore possible that it links mitochondria to ODFs in a microtubule-independent way. Whether these linker proteins interact with each other or function

alone at particular time remains to be determined. In GOPC or PICK1 knock out mice, the mitochondrial sheath arranges abnormally, which is the main feature of globozoospermia [74-76]. PICK1 locates at the mitochondrial membrane and recruits PKCα implicated in phosphorylating some proteins [77]. Moreover, the PICK1/PKCα complex has been demonstrated to be involved in anti-apopotosis by affecting the Bcl2 factor [78]. In Pick1$^{-/-}$ mice, the mitochondrial sheath is abnormal, and some mitochondria migrate to the deformed nucleus, resulting in low sperm motility [76]. However, the detailed mechanism of PICK1 involved in mitochondria sheath formation is unclear. Some observations revealed that the PKCα signaling pathway may modulate the activity of motors responsible for mitochondrial movement and participate in mitochondria mediated apoptosis of the abnormal sperm. Sertoli cells produce some paracrine mitochondrial maturation factor (PMMF) such as activin and follistatin, which regulate the shape and distribution of mitochondria during spermiogenesis in a paracrine way [79]. Accordingly, the mitochondrial membrane in the midpiece contains estrogen receptor β and androgen receptors, indicating that hormones may influence the mitochondrial motility directly [80].

Further identification and characterization of related molecular motors and proteins can help us to understand more about the mechanism of spermiogenesis. Sperm cell culture and spermatogenic stem cell induction are the limiting factors, but these seem to be effective in investigating these issues.

4. SPERM MOTILITY AND ENERGETICS

Mammalian sperm need to sustain motility to reach and fertilize the egg. Mitochondrial aerobic respiration and glycolysis are two metabolic pathways to generate ATP for sperm movement and protein phosphorylation in sperm. Some evidence supports the notion that mitochondria are the only energy source for sperm motility. In mammal sperm, the overall mitochondrial volume shows a positive correlation with the flagellum length, hence, sperm motility is highly dependent on the number and size of mitochondria [4,81]. The sperm even keep their motility when the media contain no glucose or the metabolic pathway of glycolysis is inhibited [7]. The ATP being produced by mitochondria diffuse to the distal end to meet the high energy demand through shuttle mechanisms such as mediated by creatine kinase, adenylate kinase and phosphoglycerate kinase shuttles [5, 82]. However, different species may use different mechanism to deliver ATP produced by oxidative phosphorylation to the distal sperm tail.

Conversely, Malo *et al.* (2006) found that the longer the midpiece is, the slower the sperm moves; sperm motility also positively correlates with the head length and the length of the remaining tail [83]. Other mechanisms are possible to provide energy for sperm motility. Many observations reveal multiple glycolytic enzymes localized in the sperm fibrous sheath. Glycolysis contributes largely to sperm motility. In addition, glycolysis is sufficient to maintain sperm motility when oxidative phosphorylation is inhibited [5,6]. A newly developed technology combining laser and microscopic systems provides a useful tool to study the relation between sperm motility and energy metabolism [84]. With this tool, Nascimento *et al.* (2008) discovered that glycolysis provides more ATP molecules than oxidative phosphorylation to maintain sperm motility in mammals [85]. The Ca^{2+} pathway and cAMP/PKA pathway are two important ways of signal transduction involved in sperm motility control [86-88]. Some other proteins such as protease activated receptor 2, the epidermal growth factor receptor, and pathways including the PI3-K cascade mediate sperm motility [89,90].

Both mitochondrial respiration and glycolysis provide energy during spermiogenesis. Whether these two pathways are stage specific, or might compensation each other remains unclear. It also remains open for future studies to what extent the two pathways are required in different species.

5. UBIQUITINATION OF SPERM MITOCHONDRIA

Ubiquitination, a significant post-translated modification, has multiple biological effects, involved in protein degradation, endocytosis and signaling, activation of transcriptional factors, cell cycle, cell differentiation, immune responses and others [91-94]. In this process, ubiquitin or ubiquitin-like proteins target the substrate through different modifications, such as by different numbers of ubiquitin conjugated, and by various types of linkers among ubiquitins. For instance, monoubiquitin usually results in the target degradation by proteosome or lysosomes.

Mitochondria are ubiquitinated during spermiogenesis. The defective mitochondria will be degraded after ubiquination. In normal mitochondria in the midpiece, cross-linking disulfide bonds cover the ubiquitin tag so as not to be proteolyzed until fertilization, which appears to be a mechanism to maintain the mitochondrial maternal inheritance [15]. Prohibitin is a constitutive protein localized on the mitochondrial membrane in the midpiece, which serves as an ubiquitinated substrate and determines the mitochondrial destination [95]. Defective sperm exhibit high level ubiquitination of mitochondria, they are discarded during spermiogenesis or in the epididymis. Ubiquitination of sperm mitochondria is useful in indentifying sperm quality and act as a criterion for infertility diagnosis. Deep and extensive studies on sperm mitochondria ubiquitination process will provide us with a better understanding of the molecular mecha-

nisms involved, as well as develop more feasible strategies and drugs in clinical trials.

6. MITOCHONDRIA IN MALE INFERTILITY

Defects in mitochondrial transport processes, ion channels and metabolic pathways cause various diseases, such as Parkinson's and Alzheimer's disease. Asthenozoospermia defined by low sperm motility and oligospermia characterized by reduced sperm number are two main causes for male infertility. The mitochondrial sheath dysfunction is the main cause for asthenozoospermia [96].

Mitochondria produce ATP for sperm survival and fertilization. Defective mitochondria cause low sperm motility [97]. Mitochondrial DNA mutations also affect sperm motility [98]. Both point mutation and fragment deletions may lead to abnormal mitochondrial structure and function, which in turn may cause male infertility [97-101]. Quantitative conventional PCR and mutant mice models are useful in the identification of genes related to male infertility [75,102,103]. Mitochondria are a major source of reactive oxygen species (ROS) generation, leading to apoptosis, and excessive ROS is a cause of male infertility. Antioxidant compounds are beneficial to improve fertility, and may serve as preventive drugs [104]. From this point of view, we may employ genetic therapy that combined with other therapeuticas to cure diseases at their place of origin in the future.

Some chemical compounds are toxic to mitochondria and interfere with male fertility. An environmental contaminant, TCCD, induces oxidative stress, with the consequence of reduced male fertility [105]. Parabens, a kind of food preservatives, may affect mitochondrial respiration and apoptosis that is mediated by mitochondria [106]. Toxicity to mitochondria in testes may serve as a criterion for the estimation of chemical side effects in the future.

7. CONCLUSIONS AND PERSPECTIVE

Mitochondria have effects on cell metabolism, cell signaling and apoptosis. Considering this, the intracellular localization of mitochondria is a critical factor. Under related cell signal transduction and regulatory mechanisms, some molecular motors transport the mitochondria from the cell periphery to the midpiece, and then form the mitochondrial sheath consisting of four mitochondria helices in mammals. Comparing numbers, mitochondria are much less in molluscs and teleosts than in mammals, which imply an adaption to the internal fertilization. Energy for sperm motility is provided by different mechanisms in the different parts of the spermatozoon. Whereas oxidative phosphorylation takes place within mitochondria that are located in the midpiece, glycolysis takes place along the principal piece. Ubiquitination assumes the responsibility for sperm quality control and maternal inheritance. To a great extend is male infertility caused by defective sperm and low sperm motility.

Since mitochondria more and more turned out to be relevant for human health, research on mitochondria deserves increased attention. Dynamics of mitochondrial structure, motility and function during spermiogenesis have become an exciting field of research. What kinds of molecular motors are involved, how these are coordinated to transport mitochondria, how oxidative phosphorylation and glycolysis are regulated, and the underlying ubiquitination mechanisms requires to be clarified. The same holds for mitochondria related pathogenic mechanisms in human diseases. Investigating these issues provide an intriguing approach to future studies, particularly at the molecular level.

8. ACKNOWLEDGEMENTS

We are grateful to all members of the Sperm Laboratory at Zhejiang University. This work was supported by the National Natural Science Foundation of China, Grant number: No. 30671606 and 40776079; National Basic Research Program of China (973 Program), Grant number: No 2007CB948104.

REFERENCES

[1] Abou-Haila, A. and Tulsiani, D.R. (2000) Mammalian sperm acrosome: Formation, contents, and function. *Archives of Biochemistry and Biophysics*, **379(2)**, 173-182.

[2] Fawcett, D.W. (1975) The mammalian spermatozoon. *Developmental Biology*, **44(2)**, 394-436.

[3] Kamp, G., Büsselmann, G. and Lauterwein, J. (1996) Spermatozoa: Models for studying regulatory aspects of energy metabolism. *Experientia*, **52(2)**, 487-493.

[4] Ruiz-Pesini, E., Diez, C., Lapeña, A.C., Pérez-Martos, A., Montoya, J., Alvarez, E., Arenas, J. and López-Pérez, M.J. (1998) Correlation of sperm motility with mitochondrial enzymatic activities. *Clinical Chemistry*, **44(8)**, 1616-1620.

[5] Krisfalusi, M., Miki, K., Magyar, P.L. and O'Brien, D.A. (2006) Multiple glycolytic enzymes are tightly bound to the fibrous sheath of mouse spermatozoa. *Biology of Reproduction*, **75(2)**, 270-278.

[6] Molloy, P.P., Goodwin, N.B., Côté, I.M., Reynolds, J.D., Gage, M.J. Mukai, C. and Okuno, M. (2004) Glycolysis plays a major role for adenosine triphosphate supplementation in mouse sperm flagellar movement. *Biology of Reproduction*, **71(2)**, 540-547.

[7] Ford, W.C.L. (2006) Glycolysis and sperm motility: Does a spoonful of sugar help the flagellum go round? *Human Reproduction Update*, **12(3)**, 269-274.

[8] Waterman-Storer, C.M., Karki, S.B., Kuznetsov, S.A., Tabb, J.S., Weiss, D.G., Langford, G.M. and Holzbaur, E.L. (1997) The interaction between cytoplasmic dynein and dynactin is required for fast axonal transport. *Proceedings of the National Academy of Sciences*, **94(22)**, 12180-12185

[9] Tanaka, Y., Kanai, Y., Okada, Y., Nonaka, S., Takeda, S.,

Harada, A. and Hirokawa, N. (1998) Targeted disruption of mouse conventional kinesin heavy chain, *kif5b*, results in abnormal perinuclear clustering of mitochondria. *Cell*, **93(7)**, 1147-1158.

[10] Nangaku, M., Sato-Yoshitake, R., Okada, Y., Noda, Y., Takemura, R., Yamazaki, H. and Hirokawa, N. (1994) KIF1B, a novel microtubule plus end-directed monomeric motor protein for transport of mitochondria. *Cell*, **79(7)**, 1209-1220.

[11] Hirokawa, N. and Takemura, R. (2005) Molecular motors and mechanisms of directional transport in neurons. *Nature Reviews Neuroscience*, **6(3)**, 201-214.

[12] Boldogh, I.R. and Pon, L.A. (2007) Mitochondria on the move. *TRENDS in Cell Biology*, **17(10)**, 502-510.

[13] Altmann, K., Frank, M., Neumann, D., Jakobs, S. and Westermann, B. (2008) The class V myosin motor protein, myo2, plays a major role in mitochondrial motility in *Saccharomyces cerevisiae*. *The Journal of Cell Biology*, **181(1)**, 119-130.

[14] Quintero, O.A., Divito, M.M., Adikes, R.C., Kortan, M.B., Case, L.B., Lier, A.J., Panaretos, N.S., Slater, S.Q., Rengarajan, M., Feliu, M., and Cheney, R.E. (2009) Human Myo19 is a novel myosin that associates with mitochondria. *Current Biology*, **19(23)**, 2008-2013.

[15] Sutovsky, P. (2003) Ubiquitin-dependent proteolysis in mammalian spermatogenesis, fertilization, and sperm quality control: Killing three birds with one stone. *Microscopy Research and Technique*, **61(1)**, 88-102.

[16] Clermont, Y. and Leblond, C.P. (1955) Spermiogenesis of man, monkey, ram and other mammals as shown by the "periodic acid-schiff technique". *American Journal of Anatomy*, **96(2)**, 229-253.

[17] Bedford, J.M. and Nicander, L. (1971) Ultrastructural changes in the acrosome and sperm membranes during maturation of spermatozoa in the testis and epididymis of the rabbit and monkey. *Journal of Anatomy*, **108(3)**, 527-543.

[18] Clermont, Y., Oko, R. and Hermo, L. (1991) Cell biology of mammalian spermiogenesis. In: Desjardins, C. and Ewing, L.L., Ed., *Cell and Molecular Biology of the Testis*, Oxford University Press, New York, 332-376.

[19] Breed, W.G. (2004) The spermatozoon of Eurasian murine rodents: Its morphological diversity and evolution. *Journal of morphology*, **261(1)**, 52-69.

[20] Afzelius, B. (1959) Electron microscopy of the sperm tail; results obtained with a new fixative. *Journal of Biophysical and Biochemical Cytology*, **5(2)**, 269-278.

[21] Eddy, E.M., Toshimori, K. andO'Brien, D.A. (2003) Fibrous sheath of mammalian spermatozoa. *Microscopy Research and Technique*, **61(1)**, 103-115.

[22] Breucker, H., Schäfer, E. and Holstein, A.F. (1985) Morphogenesis and fate of the residual body in human spermiogenesis. *Cell and Tissue Research*, **240(2)**, 303-309.

[23] Fawcett, D.W. (1970) A comparative view of sperm ultrastructure. *Biology of Reproduction Supplement*, **2(2)**, 90-127.

[24] De Martino, C., Floridi, A., Marcante, M.L., Malorni, W., Barcellona, P.S., Bellocci, M. and Silvestrini, B. (1979) Morphological, histochemical and biochemical studies on germ cell mitochondria of normal rats. *Cell and Tissue Research*, **196(1)**, 1-22.

[25] Ho, H.C. and Wey, S. (2007) Three dimensional rendering of the mitochondrial sheath morphogenesis during mouse spermiogenesis. *Microscopy Research and Technique*, **70(8)**, 719-723.

[26] Buckland-Nicks, J. and Scheltema, A. (1995) Was internal fertilization an innovation of early bilateral evidence from sperm structure of a mollusc. *Proceedings of Biological Sciences*, **261(1360)**, 11-18.

[27] Healy, J.M., Keys, J.L. and Daddow, L.Y.M. (2000) Comparative sperm ultrastructure in pteriomorphia bivalves with special reference to phylogenetic and taxonomic implications. In Harper, E., Taylor, J.D. and Crame, J.A., Ed., *Evolutionary Biology of the Bivalvia*, Geological Society, London, Special Publications, **177**, 169-190.

[28] Gwo, J.C., Yang, W.T., Sheu, Y.T. and Cheng, H.Y. (2002) Spermatozoan morphology of four species of bivalve (Heterodonta, Veneridae) from Taiwan. *Tissue and Cell*, **34(1)**, 39-43.

[29] Gwo, J.C., Chiu, J.Y., Lin, C.Y., Su, Y. and Yu, S.L. (2005) Spermatozoan ultrastructure of four Sparidae fishes: *Acanthopagrus berda*, *Acanthopagrus australis*, *Lagodon rhomboids* and *Archosargus probatocephus*. *Tissue and Cell*, **37(2)**, 109-115.

[30] Zhu, J.Q., Dahms, H.U. and Yang, W.X. (2008) Ultrastructure of the mature spermatozoon of the bivalve *Scapharca broughtoni*. (Mollusca: Bivalvia: Arcidae). *Micron*, **39(8)**, 1205-1209.

[31] Zhu, J.Q. and Yang, W.X. (2009) Ultrastructure of the mature spermatozoon of the bivalve *Estellarca olivacea* (Mollusca: Bivalvia: Arcidae) and its phylogenetic implications. *Acta Biologica Hungarica*, **60(1)**, 27-34.

[32] Maxwell, W.L. (1975) Spermiogenesis of *Eusepia officinalis* (L.), *Loligo forbesi* (Steenstrup) and *Alloteuthits subuclata* (L.) (Cephalopoda, Decapoda). *Proceedings of Biological Sciences*, **191(1105)**, 527-535.

[33] Selmi, M.G. (1996) Spermatozoa of two Eledone species (Cephalopoda, Octopoda). *Tissue and Cell*, **28(5)**, 613-620.

[34] Zhu, J.Q., Yang, W.X., You, Z.J. and Jiao, H.F. (2005) The ultrastructure of the spermatozoon of *Octopus tankahkeei*. *Journal of Shellfish Research*, **24(4)**, 1203-1207.

[35] Roura, A., Guerra, A., González, A.F. and Pascual, S. (2010) Sperm ultrastructure in *Bathypolypus bairdii* and *B. sponsalis* (Cephalopoda, Octopoda). *Journal of Morphology*, **271(2)**, 143-151.

[36] Quagio-Grassiotto, I., Antoneli, F.N. and Oliveira, C. (2003) Spermiogenesis and sperm ultrastructure in *Cichla intermedia* with some considerations about Labroidei spermatozoa (Teleostei, Perciformes, Cichlidae). *Tissue and Cell*, **35(6)**, 441-446.

[37] Gusmão-Pompiani, P., Oliveira, C. and Quagio-Grassiotto, I. (2005) Spermatozoa ultrastructure in Sciaenidae and Polynemidae (Teleostei: Perciformes) with some consideration on Percoidei spermatozoa ultrastructure. *Tissue and Cell*, **37(3)**, 177-191.

[38] Gage, M.J. (1998) Mammalian sperm morphometry. *Proceedings of Biological Sciences/The Royal Society*, **265(1391)**, 97-103.

[39] Gomendio, M. and Roldan, E.R. (2008) Implications of diversity in sperm size and function for sperm competi-

tion and fertility. *International Journal of Developmental Biology*, **52(5-6)**, 439-447.

[40] Ball, M.A. and Parker, G.A. (1996) Sperm competition games: External fertilization and "adapative" infertility. *Journal of Theoretical Biology*, **180(2)**, 141-150.

[41] Hirokawa, N., Noda, Y. and Okada, Y. (1998) Kinesin and dynein superfamily proteins in organelle transport and cell division. *Current Opinion in Cell Biology*, **10(1)**, 60-73.

[42] Hirokawa, N. (1998) Kinesin and dynein superfamily proteins and the mechanism of organelle transport. *Science*, **279(5350)**, 519-526.

[43] Wozniak, M.J., Melzer, M., Dorner, C., Haring, H.U. and Lammers, R. (2005) The novel protein KBP regulates mitochondria localization by interaction with a kinesin-like protein. *BMC Cell Biology*, **6(1)**, 1-15.

[44] Khodjakov, A., Lizunova, E.M., Minin, A.A., Koonce, M.P. and Gyoeva, F.K. (1998) A specific light chain of kinesin associates with mitochondria in cultured cells. *Molecular Biology of the Cell*, **9(2)**, 333-343.

[45] Cai, Q., Gerwin, C. and Sheng, Z.H. (2005) Syntabulin-mediated anterograde transport of mitochondria along neuronal processes. *The Journal of Cell Biology*, **170(6)**, 959-969.

[46] Horiuchi, D., Barkus, R.V., Pilling, A.D., Gassman, A. and Saxton, W.M. (2005) APLIP1, a kinesin binding JIP-1/JNK scaffold protein, influences the axonal transport of both vesicles and mitochondria in *Drosophila*. *Current Biology*, **15(23)**, 2137-2141.

[47] Glater, E.E., Megeath, L.J., Stowers, R.S. and Schwarz, T.L. (2006) Axonal transport of mitochondria requires milton to recruit kinesin heavy chain and is light chain independent. *The Journal of Cell Biology*, **173(4)**, 545-557.

[48] MacAskill, A.F., Brickley, K., Stephenson, F.A. and Kittler, J.T. (2009) GTPase dependent recruitment of Grif-1 by Miro1 regulates mitochondrial trafficking in hippocampal neurons. *Molecular and Cellular Neuroscience*, **40(3)**, 301-312.

[49] Frederick, R.L., McCaffery, J.M., Cunningham, K.W., Okamoto, K. and Shaw, J.M. (2004) Yeast Miro GTPase, Gem1p, regulates mitochondrial morphology via a novel pathway. *The Journal of Cell Biology*, **167(1)**, 87-98.

[50] MacAskill, A.F., Rinholm, J.E., Twelvetrees, A.E., Arancibia-Carcamo, I.L., Muir, J., Fransson, A., Aspenstrom, P., Attwell, D. and Kittler, J.T. (2009) Miro1 is a calcium sensor for glutamate receptor-dependent localization of mitochondria at synapses. *Neuron*, **61(4)**, 541-55.

[51] Russo, G.J., Louie, K., Wellington, A., Macleod, G.T., Hu, F., Panchumarthi, S. and Zinsmaier, K.E. (2009) Drosophila Miro is required for both anterograde and retrograde axonal mitochondrial transport. *Journal of Neuroscience*, **29(17)**, 5443-5455.

[52] Horiuchi, D., Collins, C.A., Bhat, P, Barkus, R.V., Diantonio, A. and Saxton, W.M. (2007) Control of a kinesin-cargo linkage mechanism by JNK pathway kinases. *Current Biology*, **17(15)**, 1313-1317.

[53] Varadi, A., Johnson-Cadwell, L.I., Cirulli, V., Yoon, Y., Allan, V.J. and Rutter, G.A. (2004) Cytoplasmic dynein regulates the subcellular distribution of mitochondria by controlling the recruitment of the fission factor dynamin-related protein-1. *Journal of Cell Science*, **117(19)**, 4389-4400.

[54] Haghnia, M., Cavalli, V., Shah, S.B., Schimmelpfeng, K., Brusch, R., Yang, G., Herrera, C., Pilling, A. and Goldstein, L.S. (2007) Dynactin is required for coordinated bidirectional motility, but not for dynein membrane attachment. *Molecular Biology of the Cell*, **18(6)**, 2081-2089.

[55] Pilling, A.D., Horiuchi, D., Lively, C.M. and Saxton, W.M. (2006) Kinesin-1 and dynein are the primary motors for fast transport of mitochondria in drosophila motor axons. *Molecular Biology of the Cell*, **17(4)**, 2057-2068.

[56] Ligon, L.A., Tokito, M., Finklestein, J.M., Grossman, F.E. and Holzbaur, E.L. (2004) A direct interaction between cytoplasmic dynein and kinesin I may coordinate motor activity. *Journal of Biological Chemistry*, **279(18)**, 19201-19208.

[57] De Vos, K., Severin, F., Van Herreweghe, F., Vancompernolle, K., Goossens, V., Hyman, A. and Grooten, J. (2000) Tumor necrosis factor induces hyperphosphorylation of kinesin light chain and inhibits kinesin-mediated transport of mitochondria. *The Journal of Cell Biology*, **149(6)**, 1207-1214.

[58] Reynolds, I.J. and Rintoul, G.L. (2004) Mitochondrial stop and go: Signals that regulate organelle movement. *Science's STKE*, **2004(251)**, 46.

[59] Chada, S.R. and Hollenbeck, P.J. (2003) Mitochondrial movement and positioning in axons: The role of growth factor signaling. *The Journal of Experimental Biology*, **206(12)**, 1985-1992.

[60] Itoh, T., Watabe, A., Toh-E, A. and Matsui, Y. (2002) Complex formation with Ypt11p, a rab-Type small GTPase, is essential to facilitate the function of myo2p, a class V Myosin, in mitochondrial Ddistribution in *Saccharomyces cerevisiae*. *Molecular and Cellular Biology*, **22(22)**, 7744-7757.

[61] Kierszenbaum, A.L. (2002). Intramanchette transport (IMT): Managing the making of the spermatid head, centrosome, and tail. *Molecular Reproduction and Development*, **63(1)**, 1-4.

[62] Yoshida, T., Ioshii, S.O., Imanaka-Yoshida, K. and Izutsu, K. (1994) Association of cytoplasmic dynein with manchette microtubules and spermatid nuclear envelope during spermiogenesis in rats. *Journal of Cell Science*, **107(3)**, 625-633.

[63] Cole, D.G., Diener, D.R., Himelblau, A.L., Beech, P.L., Fuster, J.C. and Rosenbaum, J.L. (1998) Chlamydomonas kinesin-II-dependent intraflagellar transport (IFT): IFT particles contain proteins required for ciliary assembly in *Caenorhabditis elegans* sensory neurons. *The Journal of Cell Biology*, **141(4)**, 993-1008.

[64] Miller, M.G., Mulholland, D.J. and Vogl, A.W. (1999) Rat testis motor proteins associated with spermatid translocation (dynein) and spermatid flagella (kinesin-II). *Biology of Reproduction*, **60(4)**, 1047-1056.

[65] Kierszenbaum, A.L., Rivkin, .E and Tres, L.L. (2003) The actin-based motor myosin Va is a component of the acroplaxome, an acrosome-nuclear envelope junctional plate, and of manchette-associated vesicles. *Cytogenetic and Genome Research*, **103(3-4)**, 337-344.

[66] Hayasaka, S., Terada, Y., Suzuki, K., Murakawa, H., Tachibana, I., Sankai, T., Murakami, T., Yaegashi, N. and

Okamura, K. (2008) Intramanchette transport during primate spermiogenesis: expression of dynein, myosin Va, motor recruiter myosin Va, VIIa-Rab27a/b interacting protein, and Rab27b in the manchette during human and monkey spermiogenesis. *Asian Journal of Andrology*, **10(4)**, 561-568.

[67] Ou, G., Blacque, O.E., Snow, J.J., Leroux, M.R. and Scholey, J.M. (2005) Functional coordination of intraflagellar transport motors. *Nature*, **436(7050)**, 583-587.

[68] Hancock, W.O. (2008) Intracellular transport: Kinesins working together. *Current Biology*, **18(16)**, R715-17.

[69] Bouchard, M.J., Dong, Y., McDermott, B.M. Jr., Lam, D.H., Brown, K.R., Shelanski, M., Bellvé, A.R. and Racaniello, V.R. (2000) Defects in nuclear and cytoskeletal morphology and mitochondrial localization in spermatozoa of mice lacking nectin-2, a component of cell-cell adherens junctions. *Molecular and Cellular Biology*, **20(8)**, 2865-2873.

[70] Doiguchi, M., Mori, T., Toshimori, K., Shibata, Y. and Iida, H. (2002) Spergen-1 might be an adhesive molecule associated with mitochondria in the middle piece of spermatozoa. *Developmental Biology*, **252(1)**, 127-137.

[71] Doiguchi, M., Yamashita, H., Ichinose, J., Mori, T., Shibata, Y. and Iida, H. (2002) Complementary DNA cloning and characterization of rat spergen-1, a spermatogenic cell-specific gene-1, containing mitochondria-targeting signal. *Biology of Reproduction*, **66(5)**, 1462-1470.

[72] Junco, A., Bhullar, B., Tarnasky, H.A. and van der Hoorn, F.A. (2001) Kinesin light-chain KLC3 expression in testis is restricted to spermatids. *Biology of Reproduction*, **64(5)**, 1320-1330.

[73] Zhang, Y., Oko, R. and van der Hoorn, F.A. (2004) Rat kinesin light chain 3 associates with spermatid mitochondria. *Developmental Biology*, **275(1)**, 23-33.

[74] Yao, R., Ito, C., Natsume, Y., Sugitani, Y., Yamanaka, H., Kuretake, S., Yanagida, K., Sato, A., Toshimori, K. and Noda, T. (2002) Lack of acrosome formation in mice lacking a Golgi protein, GOPC, **99(17)**, 11211–11216.

[75] Escalier, D. (2006) Knockout mouse models of sperm flagellum anomalies. *Human Reproduction Update*, **12(4)**, 449-461.

[76] Xiao, N., Kam, C., Shen, C., Jin, W., Wang, J., Lee, K.M., Jiang, L. and Xia, J. (2009) PICK1 deficiency causes male infertility in mice by disrupting acrosome formation. *Journal of Clinical Investigation*, **119(4)**, 802-812.

[77] Wang, W.L., Yeh, S.F., Chang, Y.I., Hsiao, S.F., Lian, W.N., Lin, C.H., Huang, C.Y. and Lin, W.J. (2003) PICK1, an anchoring protein that specifically targets protein Kinase Cα to mitochondria selectively upon serum stimulation in NIH 3T3 cells. *The Journal of Biological Chemistry*, **278(39)**, 37705-37712.

[78] Wang, W.L., Yeh, S.F., Huang, E.Y.K., Lu, Y.L. and Wang, C.F. (2007) Mitochondrial anchoring of PKCα by PICK1 confers resistance to etoposide-induced apoptosis. *Apoptosis*, **12(10)**, 1857-1871.

[79] Meinhardt, A. and Wilhelm, B., Seitz, J. (1999) Expression of mitochondria marker proteins during spermatogenesis. *Human Reproduction Update*, **5(2)**, 108-119.

[80] Solakidi, S., Psarra, A.M., Nikolaropoulos, S. and Sekeris, C.E. (2005) Estrogen receptors α and β (ERα and ERβ) and androgen receptor (AR) in human sperm: localization of ERβ and AR in mitochondria of the midpiece. *Human Reproduction*, **20(12)**, 3481-3487.

[81] Cardullo, R.A. and Baltz, J.M. (1991) Metabolic regulation in mammalian sperm: mitochondrial volume determines sperm length and flagellar beat frequency. *Cell Motility and the Cytoskeleton*, **19(3)**, 180-188.

[82] Tombes, R.M. and Shapiro, B.M. (1985) Metabolite channeling: A phosphorylcreatine shuttle to mediate high energy phosphate transport between sperm mitochondrion and tail. Robert M. *Cell*, **41(1)**, 325-334.

[83] Malo, A.F., Gomendio, M., Garde, J., Lang-Lenton, B., Soler, A.J. and Roldan, E.R. (2006) Sperm design and sperm function. *Biology Letters*, **2(2)**, 246-249.

[84] Shi, L.Z., Nascimento, J.M., Chandsawangbhuwana, C., Botvinick, E.L. and Berns, M.W. (2008) An automatic system to study sperm motility and energetics. *Biomedical Microdevices*, **10(4)**, 573-583.

[85] Nascimento, J.M., Shi, L.Z., Tam, J., Chandsawangbhuwana, C., Durrant, B., Botvinick, E.L. and Berns, M.W. (2008) Comparison of glycolysis and oxidative phosphorylation as energy sources for mammalian sperm motility, using the combination of fluorescence imaging, laser tweezers, and real-time automated tracking and trapping. *Journal of Cellular Physiology*, **217(3)**, 745-751.

[86] Ho, H.C., Granish, K.A. and Suarez, S.S. (2002) Hyperactivated motility of bull sperm is triggered at the axoneme by Ca^{2+} and not cAMP. *Developmental Biology*, **250(1)**, 208-217.

[87] Turner, R.M. (2003) Tales from the tail: What do we really know about sperm motility? *Journal of Andrology*, **24(6)**, 790-803.

[88] Ishijima, S., Mohri, H., Overstreet, J.W. and Yudin, A.I. (2006) Hyperactivation of monkey spermatozoa is triggered by Ca^{2+} and Completed by cAMP. *Molecular Reproduction and Development*, **73(9)**, 1129-1139.

[89] Zitta, K., Albrecht, M., Weidinger, S., Mayerhofer, A. and Köhn, F. (2007) Protease activated receptor 2 and epidermal growth factor receptor are involved in the regulation of human sperm motility. *Asian Journal of Andrology*, **9(5)**, 690-696.

[90] Ashizawa, K., Omura, Y., Katayama, S., Tatemoto, H., Narumi, K. and Tsuzuki, Y. (2009) Intracellular signal transduction pathways in the regulation of fowl sperm motility: Evidence for the involvement of phosphatidylinositol 3-Kinase (PI3-K) cascade. *Molecular Reproduction and Development*, **76(7)**, 603-610.

[91] Hershko, A. and Ciechanover, A. (1998) The ubiquitin system. *Annual Review of Biochemistry*, **67**, 425-479.

[92] Ciechanover, A., Orian, A. and Schwartz, A.L. (2000) Ubiquitin-mediated proteolysis: Biological regulation via destruction. *Bioessays*, **22(5)**, 442-451.

[93] Ciechanover, A. and Iwai, K. (2004) The ubiquitin system: From basic mechanisms to the patient bed. *IUBMB Life*, **56(5)**, 193-201.

[94] Mukhopadhyay, D. and Riezman, H. (2007) Proteosome-independent functions of ubiquitin in endocytosis and signaling. *Science*, **315(5809)**, 201-205.

[95] Thompson, W.E., Ramalho-Santos, J. and Sutovsky, P. (2003) Ubiquitination of prohibitin in mammalian sperm mitochondria: Possible roles in the regulation of mitochondrial inheritance and sperm quality control. *Biology of Reproduction*, **69(1)**, 254-260.

[96] Mundy, A.J., Ryder, T.A. and Edmonds, D.K. (1995) Asthenozoospermia and the human sperm mid-piece. *Human Reproduction*, **10(1)**, 116-119.

[97] Folgerq, T., Bertheussen, K., Lindal, S., Torbergsen, T. and Oian, P. (1993) Mitochondrial disease and reduced sperm motility. *Human Reproduction*, **8(11)**, 1863-1868.

[98] Spiropoulos, J., Turnbull, D.M. and Chinnery, P.F. (2002) Can mitochondrial DNA mutations cause sperm dysfunction? *Molecular Human Reproduction*, **8(8)**, 719-721.

[99] St John, J.C., Jokhi, R.P. and Barratt, C.L. (2005) The impact of mitochondrial genetics on male infertility. *International Journal of Andrology*, **28(2)**, 65-73.

[100] Shamsi, M.B., Kumar, R., Bhatt, A., Bamezai, R.N., Kumar, R., Gupta, N.P., Das, T.K. and Dada, R. (2008) Mitochondria DNA mutations in etiopathogenesis of male infertility. *Indian Journal of Urology*, **24(2)**, 150-154.

[101] St John, J.C., Sakkas, D. and Barratt, C.L. (2000) A role for mitochondrial DNA and sperm survival. *Journal of Andrology*, **21(2)**, 189-199.

[102] Yan, W. (2009) Male infertility caused by spermiogenic defects: Lessons from gene knockouts. *Molecular and Cellular Endocrinology*, **306(1-2)**, 24-32.

[103] St John, J.C., Jokhi, R.P. and Barratt, C.L. (2001) Men with oligoasthenoteratozoospermia harbour higher numbers of multiple mitochondrial DNA deletions in their spermatozoa, but individual deletions are not indicative of overall aetiology. *Molecular Human Reproduction*, **7(1)**, 103-111.

[104] Lanzafame, F.M., La Vignera, S., Vicari, E. and Calogero, A.E. (2009) Oxidative stress and medical antioxidant treatment in male infertility. *Reproductive Biomedicine Online*, **19(5)**, 638-659.

[105] Latchoumycandane, C., Chitra, K.C. and Mathur, P.P. (2002). The effect of 2, 3, 7, 8-tetrachlorodibenzo-p-dioxin on the antioxidant system in mitochondrial and microsomal fractions of rat testis. *Toxicology*, **171(2-3)**, 127-135.

[106] Tavares, R.S., Martins, F.C., Oliveira, P.J., Ramalho-Santos, J. and Peixoto, F.P. (2008) Parabens in male infertility—Is there a mitochondrial connection? *Reproductive Toxicology*, **27(1)**, 1-7.

Advances in Bioscience and Biotechnology, 2010, 1, 110-114 **ABB**
doi:10.4236/abb.2010.12015 Published Online June 2010 (http://www.SciRP.org/journal/abb/)

A study of aqueous humour proteins in patients of primary open angle glaucoma

Meena Zaidi[1*], Azra Jilani[1], Padmawati Bhattacharya[1], Najmul Islam[2], Shahid Alam[1]

[1]Institute of Ophthalmology, JawaharLal Nehru Medical College, Aligarh Muslim University, Aligarh, India;
[2]Department of Biochemistry, JawaharLal Nehru Medical College, Aligarh Muslim University, Aligarh, India.
Email: meenazaidi@rediffmail.com

Received 15 March 2010; revised 7 April 2010; accepted 9 April 2010.

ABSTRACT

Aims: To investigate the changes in the protein composition of aqueous humour in primary open angle glaucoma patients and non-glaucomatous subjects. Patients and Methods: Case control study was conducted at a university hospital to compare the protein profile of aqueous humour obtained from patients of primary open angle glaucoma with those of non-glaucomatous subjects. Protein concentration of the aqueous humour samples collected from both glaucomatous and non-glaucomatous patients at the time of surgery was estimated by the Bradford protein assay method. Sodium dodecylsulfate polyacrylamide gel electrophoresis of the samples was also performed. Results: Geometric mean of protein concentration of the samples was 55.73 mg/dl (range: 31-72) in the test group and 46.46 mg/dl (range: 27-65) in the control group and a statistically significant ($p \leq 0.001$) difference in protein concentration of aqueous humour between the two groups was observed. Electrophoretic study revealed differences in the aqueous protein composition of the two groups. The glaucomatous group exhibited protein bands of 10 kDa, 20 kDa, 30 kDa, 50 kDa, 60 kDa, 70 kDa, and 90 kDa while the control subjects demonstrated bands of 6 kDa, 10 kDa, 30 kDa, 70 kDa, 90 kDa. Interestingly, almost all the proteins detected in this study corresponded to the molecular weights of heat shock proteins. Conclusions: Primary open angle glaucoma patients differed in protein compositions and had higher concentration of aqueous humour proteins than non-glaucomatous patients.

Keywords: Aqueous Humour; Open Angle Glaucoma; Proteins

1. INTRODUCTION

Adult-onset primary open-angle glaucoma (POAG) is the most common form of glaucoma, usually manifesting itself after the age of 40 years. The prevalence of POAG is about 1-2% over age 40 years in white populations and 3-4 times greater in black populations of the same age [1]. Recent projections estimate that worldwide, 60.5 million people will suffer from some form of glaucoma by 2010, with primary open angle glaucoma (POAG) accounting for about 74% of cases [2].

Unfortunately, despite the magnitude of the problem, the accurate etiopathogenesis of this silent stealer of sight still remains a mystery. Compared to other forms of glaucoma, the optic neuropathy of POAG is multifactorial, with IOP, being the most important risk factor [3]. It is also the only risk factor that is therapeutically modifiable.

It is generally believed that like all other forms of glaucoma, it is ultimately a mechanical blockade of aqueous outflow that increase IOP of POAG. But the exact cause or site of this blockade is yet to be definitely determined. However, a change in the composition of aqueous humor prevents its smooth outflow. Normally, aqueous humour has 0.02% protein (20 mg/dl) as compared with 7% reported in plasma. In a study, the total protein concentration in primary open-angle glaucoma aqueous humour was approximately two times higher than that in non-glaucomatous subjects [4]. The most abundant protein identified in aqueous humour is albumin (50% of all the protein content) and transferrin, when analysed by high performance gel filtration chromatography (HPGFC) [5] or by crossed immune-electrophoresis [6] or SDS-PAGE [7]. However, biochemical investigation of the aqueous, considering such aspect in the various forms of open angle glaucoma, has so far received relatively little attention. Due to lack of sufficient information on the role of proteins involved in the pathogenesis of open angle glaucoma (especially POAG), the present study was undertaken to assess the changes in the protein composition of aqueous humour of primary open angle glaucoma and to compare it with those of non-glaucomatous patients. A better understanding of the mechanism of POAG is likely to lead to more effective treatment of this disease.

2. PATIENTS AND METHODS

This was a case-control study conducted at a university hospital of Aligarh Muslim University, India, between November 2007 to September 2008. An informed written consent was obtained from all the chosen patients following the guidelines of Helsinki Declaration. The patients were divided into two groups – (Group I) TEST group included patients above 50 years old with established cases of primary open angle glaucoma undergoing trabeculectomy due to uncontrolled intraocular pressure with optimal medical therapy. The diagnostic criteria for primary open-angle glaucoma were: 1) presence of glaucomatous optic disc damage 2) corresponding glaucomatous changes in the visual field 3) open angle of anterior chamber 4) absence of alternative causes of optic neuropathy (e.g., infection, inflammation, meningeal disease, ischemic disease, and compressive lesions) and 5) no features of secondary glaucomas. Group II (Control group) included, age matched patients of senile cataract, without any evidence of glaucoma, undergoing cataract surgery. The following criteria were used for exclusion for both groups: 1) evidence of ocular surgery including laser within 6 months 2) evidence of intraocular inflamemation 3) complicated cataract 4) history of uveitis 5) history of ocular trauma and 6) diabetic retinopathy.

2.1. Sample Collection

Aqueous humour samples were collected at the beginning of the surgery, before entering the anterior chamber. A 0.1ml aqueous humour fluid was removed from the anterior chamber under sterile conditions using a tuberculin syringe and stored in microtubes at −20˚C until analysis. All surgical procedures were performed by experienced ophthalmic surgeons. The protein contents in the aqueous humor were estimated following the method of Bradford [8]. The molecular weight of proteins in aqueous humour of the test and control samples were analyzed by sodium dodecylsulfate polyacrylamide gel electrophoresis (SDS-PAGE).

3. RESULTS

The geometric mean of total protein concentration of the aqueous humor samples was 55.73 mg/dl (ranging from 31 to72 mg/dl) in the POAG group and 46.46 mg/dl (ranging from 27 to 65 mg/dl) in the control group. The difference in the protein contents of the two groups was statistically significant ($p \leq 0.001$). Furthermore, a remarkable difference in the electrophoretic patterns of the protein in aqueous humour of the two groups was observed when analysed by sodium dodecyl sulfate polyacrylamide gel electrophoresis (SDS-PAGE). Seven well defined protein bands of molecular weight 10 kDa, 20 kDa, 30 kDa, 50 kDa, 60 kDa, 70 kDa, 90 kDa were detected in the POAG group (**Figure 1**). In contrast, the control group exhibited fewer protein bands whose molecular weights were 10 kDa, 30 kDa, 70 kDa, 90 kDa. Thus, in this study, the 20 kDa, 50 kDa and 60 kDa proteins were detected only in the samples collected from the patients suffering from POAG. The 70 kDa protein

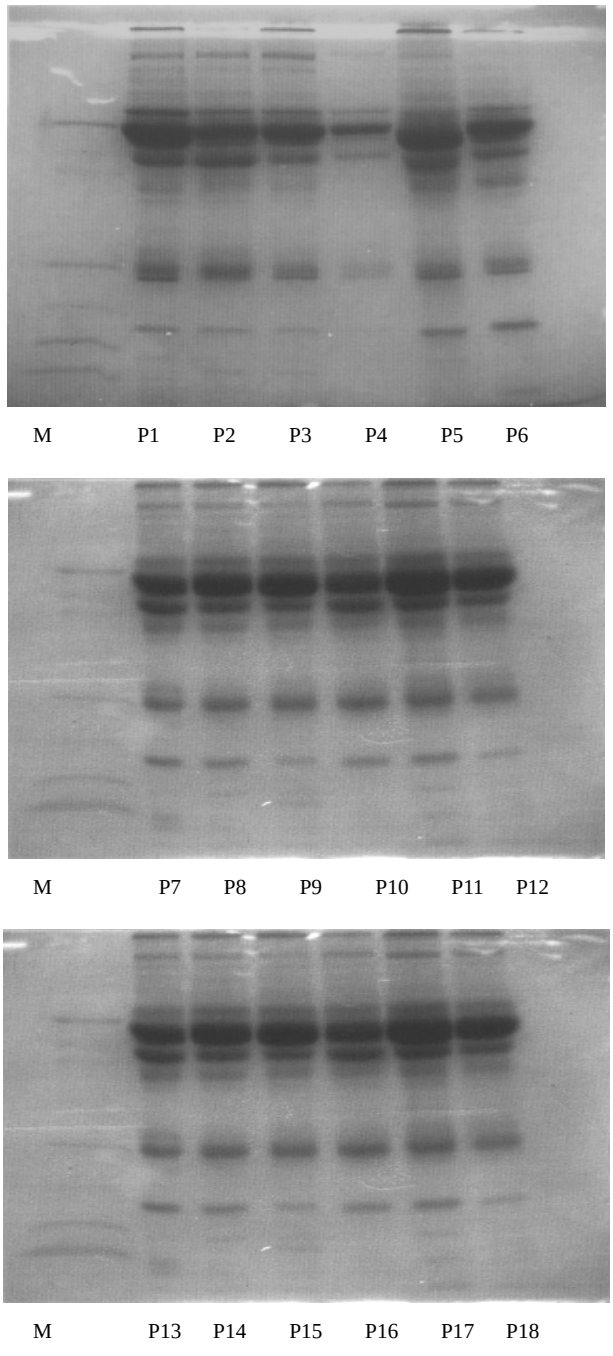

Figure 1. SDS-PAGE of protein lysates in aqueous humour of POAG group. Lanes P1 to P18 represents patient samples while lane M represents standard molecular weight marker.

though detected in both the groups, it exhibited a suppressed expression on gel in the controls relative to the POAG group. Among the POAG group samples, 24 had a higher magnitude expression while two showed only appreciable magnitude expression. On the contrary, proteins of varying molecular weight between 71-90 kDa were over expressed and densely stained in controls and, hence, finer resolution into separate molecular weights was not possible.

Another interesting observation of this study was the expression of a 60 kDa protein in aqueous humour samples of POAG patients which was not detected in control samples. However, except for two cases, 92.3% of the total POAG group samples demonstrated a low magnitude expression of 60kDa protein. Of the 26 POAG group samples, 84.6% (22 samples) showed low magnitude expression of 50kDa proteins whereas aqueous humour of controls showed no such protein bands during SDS-PAGE analysis. Generally, the 30kDa protein, like the 70 kDa protein, was detected in all samples of both the POAG and control samples. Of the total 26 POAG samples, 80.76% (21 samples) displayed low magnitude expression of 20 kDa protein, but none of the control samples showed the protein of such molecular weight. Though, the 10 kDa protein was expressed in the samples of each group, 60 kDa protein was recorded only in one control sample.

4. DISCUSSION

Outflow facility is reported to be significantly reduced in patients with uveitis who have high aquous humour protein level. Such elevated aqueous humour protein level in turn, leads to the development of glaucoma by decreasing aqueous humour outflow facility [9]. Therefore, we analyzed and compared the concentration of total proteins in both glaucomatous and non-glaucomatous patients. In our SDS-PAGE analysis of the test sample, we found that not only the total aqueous protein concentration increased in POAG, but also the aqueous protein composition differs from non-POAG eyes. The differences in protein concentrations in POAG patients cannot be attributed to the drug because increase in protein concentration in aquous humor is reported only in topical application of timilol and is not reported by other topical anti-glaucoma drugs. Further, the increase in protein concentration is not due to increase in protein production but is due to reduced concentration of aquous humor. So, this is not likely to alter the chemical composition of protein in aquous humor [10,11]. Furthermore, increase in the total concentration of proteins in aqueous humor after oral administration of 500 mg of acetazolamide has also been reported [12]. The effect of this drug on the protein concentrations of the POAG patients, who were using it, can be ruled out because two dosage of acetazolamide is routinely administered as pre-operative medication before cataract surgery at our centre.

In other study, the PG analogues though induced MMPs but the molecular weight of protein observed in our study was smaller than those reported for PG induced proteins in the ciliary body [13]. However, unlike the findings of Herschler *et al.* [14] or Lee *et al.* [15] we did not record any high molecular proteins in the aqueous humor obtained from patients of primary open angle glaucoma. Interestingly, almost all the proteins detected in this study had molecular weights corresponding to the heat shock proteins (Hsp). Synthesis of such heat shock proteins has been found *in vivo* and in organ cultures of several mammalian tissues which were subjected to heat shock or other forms of stress [16,17]. Heat shock proteins act as protective proteins and aid in maintaining cellular homeostasis under environmental stress [18-20]. Some of the common stressors include heat shock, ischemia, oxidative stress, pH extremes, nutrient limitation, osmotic variation, hypoxia etc. Of the various heat shock proteins, Hsp 70 is normally produced by the epithelial cells of the natural lens and retinal ganglion cells even in unstressed conditions. However, heat shock proteins can be expressed constitutively or be induced but its production is reported to be increased by cellular stress [21]. This may be the reason a 70kDa protein was though observed in both POAG and control groups, but it was over expressed in the POAG group only. The 60 kDa protein noticed in 92.3% of the POAG samples was not found in any of the samples collected from controls subjects. In similar studies, Tripathi [22] reported a 60 kDa protein in aqueous humor of cataract cases while serum auto antibodies to Hsp 60 in various open angle glaucomas, including POAG is also reported [23]. Increased expression of Hsp 60 has been observed in retina and optic nerve head in human donor eyes with glaucoma [24].

The kDa 50 fraction was the only protein expressed in the study samples whose molecular weight does not correspond to a heat shock protein. Plasminogen activator inhibitor1(PAI-1), an approximately 50 kDa, inducible protein has been reported to be increased in aqueous humor of open angle glaucoma patients by Dan *et al.* [25]. The tPA and uPA, the target enzymes for PAI-1, were previously detected in the human aqueous humour [26,27]. Previously it was roughly estimated that most of the tPA was complexed with PAI-1, with only a small free fraction available for proteolysis [27]. Thus, the equilibrium may normally be shifted, perhaps delicately, toward fibrinolysis and proteolysis, which could be involved in the maintenance of aqueous outflow. Our results suggest that this situation may be reversed in patients with glaucoma owing to the increase in PAI-1 level in the aqueous humor. However, our study did not specifically identify this 50kDa fraction. Moreover, none of the controls exhibited this fraction, a finding which is at

variance with other studies.

Small heat shock proteins (sHsps) are a large family of proteins with monomeric molecular weight of 12-43 kDa. Unlike the high molecular weight Hsps, which are involved in protein folding *in vivo*, under normal conditions, sHsps play an important role in protecting organism from stress. Such small heat shock proteins are reported to share an evolutionarily conserved sequence of 80-100 amino acids, located in the C-terminal region, called the alpha-crystallin [28]. Tamm *et al.* [20] have demonstrated that both monkey and human TM cell cultures stressed by heat shock, exhibited a significant increase in alpha B-crystallin mRNA. In this context, it must be emphasised that the cellular consequences of heat and ischemia are similar. Albumin, the major aqueous humor protein, acts as a escort through the trabecular meshwork in mammalian eyes, and interacts with alpha-crystallin up to the critical micelle concentration for alpha-crystallin (3.5-5 mg/ml or 0.18-0.25 mM) as reported by Doss *et al.* [29]. There is little in- teraction at or above this concentration. This binding could serve the necessary function of preventing interactions between alpha–crystallin monomers or small aggregates and hydrophobic surfaces within the trabecular meshwork. However, since the interaction between the two proteins is not very strong, the accumulation of unbound monomers/dimers of alpha–crystallin could contribute to the development of primary open angle glaucoma.

Assuming that the 20 kDa protein detected in POAG cases in our study is Hsp 20, we would like to take this hypothesis forward. What we propose is that glaucoma causes conditions of stress, which results in over expression of alpha-crystallin by the trabecular meshwork. This increased production of alpha-crystallin, overwhelms the capacity of albumin to escort it through the trabecular meshwork. This results in excess being secreted into the aqueous humor, and consequent blockade by alpha-crystallin monomers/dimer. This hypothesis is also in agreement with the observations of others [30,31]. After *in vitro* studies they concluded that the filter blocking process involves two interacting classes of blocking components, which when present simultaneously in aqueous humor, bind hydrophobically to the filtering surface. Based on these observations, it was suggested that one of the members could be albumin, the dominant protein of aqueous humor. Filtration blockage would also require a second component leading to the synthesis of 20 kDa protein as observed in our study.

In conclusion, our study revealed that primary open angle glaucoma patients had higher concentration of aqueous humor proteins than controls and that the protein composition of the aqueous humor samples was different from the normal ones. Furthermore, various protein bands detected by SDS-PAGE needs to be qualified and to establish that 20 kDa protein is indeed an alpha-crystallin. Small molecular weight aqueous humor proteins and trabecular meshwork immunohistochemistry needs further investigation to determine the etiopathogenesis of primary open angle glaucoma. Our study provides an early marker in this direction.

REFERENCES

[1] Sommer, A., Tielsch, J.M., Katz, J., *et al*. (1991) Relationship between intraocular pressure and primary open angle glaucoma among white and black patients: the Baltimore Eye Survey. *Archives of Ophthalmology*, **109(8)**, 1090-1095.

[2] Quigley, H.A. and Broman, A.T. (2006) The number of people with glaucoma worldwide in 2010 and 2020. *British Journal of Ophthalmology*, **90(3)**, 262-267.

[3] Quigley, H.A. (1996) Number of people with glaucoma worldwide. *British Journal of Ophthalmology*, **80(5)**, 389-393.

[4] Prata, T.S., Navajos, E.V., Melo, L.A., Jr., *et al*. (2007) Aqueous humor protein concentration in patients with primary open angle glaucoma under clinical treatment. *Arquivos Brasileiros de Oftalmologia*, **70(2)**, 217.

[5] Saari, K.M., Aine, E. and Parvianen, M. (1983) Determination of protein content in aqueous humour by high-performance gel filtration chromatography. *Acta Ophthalmologia* (*Copenh*), **61(4)**, 611-617.

[6] Inada, K., Muarata, T., Baba, H., *et al*. (1988) Increase of aqueous humor proteins with aging. *Japanese Journal of Ophthalmology*, **32(2)**, 126-131.

[7] Tripathi, R.C., Millard, C.B. and Tripathi, B.J. (1989) Protein composition of human aqueous humor: SDS-PAGE analysis of surgical and post-mortem samples. *Experimental Eye Research*, **48(1)**, 117-130.

[8] Bradford, M.M. (1976) A rapid and sensitive method for the quantitation of microgram quantitites of protein utilizing the principle of protein-dye binding. *Analytical Biochemistry*, **72(1-2)**, 248-254.

[9] Ladas, J.G., Fei, Y., Loo, R., *et al*. (2001) Relationship between aqueous humour protein level and outflow facility in patients with uveitis. *Investigative Ophthalmology and Visual Science*, **42(11)**, 2584-2588.

[10] Stur, M., Grabner, G., Huber-Spitzy, V., Schreiner, J. and Haddad, R. (1986) Effect of timolol on aqueous humor protein concentration in the human eye. *Archives of Ophthalmology*, **104(6)**, 899-900.

[11] Beardsley, T.L. and Shields, M.B. (1983) Effect of timolol on aqueous humor protein concentration in humans. *American Journal of Ophthalmology*, **95(4)**, 448-450.

[12] Oshika, T. and Araie, M. (1990) Time course of changes in aqueous protein concentration and flow rate after oral acetazolamide. *Investigative Ophthalmology and Visual Science*, **31(3)**, 527-534.

[13] Shahid, H., Farahdiba, J. and Crosson, C.E. (2005). Acute effects of $PGF_{2\alpha}$ on MMP-2 secretion from human ciliary muscle cells: A PKC- and ERK-dependent process. *Investigative Ophthalmology and Visual Science*, **46(5)**, 1706-1713.

[14] Herschler, J. and Litin, B.S. (1987) Biochemical abnormalities in the aqueous in chronic open angle glaucoma. *Ophthalmic Surgery*, **18(11)**, 792-795.

[15] Lee, I.S., Yu, Y.S., Kim, D.M., *et al*. (1990) Detection of specific proteins in the aqueous humor in primary open angle glaucoma. *Korean Journal of Ophthalmology*, **4(1)**, 1-4.

[16] Bagchi, M., Katar, M. and Maisel, H. (2002) Effect of exogenous stress on the tissue-cultured mouse lens epithelial cells. *Journal of Cell Biochemistry*, **86(2)**, 302-306.

[17] Banh, A., Vijayan, M.M. and Sivak, J.G. (2003) Hsp70 in bovine lenses during temperature stress. *Molecular Vision*, **9,** 323-328.

[18] Barbe, M.F., Tytell, M., Gower, D.J. and Welch, W.J. (1988) Hyperthermia protects against light damage in the rat retina. *Science*, **241(4874)**, 1817-1820.

[19] Tanaka, Y., Kobayashi, K., Kita, M., *et al*. (1996) Expression of 47 kDa heat shock protein (Hsp47) during development of mouse cornea. *Experimental Eye Research*, **63(4)**, 383-393.

[20] Tamm, E.R., Russell, P., Johnson, D.H. and Piatigorsky, J. (1996) Human and monkey trabecular meshwork accumulate alpha B-crystallin in response to heat shock and oxidative stress. *Investigative Ophthalmology and Visual Science*, **37(12)**, 2402-2413.

[21] Yao, K., Rao, H., Wu, R., *et al*. (2006) Expression of Hsp70 and Hsp27 in lens epithelial cells in contused eye of rat modulated by thermotolerance or quercetin. *Molecular Vision*, **12**, 445-450.

[22] Tripathi, R.C., Borisuth, N.S., Tripathi, B.J., *et al*. (1992) Quantitative and qualitative analysis of transferrin in aqueous humor from patients with primary and secondary glaucoma. *Investigative Ophthalmology and Visual Science*, **33(10)**, 2866-2873.

[23] Wax, M. (2001) Serum autoantibodies to heat shock proteins in glaucoma patients from Japan and the United States. *Ophthalmology*, **108(2)**, 296-302.

[24] Tezel, G., Hernandez, R. and Wax, M.B. (2000) Immunostaining of heat shock proteins in the retina and optic nerve head of normal and glaucomatous eyes. *Archives of Ophthalmology*, **118(4)**, 511-518.

[25] Dan, J., Belyea, D., Gertner, G., *et al*. (2005) Plasminogen activator inhibitor-1 in the aqueous humor of patients with and without glaucoma. *Archives of Ophthalmology*, **123(2)**, 220-224.

[26] Wang, Y., Taylor, D.M., Smalley, D.M., Cone, R.E. and O'Rourke, J. (1994) Increased basal levels of free plasminogen activator found in human aqueous humor. *Investigative Ophthalmology and Visual Science*, **35(9)**, 3561-3566.

[27] Bernatchez, S.F., Tabatabay, C. and Belin, D. (1992) Urokinase-type plasminogen activator in human aqueous humor. *Investigative Ophthalmology and Visual Science*, **33(9)**, 2687-2692.

[28] Lee, S., Carson, K., Rice-Ficht, A. and Good, T. (2005) Hsp20, a novel α-crystallin, prevents A β fibril formation and toxicity. *Protein Science*, **14(3)**, 593-601.

[29] Doss, E.W., Ward, K.A. and Koretz, J.F. (1998) Investigation of the “fines” hypothesis of primary open angle glaucoma: The possible role of alpha-crystallin. *Ophthalmic Research*, **30(3)**, 142-156.

[30] Ethier, C.R., Kamm, R.D., Johnson, M., *et al*. (1989) Further studies on the flow of aqueous humor through microporous filters. *Investigative Ophthalmology and Visual Science*, **30(4)**, 739-746.

[31] Pavao, A.F., Lee, D.A., Ethier, C.R., *et al*. (1989) Two-dimensional gel electrophoresis of calf aqueous humor, serum, and filter-bound proteins. *Investigative Ophthalmology and Visual Science*, **30(4)**, 731-738.

Advances in Bioscience and Biotechnology, 2010, 1, 115-121 **ABB**
doi:10.4236/abb.2010.12016 Published Online June 2010 (http://www.SciRP.org/journal/abb/)

Optimization of media constituents for the production of lipase in solid state fermentation by *Yarrowia lipolytica* from palm Kernal cake (*Elaeis guineensis*)

Sarat Babu Imandi[1,2], Sita Kumari Karanam[1,3], Hanumantha Rao Garapati[1,4]

[1]Center for Biotechnology, Department of Chemical Engineering, College of Engineering, Andhra University, Visakhapatnam, India;
[2]Department of Biotechnology, GITAM Institute of Technology, GITAM University, Gandhinagar, Rushikonda, Visakhapatnam, India;
[3]M.R.College of Pharmacy, Phool Baugh, Vizianagaram, India;
[4]Department of Biotechnology, Anil Neerukonda Institute of Technology and Sciences (ANITS), Sangivalasa, Bheemunipatnam, Visakhapatnam, India.
Email: saratbabuimandi@gmail.com; saratbabu_imandi@yahoo.com; sitakaranam@gmail.com; ghrao77@gmail.com

Received 9 March 2010; revised 20 March 2010; accepted 21 March 2010.

ABSTRACT

The production of extra cellular lipase in Solid State Fermentation (SSF) using *Yarrowia lipolytica* NCIM 3589 with Palm Kernal cake (*Elaeis guineensis*) has been studied. Different parameters such as incubation time, inoculum level, initial moisture content, carbon level and nitrogen level of the medium were optimized. Screening of various process variables has been accomplished with the help of Plackett-Burman design. The maximum lipase activity of 18.58 units per gram of dry fermented substrate (U/gds) was observed with the substrate of Palm Kernal cake in four days of fermentation.

Keywords: Lipase; Palm Kernal Cake; Optimization; Plackett-Burman Design; *Yarrowia Lipolytica*

1. INTRODUCTION

Lipases (triacylglycerol acylhydrolases, EC 3.1.1.3) are one of the most important classes of industrial enzymes. They hydrolyse triglycerides into diglycerides, monoglycerides, glycerol and fatty acids. In recent years, there has been an increasing interest in the study of lipases mainly due to their potential applications as medicines (digestive enzymes), food additives (flavour modifying enzymes), clinical reagents (glyceride-hydrolysing enzymes) and cleaners (detergent additives) [1]. Additionally, a promising application field for lipases is in the biodegradation of plastics such as polyhydroxyalkanoates (PHA) and polycaprolactone (PCL) [2,3]. Lipases would be economically manufactured in solid state fermentation.

Solid state fermentation (SSF) is defined as the fermentation of solids in the absence of free water; however, the substrate must possess enough moisture to support the growth and metabolism of microorganisms. Recently, several reports have been published indicating the application of this culture in upgrading the food and industrial wastes and in the production of fine chemicals and enzymes. The utilization of by-products and wastes from food and industrial sources has several advantages over submerged fermentation such as superior productivity, simple techniques, reduced energy requirements, low wastewater output, improved product recovery and the reduction in production costs [4]. In SSF, any type of substrate, including industrial wastes, could be used to enhance the production of enzymes because of their richness in fatty acids, triacylglycerols and/or sugars. The use of cheap raw materials would diminish the operating costs of the process. Moreover, total capital investment for lipase production has been reported to be significantly lower in solid state fermentation than in submerged fermentation [5]. Most studies on lipolytic enzymes production with bacteria, fungi and yeasts have been performed in submerged fermentation; however, there are only few reports on lipase synthesis in solid state fermentation. In recent years, considerable research has been carried out using agricultural wastes, which are renewable and abundantly available to produce value-added products. For example babassu oil cake [6], olive cake and sugar cane bagasse [7], gingelly oil cake [8], wheat bran [9], rice bran [10] and *Jatropha curcas* seed cake [11] have been used as the substrates for lipase production.

The global production of palm kernel cake (PKC), a by-product of oil extraction from the nut of the palm tree, *Elaeis guineensis*, is ever increasing due to the tremendous growth of the oil palm industry in many parts of Asia and Africa [12]. World producers of palm kernel

include Malayasia, Indonesia, Nigeria, Colombia, India, and Thailand. In Malaysia alone, about 3 million tonnes of palm kernel were produced in 2001 producing about 1.4 million tonnes of palm kernel oil together with 1.6 million tonnes of PKC as its byproduct. Palm trees are widely cultivated in the state of Andhra Pradesh, India. The low cost and availability of PKC have recently generated much interest in its potential use in fish diets. In recent years, the cost of imported feed ingredients used in commercial aqua feeds in many developing countries in Asia has continued to rise due to increased global demand and fluctuation in foreign currency exchange. The rising cost of imported ingredients such as fish meal, soyabean meal, corn flour and wheat flour greatly cuts into the profit margins of local fish farmers to such an extent that many local aquaculture enterprises are no longer profitable. This is especially true for the culture of lower-value fish species such as catfish, tilapia and carps. There is currently a great interest within the animal feed industry to reduce costs by using locally available feed ingredients like Palm kernel cake.

The present study aimed at developing appropriate bioprocesses for the utilization of Palm kernel cake. Palm kernel contains 16% protein, 15% crude fiber, 48% carbohydrates and 4% ash. This composition is appropriate to support good microbial growth and enzyme production. Use of Palm kernel cake as a substrate for solid state fermentation thus appears logical and worth exploring. SSF has been employed to grow microbes and to produce extracellular lipase [9,13]. Even though large number of agricultural/food residues have been worked out as suitable substrates for SSF [14], there is no report on SSF of Palm kernel cake so far to the best of our knowledge.

Hence an attempt is made in this paper to utilize the PKC as a substrate for the production of lipase by solid state fermentation. It was under taken to optimize the key process variables, including incubation time, inoculum level, initial moisture content, carbon level, and nitrogen level of the medium for the production of lipase using this oil cake under SSF.

2. MATERIALS AND METHODS

2.1. Substrate

PKC, obtained from a local palm oil distillery (Jeevan Enterprises) unit of Vizianagaram, India, was used as the substrate. It was dried at 60˚C for 72 h to reduce the moisture content to around 5%, and ground to the desired size (2 mm).

2.2. Chemical Analysis of PKC

Palm kernel cake is the major byproduct of oil palm kernel oil extraction. PKC, when powdered, gives meal or flour. As such there is no significant alteration in the content of nutrients when the cake is converted to meal or flour. Palm kernel meal contains 20% protein which is the lowest among the oil seed meals. Carbohydrates are the major constituents of palm kernel meal than most of the oil seed meals. It is characterized by higher fiber content. The contents of nitrogen free extract (NFE) and crude fiber depend on the method of oil extraction from palm kernel. PKC contains a good amount of minerals: 0.69% phosphorus, 0.42% potassium, 0.29% calcium, and 0.017% iron [15]. The chemical composition of PKC was presented in **Table 1**.

2.3. Microorganism and Growth Conditions

Yarrowia lipolytica NCIM 3589, obtained from National Chemical Laboratory, Pune, India, was used throughout the study. The culture was maintained on MGYP slants having the composition (%): malt extract 0.3, glucose 1.0, yeast extract 0.3, peptone 0.5 and agar agar 2.0. The pH of the medium was adjusted to 6.4–6.8 and culture was incubated at 30˚C for 48 h. Sub-culturing was carried out once in 2 weeks and the culture was stored at 4˚C.

2.4. Inoculum and Media Preparation

The *Yarrowia* strain was cultivated in a medium containing peptone 5 g, yeast extract 3 g and sodium chloride 3 g per liter of distilled water. The cells were cultivated in this medium at 30˚C on a shaker at 200 rpm for 24 h [16]. Ten grams of substrate was weighed into a 250 ml Erlenmeyer flask and to this a supplemental salt solution was added to the desired moisture level. The composition of the salt solution was as follows (% w/w): KH_2PO_4: 0.1; $MgSO_4.7H_2O$: 0.05; $CaCl_2$: 0.01; NaCl: 0.01; H_3BO_3: 0.00005; $CuSO_4.5H_2O$: 0.000004; KI: 0.00001; $FeCl_3.4H_2O$: 0.00002; $ZnSO_4.7H_2O$: 0.00004; $MnSO_4.H_2O$: 0.00004 [17]. Out of various compounds tried, glucose and urea were ultimately selected as carbon and nitrogen sources respectively as per the Plackett-Burman design. The contents were thoroughly mixed and autoclaved at 121˚C (15 psi) for 20 min.

2.5. Solid State Fermentation and Extraction of Lipase

The sterilized substrate along with media as shown in the above section was inoculated with 2 ml of inoculum.

Table 1. Chemical composition of PKC [17].

Constituents	Quantity (%w/w)
Crude protein	16.1
Ether extract	0.8
Crude fiber	15.2
Ash	4.0
Nitrogen free extract	63

The contents were mixed thoroughly and incubated in a slanting position at 30˚C. All the experiments were carried out in duplicate and samples were withdrawn after 4 days of incubation. The crude enzyme from the fermented material was recovered by simple extraction method. For this, the fermented substrate was mixed thoroughly with 100 ml of distilled water and the contents were agitated for 1 h at the room temperature in a rotary shaker at 150 rpm. At the end of extraction, the liquid was filtered off through Whatman No.1 filter paper and the resulting clear filtrate was used for lipase assay.

2.6. Lipase Assay

Lipase activity was assayed by the colorimetric method of Winkler and Stuckmann, [18] by measuring the micromoles of 4-nitrophenol released from 4-nitrophenyl palmitate. One unit of lipase activity was defined as the enzyme amount that releases 1µmol of *p*-nitrophenol per minute under assay conditions. Enzyme activity was expressed as units/gram of the initial dry substrate (U/gds).

3. EXPERIMENTAL DESIGN AND OPTIMIZATION

3.1. Plackett-Burman Design

The purpose of this optimization step was to identify which ingredients of the medium had a significant effect on lipase activity. The Plackett–Burman [19] statistical experimental design is a versatile method for screening the important variables. The total number of experiments to be carried out is $K + 1$, where K is the number of variables. Each variable is represented at two levels, high and low denoted by (+) and (–) respectively. The statistical software package STATISTICA 6.0 (Stat-Ease Inc., Tulsa, OK, USA) was used for analyzing the experimental data.

The effect of each variable on lipase activity was calculated by using the following Equation:

$$E_{(Xi)} = \frac{\Sigma Y_{(+)i} - \Sigma Y_{(-)i}}{L/2} \quad (1)$$

where $E_{(Xi)}$ is the effect of levels of the tested variables, $Y_{(+)i}$ and $Y_{(-)i}$ are the lipase activity from the experimental runs in which the variables being tested are added to the medium at their maximum and minimum levels respectively and L is the number of experiments carried out. When the value of concentration effect ($E_{(Xi)}$) of the tested variable is positive, the influence of the variable is greater at the high concentration, and when it is negative, the influence of the variable is greater at the low concentration.

4. RESULTS AND DISCUSSION

4.1. Effect of Incubation Time

The incubation time is an important factor for the production of extracellular lipase by the microorganisms [20]. The amount of lipase activity was observed daily during a period of five days. The maximum lipase activity was observed on fourth day as shown in **Table 2**. At longer incubation periods, the lipase activity decreased which might be due to the depletion of nutrients, accumulation of toxic end products, and the change in pH of the medium, or loss of moisture. Several researchers have reported different incubation periods for optimal lipase production. Maximum lipase activity was achieved after 48 h of incubation by Ul-Haq *et al.*, [21] with *Rhizopus oryzae.* Cordova *et al.*, [7] reported the maximum lipase activity by *R.pullis* after 24 h of incubation using the mixture of olive oil cake and sugar cane bagasse as substrate. In another study, the maximum lipase activity by *Aspergillus niger* occurred after 5 days of incubation [9]. Benjamin and Pandey, [22] obtained maximum production of lipase by *Candida rugosa* after 3 days of incubation.

4.2. Effect of Inoculum Level

Different levels of the inoculum were tried to study their effect on lipase activity (**Figure 1**) so as to find an

Table 2. Effect of incubation time on lipase activity.

Incubation time (hrs)	Lipase activity (U/gds)
24	-
48	0.46
72	4.92
96	**6.48**
120	5.04

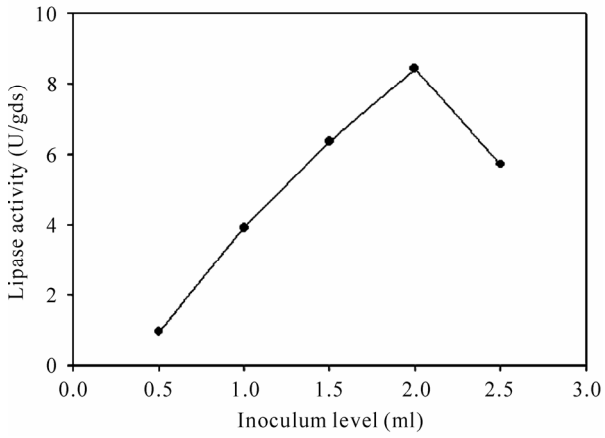

Figure 1. Effect of inoculum level on lipase activity.

optimum inoculum level in the fermentation process. A lower inoculum may give insufficient biomass causing reduced product formation, whereas a higher inoculum may produce too much biomass leading to the poor product formation [23]. In this study, the maximum lipase activity (8.43 U/gds) was obtained with 2 ml (20% v/w) inoculum level. Various investigators have used different levels of inoculum for lipase production employing different microorganisms. Maximum lipase production by *Rhizopus oligosporus* was achieved by Ul-Haq *et al.*, [21] with 1 ml of inoculum. An inoculum concentration of 1.07×10^8 spores/10 g of substrate were found to be optimal for lipase production by *Aspergillus niger* [8]. Diaz *et al.*, [13] used an inoculum concentration of 3×10^7 spores/g of dry substrate for maximum lipase production by *R. homothallicus*.

4.3. Effect of Initial Moisture Content

Moisture content of substrate plays a vital role for the microbial growth and for effecting biochemical activities in SSF [24]. The maximum lipase activity was obtained at 70% v/w initial moisture content as presented in **Figure 2**. Lipase production was decreased at very higher moisture content which may be attributed to the decrease in porosity and hence decrease in gaseous exchange leading to suboptimal growth and less enzyme production as indicated by Silman *et al.*, [25]. Less lipase activity was observed at lower moisture content due to the reduction in the solubility of nutrients of the substrate, lowers the degree of swelling, and creates higher water tension as suggested by Perez-Guerra *et al.*, [26]. Mahanta *et al.*, [11] reported initial moisture content at 50% of substrate as ideal for lipase production using *Jatropha curcas* seed cake as the substrate.

4.4. Identification of Important Nitrogen Source Using Plackett-Burman Design

A total of ten nitrogen sources were screened through twelve experimental runs. The experimental plan and corresponding lipase production were shown in **Table 3**. The pareto graph (**Figure 3**) was used to show the effect of all nitrogen sources (both organic and inorganic) on lipase production. A *p*-value of less than 0.05 for the six variables viz., urea, peptone, malt extract, yeast extract, $(NH_4)_2SO_4$, and $NH_4H_2PO_4$ indicates that they are significant. From the statistical analysis, it was also found that lipase production was affected by the above six nitrogen sources as evident from their *F*-values and *p*-values as shown in **Table 4**. In addition, the coefficient of determination (R^2) of the model was found to be 0.9992 which explains the 99.92% variability of the data. Urea had the confidence level more than 95% in comparison to the other variables and thus considered to be highly significant for lipase production. Here one dummy variable (DV) was employed to evaluate the standard errors of the experiment. Further studies were conducted by taking urea at different concentrations. **Figure 4** shows that 1.5 (%w/w) of urea yielded maximum lipase activity. However, at higher levels the

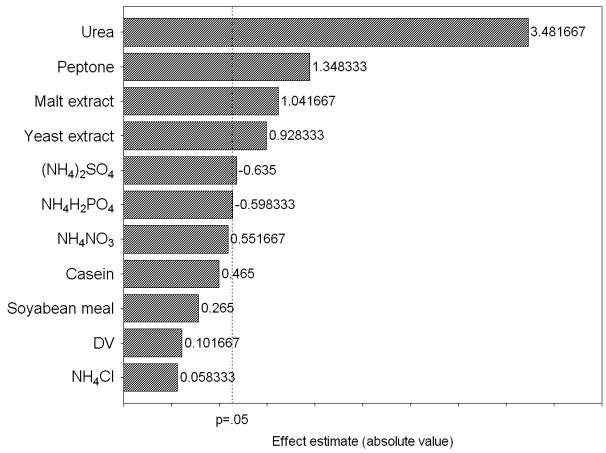

Figure 3. Pareto graph showing effect of various nitrogen sources on lipase production based on the observation of Plackett–Burman design.

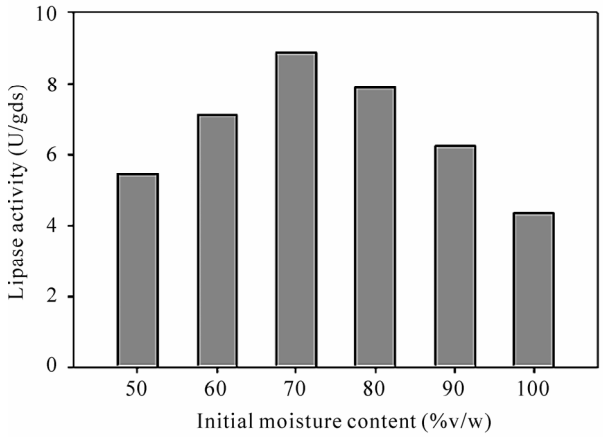

Figure 2. Effect of initial moisture content on lipase activity.

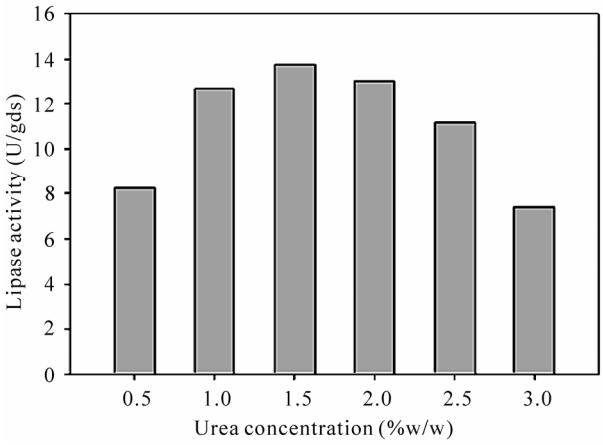

Figure 4. Effect of urea concentration on lipase activity.

Table 3. Plackett–Burman experimental design matrix for screening of various nitrogen sources for lipase production.

Run no.	Levels	Variables (% w/w)											Lipase activity (U/gds)
		Soyabean meal	Casein	Yeast extract	Malt extract	Peptone	Urea	NH_4Cl	$NH_4H_2PO_4$	$(NH_4)_2SO_4$	NH_4NO_3	DV	
	+	5.0	5.0	5.0	5.0	5.0	3.0	3.0	3.0	3.0	3.0	–	
	–	1.0	1.0	1.0	1.0	1.0	0.5	0.5	0.5	0.5	0.5	–	
1		+	–	+	–	–	–	+	+	+	–	+	6.31
2		+	+	–	+	–	–	–	+	+	+	–	7.28
3		–	+	+	–	+	–	–	–	+	+	+	8.95
4		+	–	+	+	–	+	–	–	–	+	+	12.56
5		+	+	–	+	+	–	+	–	–	–	+	9.47
6		+	+	+	–	+	+	–	+	–	–	–	12.08
7		–	+	+	+	–	+	+	–	+	–	–	11.53
8		–	–	+	+	+	–	+	+	–	+	–	9.52
9		–	–	–	+	+	+	–	+	+	–	+	10.93
10		+	–	–	–	+	+	+	–	+	+	–	11.26
11		–	+	–	–	–	+	+	+	–	+	+	10.25
12		–	–	–	–	–	–	–	–	–	–	–	6.19

DV: Dummy Variable

Table 4. Effects of different nitrogen sources for lipase production from the results of Plackett-Burman design.

Variables	Effect (*E*)	*t*-value	*p*-value
Soyabean meal	0.265000	5.6761	0.111019
Casein	0.465000	9.9599	0.063705
Yeast extract	0.928333	19.8841	0.031990[a]
Malt extract	1.041667	22.3116	0.028514[a]
Peptone	1.348333	28.8801	0.022035[a]
Urea	3.481667	74.5742	0.008536[a]
NH_4Cl	0.058333	1.2494	0.429690
$NH_4H_2PO_4$	–0.598333	–12.8158	0.049574[a]
$(NH_4)_2SO_4$	–0.635000	–13.6011	0.046722[a]
NH_4NO_3	0.551667	11.8162	0.053749
DV	0.101667	2.1776	0.274061

Standard error = 0.046687
[a]Significant at $p \leq 0.05$.

production was reduced due to the inhibitory effects of urea. Banjamin and Pandey [22] reported that urea was found to be best nitrogen source for lipase production with *C.rugosa*.

4.5. Identification of Important Carbon Source Using Plackett-Burman Design

Five carbon sources were screened by eight experimental runs. The experimental plan and corresponding lipase production were shown in **Table 5**. The pareto graph (**Figure 5**) was used to show the effect of all the carbon sources on lipase production. A *p*-value less than 0.05 for the three variables viz., glucose, sucrose, and fructose indicates that they are significant. From the analysis, it was also found that lipase production was affected by the above three carbon sources as evident from their *F*-values and *p*-values as shown in **Table 6**. In addition, the coefficient of determination (R^2) of the model was 0.9998 which explains the 99.98% variability of the data. Glucose had a confidence level of above 95% in comparison to other variables and thus considered to be highly significant for lipase production. Two dummy variables (DV1 & DV2) were employed to evaluate the standard errors of the experiment. **Figure 6** presents the results of different concentrations of glucose on lipase activity.

5. CONCLUSIONS

The Palm kernel cake supported good microbial growth and enzyme production as evident by its chemical composition. Marine yeast *Yarrowia lipolytica* NCIM 3589 was used for the fermentation. The presence of PKC

Table 5. Plackett–Burman experimental design matrix for screening of different carbon sources for lipase production.

Run no.	Levels	Variables (%w/w)							Lipase activity (U/gds)
		Glucose	Sucrose	Fructose	Lactose	Starch	DV1	DV2	
	+	9	9	9	9	9	–	–	
	–	1	1	1	1	1	–	–	
1		–	–	–	+	+	+	–	8.94
2		+	–	–	–	–	+	+	12.61
3		–	+	–	–	+	–	+	10.64
4		+	+	–	+	–	–	–	13.51
5		–	–	+	+	–	–	+	10.15
6		+	–	+	–	+	–	–	13.91
7		–	+	+	–	–	+	–	11.18
8		+	+	+	+	+	+	+	14.15

DV: Dummy Variables

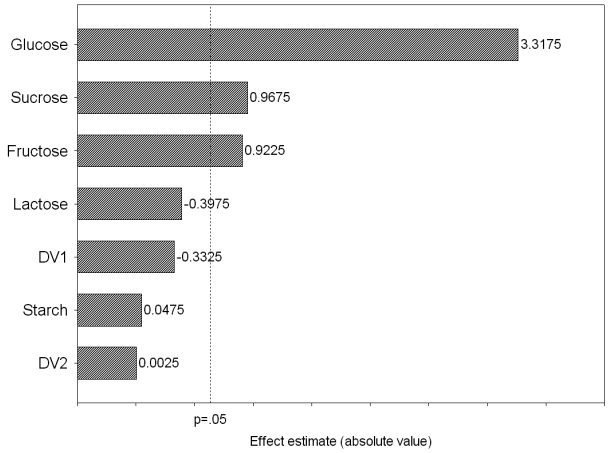

Figure 5. Pareto graph showing effect of various carbon sources on lipase production basedon the observation of Plackett-Burman design.

Table 6. Effects of different carbon sources for lipase production from the results of Plackett-Burman design.

Variables	Effect (*E*)	*t*-value	*p*-value
Glucose	3.3175	65.2623	0.009754[a]
Sucrose	0.9675	19.0328	0.033418[a]
Fructose	0.9225	18.1475	0.035045[a]
Lactose	–0.3975	–7.8197	0.080973
Starch	0.0475	0.9344	0.521572
DV1	–0.3325	–6.5410	0.096580
DV2	0.0025	0.0492	0.968716

Standard error = 0.050833
[a]Significant at $p \leq 0.05$.

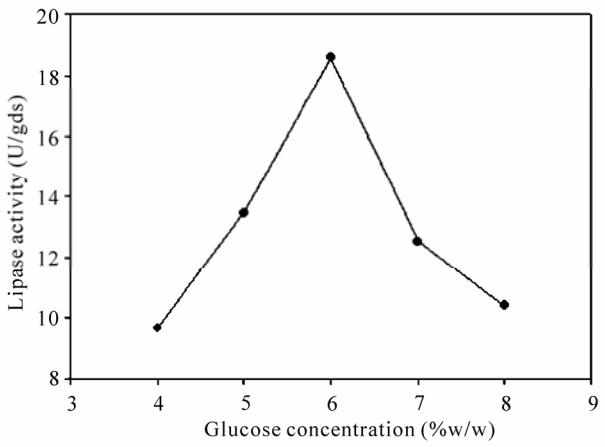

Figure 6. Effect of glucose concentration on lipase activity.

with 70% moisture content yielded the maximum lipase activity (18.58 U/gds) in four days. The high lipase activity achieved in conjunction with the abundantly available palm kernel cake in the state of Andhra Pradesh, India, paved a way for the industrial exploitation of this substrate under solid state fermentation using the indigenous *Yarrowia lipolytica* NCIM 3589 as a suitable micro organism.

REFERENCES

[1] Sharma, R., Chisti, Y. and Banerjee, U.C. (2001) Production, purification, characterization, and applications of lipases. *Biotechnology Advances*, **19(8)**, 627-662.

[2] Jaeger, K.E., Steinbuchel, A. and Jendrossek, D. (1995) Substrate specificities of bacterial polyhydroxyalkanoate depolymerases and lipases: Bacterial lipases hydrolyze

poly(ω-hydroxyalkanoates). *Applied Environmental and Microbiology*, **61(8)**, 3113-3118.

[3] Mochizuki, M., Hirano, M., Kanmuri, Y., Kudo, K. and Tokiwa, Y. (1995) Hydrolysis of polycaprolactone by lipase: effects of draw ratio on enzymatic degradation. *Journal of Applied Polymer Science*, **55(2)**, 289-296.

[4] Ashok, P. (2003) Solid state fermentation. *Biochemical Engineering Journal*, **13(2-3)**, 81-84.

[5] Castilho, L.R., Polato, C.M.S., Baruque, E.A., Sant Anna Jr, G.L. and Freire, D.M.G. (2000) Economic analysis of lipase production by *Penicillium restrictum* in solid-state and submerged fermentations. *Biochemical Engineering Journal*, **4(33)**, 239-247.

[6] Gombert, A.K., Pinto, A.L., Castilho, L.R. and Freire, D.M.G. (1999) Lipase production by *Penicillium restrictum* in solid-state fermentation using babassu oil cake as substrate. *Process Biochemistry*, **35(1-2)**, 85-90.

[7] Cordova, J., Nemmaoui, M., Ismaili-Alaoui, M., Morin, A., Roussos, S., Raimbault, M. and Benjilali, B. (1998) Lipase production by solid state fermentation of olive cake and sugar cane bagasse. *Journal of Molecular Catalysis B*: *Enzymatic*, **5(1-4)**, 75-78.

[8] Kamini, N.R., Mala, J.G.S. and Puvanakrishnan, R. (1998) Lipase production from *Aspergillus niger* by solid-state fermentation using gingelly oil cake. *Process Biochemistry*, **33(5)**, 505-511.

[9] Mahadik, N.D., Puntambekar, U.S., Bastawde, K.B., Khire, J.M. and Gokhale, D.V. (2002) Production of acidic lipase by *Aspergillus niger* in solid state fermentation. *Process Biochemistry*, **38(5)**, 715-721.

[10] Rao, P.V., Jayaraman, K. and Lakshmanan, C.M. (1993) Production of lipase by *Candida rugosa* in solid state fermentation. 1: Determination of significant process variables. *Process Biochemistry*, **28(6)**, 385-389.

[11] Mahanta, N., Gupta, A. and Khare, S.K. (2008) Production of protease and lipase by solvent tolerant *Pseudomonas aeruginosa PseA* in solid-state fermentation using *Jatropha curcas* seed cake as substrate. *Bioresource Technology*, **99(6)**, 1729-1735.

[12] PORLA (2000) Palm Oil Statistics. Ministry of Primary Industries, Kuala Lumpur.

[13] Diaz, M.J.C., Rodríguez, J.A., Roussos, S., Cordova, J., Abousalham, A., Carriere, F. and Baratti, J. (2006) Lipase from the thermotolerant fungus *Rhizopus homothallicus* is more thermostable when produced using solid state fermentation than liquid fermentation procedures. *Enzyme and Microbial Technology*, **39(5)**, 1042-1050.

[14] Raimbault, M. (1998) General and microbiological aspects of solid substrate fermentation. *Electronic Journal of Biotechnology*, **1(3)**, 174 189.

[15] Salunkhe, D.K., Chavan, J.K., Adsule, R.N. and Kadam, S.S. (1999) World oil seeds chemistry, Technology, and Utilization. Van Nostrand Reinhold, NewYork.

[16] Imandi, S.B., Bandaru, V.V.R., Somalanka, S.R., Bandaru, S.R. and Garapati, H.R. (2008) Application of statistical experimental designs for the optimization of medium constituents for the production of citric acid from pineapple waste. *Bioresource Technology*, **99(10)**, 4445-4450.

[17] Imandi, S.B. (2008) Studies on the production of lipase in solid state fermentation using Artificial Neural Networks and Genetic Algorithms. Ph.D. Thesis, Andhra University, Visakhapatnam, India.

[18] Winkler, U.K. and Stuckmann, M. (1979) Glycogen, hyaluronate and some other polysaccharides greatly enhance the formation of exolipase by *Serratia marcescens*. *Journal of Bacteriology*, **138(3)**, 663-670.

[19] Plackett, R.L. and Burman, J.P. (1946) The Design of Optimum Multifactorial Experiments. *Biometrika*, **33(4)**, 305-325.

[20] Shirazi, S.H., Rahman, S.R. and Rahman, M.M. (1998) Production of Extra cellular lipases by *Saccharomyces cerevisiae*. *World Journal of Microbiology and Biotechnology*, **14(4)**, 595-597.

[21] Ul-Haq, I., Idrees, S. and Rajoka, M.I. (2002) Production of lipases by *Rhizopus oligosporus* by solid-state fermentation. *Process Biochemistry*, **37(6)**, 637-641.

[22] Benjamin, S. and Pandey, A. (1997) Coconut cake: a potent substrate for production of lipase by *Candida rugosa* in solid state fermentation. *Acta Biotechnologica*, **17(3)**, 241-251.

[23] Mudgetti, R.E. (1986) Manual of industrial biotechnology. American Society for Microbiology, Washington DC.

[24] Babu, I.S. and Rao, G.H. (2007) Lipase production by *Yarrowia lipolytica* NCIM 3589 in solid state fermentation using mixed substrate. *Research Journal of Microbiology*, **2(5)**, 469-474.

[25] Silman, R.W., Conway, M.F., Anderson, R.A. and Bagley, E.B. (1979) Production of aflatoxin in corn by large scale solid state fermentation process. *Biotechnology and Bioengineering*, **21(10)**, 1799-1808.

[26] Pérez-Guerra, N., Torrado-Agrasar, A., López-Macias, C. and Pastrana, L. (2003) Main characteristics and applications of solid substrate fermentation. *Electronic Journal of Environmental, Agricultural and Food Chemistry*, **2(3)**, 343-350.

Advances in Bioscience and Biotechnology, 2010, 1, 122-130 **ABB**
doi:10.4236/abb.2010.12017 Published Online June 2010 (http://www.SciRP.org/journal/abb/)

Age changes in the anthropometric and body composition characteristics of the Bishnupriya Manipuris of Cachar district, Assam

Bhubon Mohan Das, Subrata K. Roy

Biological Anthropology Unit, Indian Statistical Institute, Kolkata, India.
Email: bmohan07@gmail.com; rsubrata@isical.ac.in

Received 8 March 2010; revised 12 March 2010; accepted 23 March 2010.

ABSTRACT

Generally all morphological physical features of human body change throughout ones life span, the rates of change are not constant and there are certain ages when anthropometric characteristics reach its peak. The maturity of the anthropometric characteristics varies among populations/communities and sexes due to genetic make-up, environment and other concomitants. Present study examined the nature and extent of age related changes in anthropometric and body composition characteristics among the adult Bishnupriya Manipuris of Cachar district, Assam. Some anthropometric data and body composition characteristics analysed and compared between/among 5-age cohorts to see age changes. Study results show significant age changes in some anthropometric characteristics and some body composition characteristics. However, age specific changes could not been determined due to small sample size.

Keywords: Anthropometry; BMI; Fat; Age-Changes

1. INTRODUCTION

Changes in body structure and morphology in humans occurs over its lifetime. At every stage of life, there are physical changes in the human body. Although every person experiences growth and development uniquely, the patterns are similar for all humans but the rates vary (due to nutrition, exercise, environment etc). Generally, from age 20 to 35 years, most of the physical body dimension is in peak form. Changes that occur during early stages of life and through adolescence are known as growth and development, which is characterized by fast progress. On the other hand, changes that occur during adulthood are known as age changes, which is relatively slower than earlier phase [1].

It was thought that once the human body reached its adult size, all the body measurements remain constant for many years to come but there is no clear static point in actual age or particular time of human being, when the morphological body features do not change [2]. Developmental processes or changes in body morphology continue to occur after puberty. Genetic and environmental factors play a significant role in the whole process of change in the anthropometric characteristics during adulthood among individuals [3]. Susanne [4] pointed out that the process of formation and destruction are present in all stages of life, beginning from the conception to death and the ratio between these processes are different and it is difficult to assign a period or age of complete maturation and the beginning of aging process. Anthropometric characteristics provide a better understanding of the growth process by describing changes in the body size and morphology through ages. However, all the anthropometric characteristics do not reach its peak at the same time, at the same rate or at the same extent with other. The variation may be evident between anthropometric characteristics, between populations, or between sexes.

Though, nutritional status are supposed to have a great role in making all types of changes but the variation in the anthropometric and body composition characteristics in the adulthood are primarily due to osteological changes, changes in the fat and muscle tissue. Because of the cross-sectional nature of most of the anthropological studies on adults, it is difficult to separate the changes occur due to secular changes or from continuing growth or due to aging [4,5]. Anthropometric measurements on individual seem to attain their peak at different ages. In general, height reaches the peak early in the life (*i.e.* around 20 years of age), weight attains its peak after 30 years, circumferences and some functional characteristics reaches at and around the same time, width measurements reaches its peak later ages of life [6].

In view of the importance of age changes in the anthropometric characteristics of healthy adults, which help to understand the process of change and ultimately

improve the knowledge. A large number of studies on age related changes have been conducted on different ethnic groups in India and abroad but majority of the studies have focused attention on the elderly population [7-13]. Very few studies have concentrated on age changes in anthropometric characteristics during adulthood [5,6,14-16].

In light of the above-mentioned studies, the present study examined the nature and extent of age related changes in anthropometric characteristics among the adult Bishnupriya Manipuris of Cachar district, Assam.

2. MATERIALS AND METHODS

A multi-disciplinary bio-medical research project was undertaken among the Bishnupriya Manipuris, who has been settled at Pakaipar, about 30 kilometers away from Silchar (capital town), Cachar district of Assam. Bishnupriya Manipuris of this area have been originally migrated from Manipur around 100 years before. Bishnupriya Manipuris are different from the Meiteis (dominant group of Manipur) in terms of language [17] and some physical features, although both the groups are hinduised and followers of lord Vishnu.

No statistical sampling of the households/individuals have been made, complete enumeration of the settlement have been done for demographic information. For anthropometric data, individual, who voluntarily agreed to participate in the study, have been incorporated in the sample (100 males and 146 females). Age of the individuals have been collected after verifying written record, those individuals who do not have birth record, their age was estimated by reference to important local events but those data have not been used in the present analyses. Initially, anthropometric data have been collected from 279 individuals but at the time of analysis data of 33 individuals have been excluded due to unavailability of proper birth record. Total 246 individuals have been classified into 5 groups of 10 years age cohort, *i.e.*, <25, 25-34, 35-44, 45-54 and> 54. It would be ideal to make classification with each age but due to small number of samples it was not possible.

Data types include Socio-demographic characteristics of the individuals studied like age, sex, education, occupation and per capita monthly expenditure as well as their anthropometric measurements. Socio-demographic data collected through household census schedule from 122 households. Anthropometric data have been collected from adult (above 18 years) individuals of both sexes, following standard techniques [18]. Anthropometric data includes height, weight, sitting height, upper arm circumference, calf circumference, biacromial diameter, biiliac diameter, bicondylar diameter of humerus, bicondylar diameter of femur, skinfold thickness like biceps, triceps, subscapular, suprailiac, medial calf.

Some calculated values like Body mass index (BMI), Body fat percentage, Fat mass and Fat free mass have also been presented. Fat percentages have been obtained by Beurer Body Fat Monitor, which works on the principles of Bioelectrical Impedance to measure a persons' actual body fat content. By utilizing BIA (bioelectrical impedance analysis) principles, a relatively accurate picture can be obtained of the body's fat content. The methods Bioelectrical Impedance is considered to be one of the standard techniques as stated in many literatures [19,20]. Body mass index (BMI), Fat mass (FM) and Fat free mass (FFM) data have been calculated by using the following formula:

BMI = Weight (kg)/Height (m^2)

FM (kg) (Fat mass) = (Body Fat percent/100) × Weight (kg)

FFM (kg) (Fat free mass) = Weight (kg) – Fat mass (kg)

Analysis of data: Descriptive statistics of anthropometric variables have been calculated and one-way analysis of variance (ANOVA) calculated to test the hypothesis that all the mean values of age cohorts are equal for each variable. Whenever significant ANOVA (F value) results of any variable detected, the mean values were crosschecked with Scheffe test to find out where the exact difference exists between groups. Scheffe's test is designed to allow all possible linear combinations of group means to be tested, not just pairwise comparisons but the test is more conservative than other tests, meaning that a larger difference between means is required for significance. The chance of rejecting a true hypothesis is, say 5% on each test, and when several tests are made, the chance of rejecting at least one true-hypothesis becomes considerably larger than 5%. Scheffe's multiple-comparison method overcomes this problem. In fact, using Scheffe's method, and making all possible comparisons, the probability of obtaining one or more false conclusions when all the population means are actually equal is exactly 5%. The coefficient of variation (CV) has also been calculated and has been expressed as percent. The coefficient of variation (CV) is a normalized measure of dispersion of a probability distribution, also known as "relative variability", equals the standard deviation divided by the mean. Sometime CV is expressed as percentage. The coefficient of variation describes the magnitude sample values and the variation within them and it is a useful statistic for comparing the degree of variation from one data series to another, even if the means are drastically different from each other. The coefficient of variation is useful because the standard deviation of data must always be understood in the context of the mean of the data. The coefficient of variation is a dimensionless number. The CV of a single variable aims to describe the dispersion of the variable, which does not depend on the variable's measurement

unit. The higher the value of CV is, the greater the dispersion of the variable. All the analyses have been done using SPSS 11.0 version computer package.

3. RESULTS

3.1. Socio-Economic Condition of the Study Population

Socio-demographic profile of the Bishnupriya Manipuris shows out of 246 individuals, 146 (59.30%) is female. Higher number of males (63.00%) and females (51.37%) has education up to secondary level, followed by higher secondary level (22.00% males & 18.49% females), graduation level & above (8.00% males and 6.85% females) and primary level (4.00% males & 12.33% females). Considering the occupations of the study group, large number of males are owner cultivator (25%) followed by business (22%), pension holder (21%) and service (10%), while most of the females are engaged in household work (75.34%). Economic status of the group has been determined by per-capita expenditure, shows that most of the individuals of both sexes belong to Rs.500/- to Rs.1000/- (53.00% males and 60.27% females), followed by above Rs.1000/- (33.00% males and 25.34% females) expenditure category and rest of the individual belong to below Rs.500/- (14.00% males and 14.38% females) expenditure category. Aging effect for the above mentioned variable was not possible due to present sample size but will make an impression on the subject of study.

Table 1 shows descriptive statistics pertaining to anthropometric characteristics and body composition of 5-age cohorts of male Bishnupriya Manipuris. Younger group (< 25 years) show higher mean values in stature, medial calf skinfold and fat free mass, 2nd group (25-34 years) show higher mean values in sitting height and suprailiac skinfold thickness, 3rd group (35-44 years) show higher mean values in body weight, upper arm and calf circumference, biacromial diameter and subscapular skinfold thickness, 4th group (45-54 years) show higher mean values in biiliac diameter, biepicondylar diameter of humerous as well as BMI, eldest group (> 54 years) show higher mean values in and biepicondylar diameter femur and fat. ANOVA result shows significant mean differences between/among 5 age groups in the anthropometric traits like sitting height, biepicondylar diameter of humerus and all the body composition characteristics except body mass index.

Table 2 shows Scheffe test results for group comparison, between/among 5-age cohorts. The variables considered in the test, which show significant ANOVA values in **Table 1**. Scheffe test is more robust than t-test and it rules out type I error. First 2 variables (Sitting Height and Humerus diameter) do not show significant values between/among groups. Body fat percent is significantly high in the eldest group and significantly low in the younger group, therefore, it shows significant values. Fat mass and fat free mass also show more or less similar result with slight variation.

Descriptive statistics pertaining to anthropometric characteristics and body composition of the female Bishnupriya Manipuris has been presented in **Table 3**. Younger group (< 25 years) show higher mean values in body weight, sitting height, calf circumference, medial calf skinfold and fat free mass, 2nd group (25-34 years) show higher mean values only in subscapular skinfold thickness, 3rd group (35-44 years) show higher mean values in only, upper arm circumference and 4th group (45-54 years) show higher mean values in stature, biceps and triceps skinfold thickness and BMI, eldest group (> 54 years) show higher mean values in biacromial and biiliac diameter, biepicondylar diameter of humerous, biepicondylar diameter femur, suprailiac skinfold thickness, fat% and fat free mass. ANOVA result shows significant mean differences between/among 5 age groups in the anthropometric traits like sitting height, biepicondylar diameter of humerus, medial calf skinfold thickness and all the body composition characteristics except body mass index.

Table 4 shows Scheffe test results for group comparison, between/among 5-age cohorts. The variables considered in the test, which show significant ANOVA values in **Table 3**. First 2 variables (Sitting height and medial calf skinfold) show significant difference between younger and eldest (1st vs. 5th) group. Biepiconder diameter of humerus fail to show significant difference between/among groups. Body fat percent is significantly high in the eldest group and significantly low in the younger group, therefore, it shows significant values. Fat mass and fat free mass also show more or less similar result with slight variation.

Age changes in the anthropometric and body composition characteristics have been presented (mean $\pm$ SE) in **Figure 1** and **Figure 2** for both male and female Bishnupriya Manipuris.

Table 5 shows the Coefficient of variation in percentages. Variation of skinfold measurement is greater than all other measurements and again the variation is much greater in females than males, whereas fat percent and fat mass of females show smaller variation than males.

4. DISCUSSION

Individuals reach physical maturity through growth and development at certain age, but the age of maturity of all the body components is not similar between individuals or populations. It is inevitable that after middle age the changes in physical characteristics are marked and show declining trend. Present study examines age related changes in anthropometric and body composition

Table 1. Descriptive statistics pertaining to anthropometric and body composition characteristics of 5-age cohorts of male Bishnupriya Manipuris (F value refers to ANOVA results).

Anthropometric Variables	< 25 Years (n = 16)		25-34 Years (n = 23)		35-44 Years (n = 26)		45-54 Years (n = 18)		> 54 Years (n = 17)		F Value#
	Mean	SD	Mean	SD	Mean	SD	Mean	SD	Mean	SD	
Body weight (kg)	56.17	5.43	55.38	8.77	57.87	9.44	56.23	8.68	54.64	9.97	0.426
Stature (cm)	164.84	6.45	163.36	5.68	163.75	7.27	161.29	3.80	162.11	4.68	1.001
Sitting height (cm)	86.19	2.96	87.07	2.78	86.90	3.26	84.88	2.53	84.38	2.73	3.442*
***Circumferences* (cm)**											
Mid upper arm	24.25	2.04	23.72	2.17	24.91	2.51	23.54	4.81	24.14	2.62	0.747
Medial Calf	32.01	3.02	31.51	2.99	32.57	3.21	31.73	2.49	31.08	2.94	0.766
***Diameter* (cm)**											
Biaccromial	37.69	2.03	38.19	1.71	38.39	1.68	36.99	1.46	37.61	1.69	2.123
Biiliac	26.60	1.15	26.72	1.62	26.91	1.76	27.34	1.80	27.21	2.03	0.615
Bicondylar humerus	6.47	0.44	6.16	0.39	6.47	0.54	6.56	0.40	6.51	0.32	2.809*
Bicondylar femur	9.04	0.48	8.89	0.48	9.11	0.56	9.01	0.29	9.26	0.44	1.669
***Skinfold thickness* (mm)**											
Biceps	3.38	0.77	3.99	1.60	4.01	1.47	3.51	1.48	4.29	1.48	1.260
Triceps	6.30	2.09	6.82	3.02	7.25	3.03	6.00	2.12	7.71	3.04	1.134
Sub-scapular	9.90	2.65	12.43	4.67	14.25	5.71	12.43	3.42	12.46	5.03	2.225
Suprailiac	7.38	3.60	9.85	5.72	9.08	4.91	8.10	3.77	9.46	6.32	0.749
Medial calf	8.03	3.14	6.60	2.78	6.53	2.62	5.46	2.18	5.81	2.25	2.372
Body composition											
Body Mass Index (kg/m^2)	20.66	1.49	20.72	2.91	21.59	3.33	21.62	3.28	20.73	3.35	0.545
Body Fat (%)	13.27	4.91	20.80	7.33	20.73	6.82	27.65	9.30	30.66	7.64	14.502**
Fat Mass (kg)	7.46	2.79	11.59	4.69	12.21	5.02	15.78	6.20	16.83	5.12	9.632**
Fat Free Mass (kg)	48.71	5.21	43.79	7.29	45.66	7.16	40.46	6.73	37.80	7.47	9.721**

[df = 4, 95 * $P < 0.05$, ** $P < 0.01$]

Table 2. Scheffe test between/among age groups of selected anthropometric characteristics of male, which show significant values in ANOVA (**Table 1**).

Variables	Age Groups									
	1 vs. 2	**1 vs. 3**	**1 vs. 4**	**1 vs. 5**	**2 vs. 3**	**2 vs. 4**	**2 vs. 5**	**3 vs. 4**	**3 vs. 5**	**4 vs. 5**
Male	*df* = 37	*df* = 40	*df* = 32	*df* = 31	*df* = 47	*df* = 39	*df* = 38	*df* = 42	*df* = 41	*df* = 33
Sitting Height (cm)	0.886	0.709	1.304	1.811	0.178	2.191	2.697	2.013	2.520	0.507
Humerus diameter (cm)	0.308	0.004	0.087	0.037	0.312	0.395	0.345	0.082	0.033	0.050
Body Fat Percent	7.527*	7.462*	14.381*	17.396*	0.065	6.854	9.869*	6.919	9.934*	3.015
Fat Mass (kg)	4.128	4.746	8.313*	9.369*	0.618	4.185	5.241*	3.567	4.623	1.056
Fat Free Mass (kg)	4.919	3.045	8.249*	10.902*	1.873	3.330	5.984	5.203	7.857*	2.654

* $P < 0.05$

Table 3. Descriptive statistics pertaining to anthropometric and body composition characteristics of 5-age cohorts of female Bishnupriya Manipuris (F value refers to ANOVA results).

Anthropometric Variables	< 25 Yrs. (n = 31)		25 - 34 Yrs. (n = 39)		35-44 Yrs. (n = 29)		45-54 Yrs. (n = 19)		> 54 Yrs. (n = 28)		F Value#
	Mean	SD	Mean	SD	Mean	SD	Mean	SD	Mean	SD	
Body weight (kg)	45.64	5.41	46.09	7.46	47.92	6.23	48.67	8.58	48.49	9.53	1.012
Stature (cm)	150.55	6.06	149.13	5.21	149.47	5.64	148.26	5.37	149.07	4.29	0.621
Sitting height (cm)	80.23	3.37	79.44	3.06	79.10	3.45	78.41	3.33	77.58	2.21	3.043*
***Circumferences* (cm)**											
Mid upper arm	22.15	1.75	21.77	2.07	22.89	1.99	23.34	2.43	22.68	2.57	2.325
Medial Calf	29.10	1.93	28.10	2.18	28.19	1.75	28.29	2.97	28.35	2.55	1.012
***Diameter* (cm)**											
Biaccromial	34.37	1.80	34.23	1.66	34.37	1.78	34.08	2.02	34.89	1.90	0.744
Biiliac	26.42	1.59	26.22	1.68	26.62	1.25	27.04	1.49	27.28	1.94	2.189
Bicondylar humerus	5.64	0.42	5.56	0.47	5.59	0.40	5.78	0.52	5.89	0.44	2.747*
Bicondylar femur	8.26	0.41	8.20	0.47	8.28	0.60	8.35	0.52	8.43	0.47	0.974
***Skinfolds thickness* (mm)**											
Biceps	6.47	2.57	6.41	2.87	5.99	2.33	6.77	3.25	6.74	2.98	0.337
Triceps	13.02	3.90	11.25	4.09	12.03	4.41	13.03	4.75	12.16	4.20	0.978
Sub-scapular	14.98	4.72	15.49	5.53	15.47	5.00	14.34	4.41	16.09	6.15	0.365
Suprailiac	12.35	5.50	12.11	5.68	11.12	4.42	12.19	5.66	13.12	6.37	0.472
Medial calf	10.20	3.01	8.59	3.56	7.88	2.06	7.48	3.63	7.09	2.83	4.612**
Body composition											
Body Mass Index (kg/m^2)	20.13	1.95	20.67	2.85	21.45	2.65	22.12	3.65	21.76	3.94	1.985
Body Fat (%)	29.46	4.66	33.84	5.19	36.98	5.83	39.22	6.31	43.02	7.17	23.194**
Fat Mass (kg)	13.47	2.78	15.66	3.73	17.73	3.67	19.11	4.65	21.13	5.75	15.035**
Fat Free Mass (kg)	32.17	4.23	30.44	5.08	30.19	4.75	29.56	5.85	27.36	5.02	15.167**

[df = 4, 141 *P < 0.05, **P < 0.01]

Table 4. Scheffe test between/among age groups of selected anthropometric characteristics of female, which show significant values in ANOVA (ref. **Table 3**).

Variables	Age Groups									
	1 vs. 2	**1 vs.3**	**1 vs.4**	**1 vs.5**	**2 vs.3**	**2 vs.4**	**2 vs.5**	**3 vs.4**	**3 vs.5**	**4 vs.5**
Female	*df* = 68	*df* = 58	*df* = 48	*df* = 57	*df* = 66	*df* = 56	*df* = 65	*df* = 46	*df* = 55	*df* = 54
Sitting Height (cm)	0.789	1.132	1.827	2.650*	0.344	1.038	1.861	0.695	1.518	0.823
Calf skinfold (mm)	1.610	2.317	2.716	3.114*	0.707	1.106	1.504	0.399	0.797	0.399
Humerus diameter (cm)	0.078	0.049	0.142	0.244	0.029	0.220	0.322	0.191	0.293	0.102
Body Fat Percent	4.383*	7.518*	9.763*	13.560*	3.135	5.380*	9.177*	2.245	6.042*	3.797
Fat Mass (kg)	2.192	4.260*	5.642*	7.660*	2.069	3.451	5.468*	1.382	3.400	2.018
Fat Free Mass (kg)	1.739	1.981	2.610	4.813*	0.243	0.872	3.074	0.629	2.831	2.202

*P < 0.05

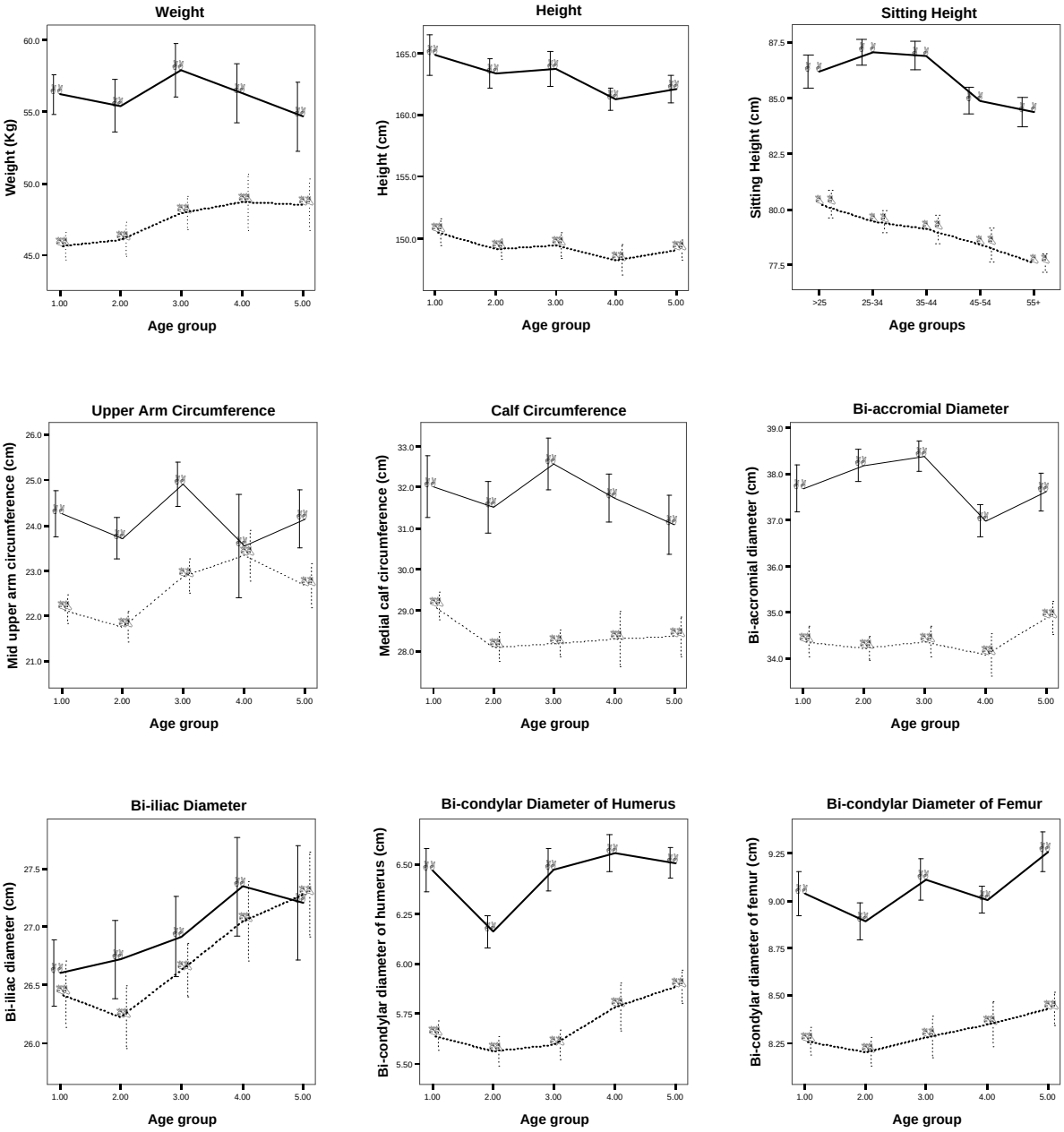

Legends: ----o---- **Male** Δ **Female**
Age Group: 1 = <25 years, 2 = 25-34 years, 3 = 35-44 years, 4 = 45-54 years and 5 = > 54 years

Figure 1. Age changes in the anthropometric characteristics in 10-yearly age cohort.

characteristics of the Bishnupriya Manipuris of Cachar district, Assam. The study population belongs to similar socio-economic background and shares a common physical environment. Study protocols were similar for all the individuals studied.

Present study shows significant difference in the anthropometric traits like, sitting height, humerus diameter, medial calf skinfold thickness; and in all body composition variables except body mass index between/among 10-yearly age cohorts in both sexes. Present study shows maximum mean height in the age group of < 25 years and thereafter it is slightly decreasing with increase of age irrespective of sex. Similarly, sitting height of both sexes demonstrate a significant decreasing trend with increasing age and this trend is very clear in females, which is corroborative with few empirical studies [21,22]. Most other anthropometric characteristics reached its peak at 35-44 yrs. age cohort (e.g. Body

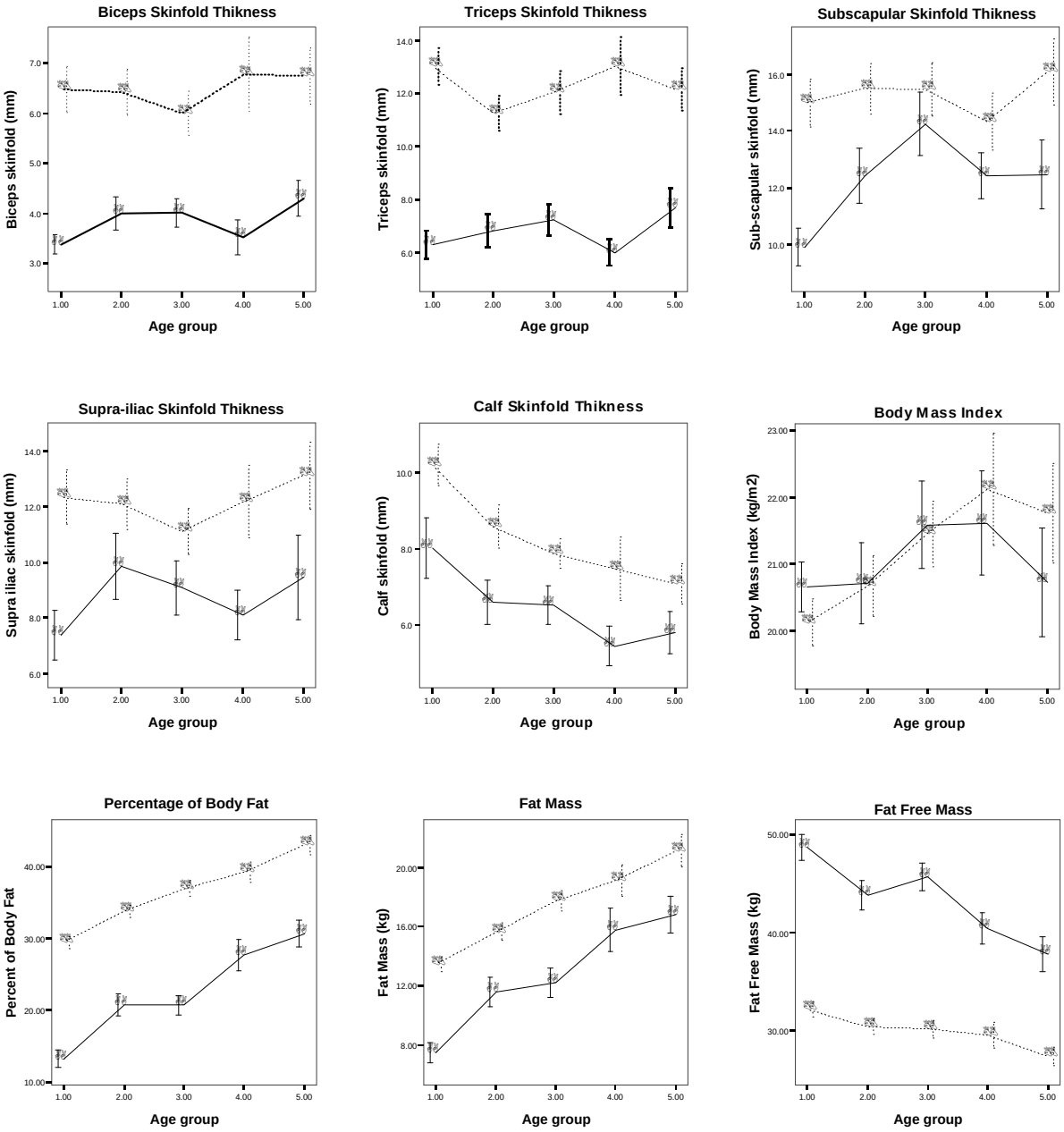

Legends: ----o---- **Male** Δ **Female**
Age Group: 1 = < 25 years, 2 = 25-34 years, 3 = 35-44 years, 4 = 45-54 years and 5 = > 54 years

Figure 2. Age changes in the body composition characteristics among 10-yearly age cohort.

weight, Sitting height, Upper arm circumference, calf girth and so on) and few other characteristics reached its peak at 45-54 yrs. age cohort (e.g. Biiliac diameter, bicondylar diameter of humerus), which is corroborative with the study of Oraon agricultural labourer of Jalpaiguri [5]. After peakedness, anthropometric characteristics show a decreasing trend with the increment of age may be due to the shrinkage of inter-vertebral space and increasing curvature of spine. Prokopec [6] (1987) observed that weight increase upto 40 years and then decline, which is corroborates with the present study in male but female show decreasing trend in weight in the age group of >54 years, which is corroborative with the study of Dangour [21] (2003) and Norris *et al.* [23] (1963).

Medial calf skinfold thickness significantly depicts a declining trend from first age group, *i.e.*, < 25 years, which is corroborates with the study of Roy and Pal

Table 5. Coefficient of variation (CV) in anthropometric and body composition characteristics of different age cohorts of the study population (expressed in percentage).

Variables	Male					Female				
	< 25y	25-34y	35-44y	45-54y	> 54y	< 25y	25-34y	35-44y	45-54y	> 54y
Weight	9.667	15.832	16.313	15.441	18.245	11.859	16.176	13.002	17.627	19.649
Stature	3.913	3.476	4.441	2.359	2.885	4.025	3.495	3.770	3.620	2.876
Sitting Height	3.431	3.192	3.748	2.980	3.232	4.197	3.856	4.368	4.249	2.854
Circumference										
Upper arm	8.400	9.129	10.062	20.446	10.852	7.920	9.517	8.691	10.398	11.345
Medial Calf	9.441	9.498	9.843	7.850	9.462	6.627	7.770	6.193	10.512	9.003
Diameter										
Bi-accromial	5.395	4.470	4.378	3.937	4.486	5.240	4.840	5.183	5.930	5.438
Bi-iliac	4.332	6.055	6.556	6.595	7.456	6.011	6.411	4.691	5.503	7.129
Humerus	6.791	6.281	8.389	6.039	4.905	7.390	8.384	7.119	8.914	7.481
Femur	5.266	5.361	6.117	3.242	4.740	4.981	5.747	7.199	6.230	5.629
Skinfold thickness										
Biceps	22.887	40.015	36.576	42.096	34.388	39.738	44.711	38.943	48.014	44.134
Triceps	33.235	44.253	41.810	35.369	39.502	29.925	36.381	36.605	36.467	34.559
Sub-scapula	26.720	37.607	40.058	27.499	40.375	31.488	35.700	32.356	30.771	38.212
Supra-iliac	48.873	58.089	54.078	46.551	66.834	44.546	46.896	39.770	46.438	48.523
Medial calf	39.140	42.178	40.097	39.977	38.637	29.507	41.483	26.179	48.531	39.943
Body Composition										
BMI	7.200	14.053	15.432	15.185	16.159	9.712	13.771	12.338	16.521	18.114
Fat percent	37.037	35.271	32.920	33.621	24.915	15.822	15.324	15.774	16.083	16.665
Fat mass	37.333	40.441	41.101	39.320	30.399	20.639	23.812	20.719	24.354	27.217
Fat free mass	10.700	16.641	15.674	16.633	19.751	13.132	16.706	15.748	19.777	18.363

[5] (2003). Other skinfold thickness measurements do not show any such trend, however, biceps and triceps skinfold show its peak at 45-54 yrs. age cohort.

Body mass index is generally considered to be as a measurement of fatness [24,25], while it also gives information about fat free mass. The same adult BMI value corresponds to a more fatty body composition in the elder individual, because fat mass increases and fat free mass decreases in this particular period of life [26]. BMI (Body Mass Index) of the present population show peaked ness at 45-54 yrs. age cohort, similar trend has been revealed from other studies [21,27] conducted in developing countries like India. Whereas fat percent as well as fat mass show its peak at the last age group, while fat free mass shows significant reverse trend with age, which is not corroborative with other studies [13, 16]. This trend may be due to the degeneration of muscle and accumulation of fat mass during the older age of this particular population.

Finally, although the present study shows some significant changes and trend with increment of age in anthropometric and body composition traits of both sexes but some of the variables fail to demonstrate specific trend with increment of age. It would have been better to make age specific changes (considering each age) instead of making 10-yealy age cohorts, which could specifically able to demonstrate exact nature of change (exact age when the development for each trait ceased and when declining trend starts), however, it was not possible for the small sample size of the present study. It is important to understand the actual age changes in anthropometric and body composition characteristics of

any group in terms of greater academic interest as well as biological and social point of view. As a note of caution, future studies on age changes in any population should be careful in taking the sample sizes as much as possible in order to make a clear understanding of the age specific changes.

5. ACKNOWLEDGEMENTS

The authors are deeply indebted to the study participants for their kind cooperation. We would like to thank Indian Statistical Institute, Kolkata for providing the financial support for conducting the study.

REFERENCES

[1] Plato, C.C. (1987) The effect of aging on Bioanthropo-logical variables: Changes in bone, mineral density with increasing age. *Collegium Anthropologicum*, **11(1)**, 59-71.

[2] Åstrand, P.O. and Rodahl, K. (1977) A text book of work physiology: Physiological bases of exercise. 2nd Edition, McGraw-Hill Book Company, New York.

[3] Launer, L.J. and Harris, T. (1996) Weight, height, body mass index distribution in geographically and ethnically diverse samples of older person. *Age and Ageing*, **25(4)**, 300-306.

[4] Susanne, C. (1979) Aging, continuous changes of adulthood. In *Human Physical Growth and Maturation*: *Methodologies and Factors*, Johnston, F.E., Roche, A.F. and Susanne, C., Eds., Plenum Press, New York, 203-218.

[5] Roy, S.K. and Pal, B. (2003) Anthropometric and physiological traits: Age changes among the Oraon agricultural labourer of the Jalpaiguri district, Northern West Bengal, India. *Anthropology Anz*, **61(4)**, 445-460.

[6] Prokopec, M. (1987) Changing patterns of growth, development and aging in the population of Czechoslovakia. *Collegium Anthropologicum*, **11(1)**, 91-115.

[7] Burr, M.L. and Phillips, K.M. (1984) Anthropometric norms in the elderly. *British Journal of Nutrition*, **51(1)**, 165-169.

[8] Chumlea, W.C., Rhyne, R.L., Garry, P.J. and Hunt, W.C. (1989) Changes in anthropometric indices of body composition with age in a healthy elderly population. *American Journal of Human Biology*, **1(4)**, 457-462.

[9] Chandler, P.J. and Bock, R.D. (1991) Age changes in adult stature: Trend estimation from mixed longitudinal data. *AnnaHum Biology*, **18(5)**, 433-440.

[10] Manandhar, M.C., Ankelsaria, P.S. and Ismail, S. (1997) Weight, skinfolds and circumference characteristics of poor elderly people in Mumbai, India. *Asia Pacific Journal of Clinical Nutrition*, **6(3)**, 191-199.

[11] Chiu, H.C., Chang, H.Y., Mau, L.W., Lee, T.K. and Liu, H.W. (2000) Height, weight, and body mass index of elderly persons in Taiwan. *Journal of Jeron Biology Sciences and Medicine Sciences*, **55(11)**, M684-M690.

[12] Bose, K. and Das Chaudhuri, A.B. (2003) Age variations in adiposity and body fat composition among older Bangalee Hindu women of Calcutta, India. *Anthropology Anz*, **61(3)**, 311-321.

[13] Ghosh, A. (2004) Age and sex variation in measures of body composition among the elderly Bangalee Hindu of Calcutta, India. *Collegium Anthropologicum*, **28(2)**, 553-561.

[14] Sidhu, L.S., Sodhi, H.S. and Bhatnagar, D.P. (1975) Anthropometric changes from adulthood to old age. *Indian Journal of Physical Anthropology*, **1(2)**, 119-123.

[15] Singal, P. and Sidhu, L.S. (1983). Age changes in skinfolds, body fat and lean body mass in Jat-Sikh and Bania females during 20 to 80 years. *Anthropology Anz*, **41(3)**, 179-189.

[16] Bose, K., Bisai, S. and Chakraborty, F. (2006) Age variation in anthropometric and body composition characteristics and underweight among male Bathudis: A tribal population of Keonjhar District, Orissa, India. *Collegium Anthropolozicum*, **30(4)**, 771-775.

[17] Sinha, K.P. (1981) The Bishnupriya manipuri language. Calcutta.

[18] Weiner, J.S. and Lourie, J.A., Eds., (1981) Practical human biology. Academic Press, London.

[19] Kushner, R.F., Kunigk, A., Alspaugh, M., Andronis, P.T., Leitch, C.A. and Schoeller, D.A. (1990) Validation of bioelectrical-impedance analysis as a measurement of change in body composition in obesity. *Asia Pacific Journal of Clinical Nutrition*, **52(2)**, 219-223.

[20] Chumlea, W.C. and Baumgartner, R.N. (1989) Status of anthropometry and body composition data in elderly subjects. *Asia Pacific Journal of Clinical Nutrition*, **50 (Suppl 5)**, 1158-1166.

[21] Dangour, A.D. (2003) Cross-sectional changes in anthropometric variables among wapishana and patamona amerindian adults, *Human Biology*, **75(2)**, 227-240.

[22] Roche, A.F., Siervogel, R.M., Chumlea, W.C. and Webb, P. (1981). Grading body fatness from limited anthropometric data. *American Journal of Clinical Nutrition*, **34(12)**, 2831-2838.

[23] Norris, A.H., Lundy, T. and Shock, N.W. (1963) Trend in selected indices of body composition in men between ages of 30 and 80 years. *Annals of the New York Academy of Sciences*, **110(2)**, 623-640.

[24] Deurenberg, P., Weststrate, J.A. and Seidell, J.C. (1991) Body mass index as a measure of body fatness: Age and sex-specific prediction formula. *British Journal of Nutrition*, **65(2)**, 105-114.

[25] Daniels, S.R., Khoury, P.R. and Morrison, J.A. (1997) The utility of body mass index as a measure of body fatness in children and adolescents: Differences by race and gender. *Pediatrics*, **99(6)**, 804-807.

[26] Steen, B. (1988) Body composition and aging. *Nutrition Review*, **46(2)**, 45-51.

[27] Strickland, S.S. and Ulijaszek, S.J. (1993) Body mass index, aging and differential reported morbidity in rural Sarawak. *European Journal of Clinical Nutrition*, **47(1)**, 9-19.

Advances in Bioscience and Biotechnology, 2010, 1, 131-135 **ABB**
doi:10.4236/abb.2010.12018 Published Online June 2010 (http://www.SciRP.org/journal/abb/)

Development and validation of HPTLC method for niacin and simvastatin in binary combination

Pravish Kumar Tiwari, Padmakar Sathe

Department of Chemistry, Ramnarian Ruia College, Mumbai, India.
Email: pravishkumar1981@yahoo.com

Received 21 February 2010; revised 11 March 2010; accepted 28 March 2010.

ABSTRACT

A simple, sensitive and validated HPTLC method has been developed to determine Niacin and simvastatin simultaneously in synthetic mixture form. Chromatographic separation was achieved on a RP18 plate using a mixture of Methanol: Water: Acetic acid (80:20:0.1) at a wavelength of 236 nm. Linearity of the method was found to be in the concentration range of 12.5-37.5 µg/spot for niacin and 0.25-0.75 µg/spot for simvastatin with correlation coefficient greater than 0.999. The method can be used for simultaneous determination of Niacin and Simvastatin.

Keywords: HPTLC; Methanol; Niacin; Simvastatin

1. INTRODUCTION

Niacin (**Figure 1**) chemically designated as Pyridine 3 carboxylic acid reduce triglyceride, levels, is also effective for increasing serum HDL levels [1]. It has also been demonstrated that this drug lowers the incidence of coronary heart disease in humans [1]. A number of analytical methods have been developed for its determination in pharmaceutical formulations or in biofluids either alone or in combination with other drugs [2-8]. These include determination of niacin by liquid chromatography–mass spectrometry [9], HPLC [9-12], flow injection and spectrofluorimetric analysis.

Simvastatin (**Figure 2**), a hypolipidemic drug belonging to the class of pharmaceuticals called statins is chemically designated as [(1S,3R,7R,8S,8aR)-8-[2-[(2R,4R)-4-hydroxy-6-oxo-oxan-2-yl]ethyl]-3,7-dimethyl-1,2,3,7,8,8ahexahydronaphthalen-1-yl] 2,2-dimethylbutanoate. It is used for the treatment of hypercholesterolemia [13]. An HMG-CoA reduces ase inhibitor, acts by decreasing cholesterol synthesis and by increasing low density lipoprotein (LDL) catabolism via increased LDL receptor activity [14]. Different analytical methods have been reported for the determination of simvastatin, which include HPLC [15-17], HPLC-MS/MS [18], spectrophotometer [19].

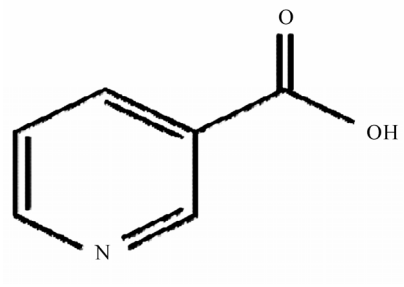

Figure 1. Niacin.

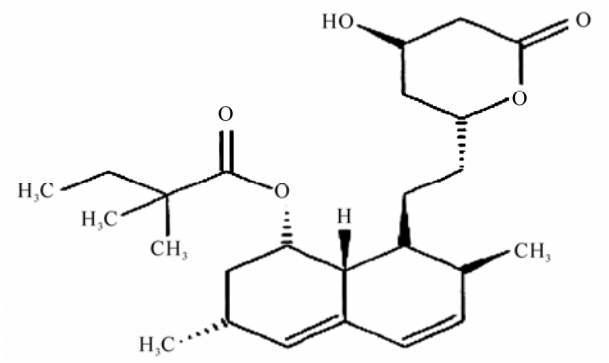

Figure 2. Simvastatin.

It was found that Simvastatin plus niacin provides marked clinical and angiographic ally measurable benefits in patients with coronary disease and low HDL levels [20]. The US Food and Drug Administration (FDA) has approved a fixed-dose combination of niacin and simvastatin for use in patients with complex lipid abnormalities where treatment with niacin or simvastatin alone is not sufficient [21] The FDA has approved maximum dose of niacin 1000mg and 20 mg of simvastatin per tab. The combine dosage form of Niacin and simvastatin are available in market.

According to the information collected from literature there is no reported method for simultaneous determination of Niacin and simvastatin. In the present work we have focused on deciding the optimum chromatographic

conditions for the simultaneous determination of Niacin and simvastatin in a pharmaceutical preparation.

We describe in this paper a simple, sensitive and validated HPTLC method for the simultaneous determination of Niacin and Simvastatin .The developed method can be applied successfully for quality control and for other analytical purposes.

2. MATERIAL AND METHODS

2.1. Chemicals and Reagents

Niacin and simvastatin reference substances with claimed purity of 99.70% and 99.65% respectively were taken from Precise Pharma (Turbhe, mumbai) Methanol (HPLC grade), Triethyl amine and acetic acid (analytical reagent grade) were purchased from Merck (Mumbai). All excepients used were of pharmaceutical grade. Mobile phase was filtered using 0.45 μm cellulose acetate filters made by Millipore (USA) whereas; Whatmann filter papers No. 41 (purchased from the local market) were used in the preparation of sample solution.

2.2. Chromatographic Conditions

The chromatographic estimation were performed using stationary phase precoated C18 aluminum sheets (10 × 10 cm, prewashed with methanol and dried in oven at 50℃ for 5 min) mobile phase, Water: Methanol: Acetic acid (20:80:0.1), chamber and plate saturation time of 30 min, migration distance allowed was 74 mm, wavelength scanning was done at 236 nm, keeping the slit dimension at 5 × 0.45 mm.

2.3. Preparation of Standard Solution

A Stock solution of niacin and simvastatin was prepared at about 10000 μg/ml and 200 μg/ml respectively in Diluent. Make standard in duplicate and spot 2.5 μl of each solution.

2.4. Determination of Simvastatin and Niacin in There Combined Dosage Forms

The content of twenty tablets where taken and weighed .powder equivalent to Niacin 1000 mg and 20 mg simvastatin in 100 ml volumetric flask add 50 ml of diluent and flask was sonicated for 5 min .The flask was sonicated and the volume was diluted to the mark with diluent .The above solution was filtered using what man filter paper No. 1.

2.5. Linearity

Linearity of the proposed method was checked by analyzing seven solutions in the range of 5000-15000 μg/ml for niacin (5000, 7500, 10000, 12500, 15000 μg/ml) and 100-300 μg/ml for simvastatin (100,150,200,250,300 μg/ml). Each level was made in triplicate and spot 2.5 μl of each solution.

2.6. Accuracy

Method accuracy was performed by adding known amounts of niacin and simvastatin to the pre analyzed sample and then comparing the added concentration with the found concentration. Three levels of solutions were made which correspond to 50, 100 and 150% of the nominal analytical concentration. Each level was made in triplicate and spot 2.5 μl of each solution.

2.7. Specificity

Commonly used exceipients (starch, microcrystalline cellulose and magnesium stearate, lactose,) were spiked in to a pre weighed quantity of drugs .The chromatogram was taken by appropriate dilution and the quantities of drug were determined.

2.8. Ruggedness

Ruggedness of the method was performed by two different parameters *i.e.* days and analyst .The results of estimation by proposed method are very much similar under variety of condition.

2.9. Precision

For evaluating the within-day precision, results of six replicate analyses of samples were calculated on a single day. The between-day precision was calculated from the same samples analyzed on different days.

2.10. LOD and LOQ

For calculating the LOD and LOQ values, solutions with known decreased concentrations of analytes were injected into the HPTLC system. The limit of detection (LOD) and quantification (LOQ) were then measured by calculating the minimum level at which the analytes can be readily detected (signal to noise ratio of 3:1) and quantified (signal to noise ratio of 10:1) with accuracy, respectively.

3. RESULTS

In the present work conditions were optimized for the development and validation of a simple and accurate HPTLC method for the simultaneous determination of niacin and simvastatin in synthetic mixture form. Method development was started with water and methanol in the ratio of 50:50 (v/v). At this composition although both components were separated large resolution but peak shape was not good. The methanol contents of the mobile phase were then increased to decrease resolution and R.F and 0.1% acetic acid was added to reduce the tailing. At the composition of 20:80:0.1(Water: Methanol: Acetic acid) both components were separated with a good resolution and good peak shape. The most appropriate mobile phase composition was thus found to be Water: Methanol; Acetic acid in the ratio of 20:80:0.1.

Under the Described experimental conditions, sharp peaks that belong to niacin and simvastatin were obtained at retention factor of 0.100 and 0.65 minutes respectively as shown in **Figure 3**.

The developed chromatographic method was validated using ICH guidelines [22]. Validation parameters performed include linearity, limit of detection and quantitation, selectivity, ruggedness, accuracy and repeatability the calibration curve was linear over the concentration range of 5000-15000 µg/ml for niacin and 100-300 µg/ml for simvastatin. The correlation coefficient in both cases was found to be greater than 0.999 which manifests a linear relationship between concentration and the peak area. The linear regression equation for niacin was found to be Y = 3.2342 X + 149.27 with correlation coefficient equal to 0.999. The linear regression equation for simvastatin was found to be Y = 11.499 X + 4.8 with value of correlation coefficient equal to 0.99997. In this study, the LOD was found to be 1200 µg/ml and 24 µg/ml for niacin and simvastatin respectively. The LOQ was found to be 4000 µg/ml and 80 µg/ml for niacin and simvastatin respectively. The recovery and the relative standard deviation for each of the analytes are given in **Table 1**.

The results of within-day and between-day precision are presented in **Table 2**.

Chromatogram of niacin and simvastatin in sample in given in **Figure 4** showing selectivity of the proposed method.

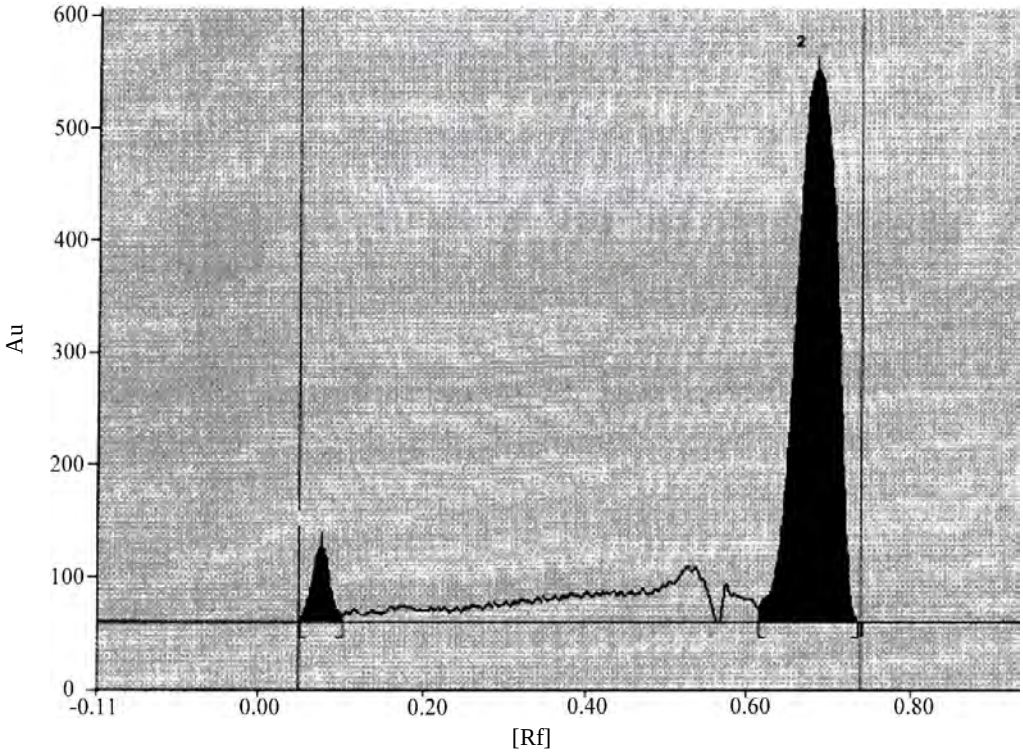

Figure 3. Chromatograms of Niacin and simvastatin reference substances.

Table 1. Accuracy of the proposed HPTLC method.

compound	Level (%)	n	Added Conc.µg/ml	Found Conc.µg/ml	% recovery	RSD (%)
Niacin	50	3	5000	4920	98.4	0.68
	100	3	10000	9880	98.8	0.35
	150	3	15000	15120	100.8	0.35
Simvastatin	50	3	100	98.00	98.0	1.63
	100	3	200	205.0	102.5	0.21
	150	3	300	302.0	100.6	0.67

Table 2. Precision of the proposed HPTLC method.

			Within a day		Between a day	
	Concn µg /ml	No of Inj	Concn. found µg/ml Mean	Rsd %	Concn. found µg/ml Mean	Rsd %
Niacin	5000	3	5000.20	0.23	5009.10	0.59
	10000	3	10030.12	0.36	10020.22	0.16
	15000	3	14996.33	0.88	15000.13	0.28
Simvasatin	100	3	100.22	0.55	100.02	0.15
	200	3	200.22	0.77	201.32	0.37
	300	3	301.55	0.99	300.15	0.68

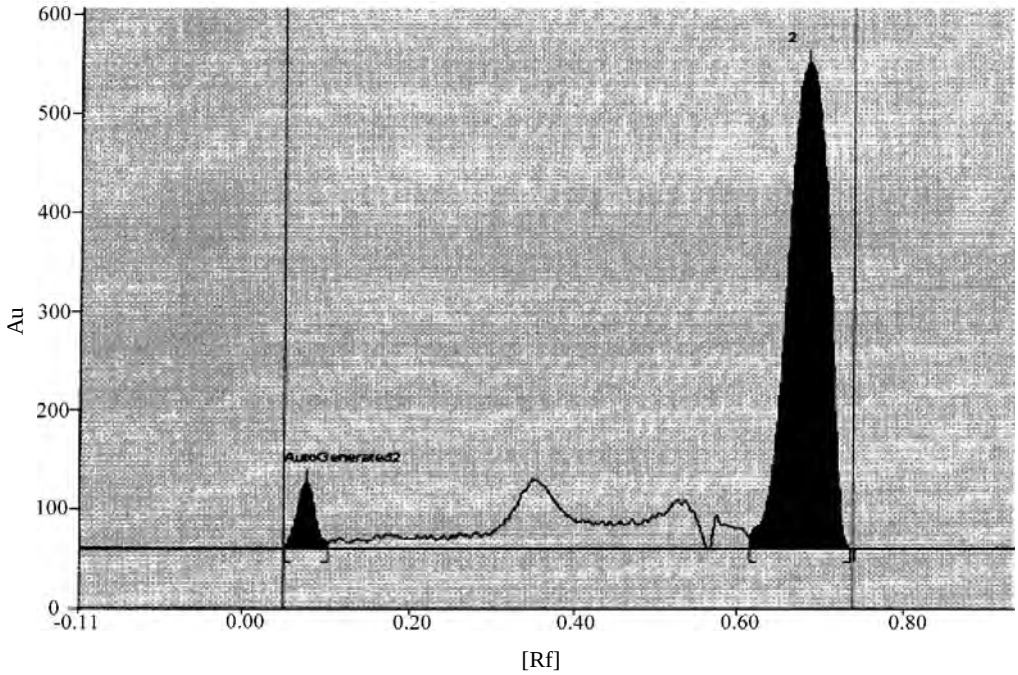

Figure 4. Chromatograms of Niacin and simvastatin in sample solution.

4. CONCLUSIONS

A simple and accurate reverse phase HPTLC method has been developed for the simultaneous determination of niacin and simvastatin. The method was validated by testing its linearity, accuracy, precision, limits of detection and quantization, selectivity and robustness.

5. ACKNOWLEDGEMENTS

The authors are great full to precise pharma for providing gift sample of simvastain and niacin.

REFERENCES

[1] Susman (1995) Niacin reduces triglycerides, increases good cholesterol in diabetics. Doctors Guide Publishing Limited.

[2] Kumar, V. and Shah, R.P., (2008) LC and LC–MS methods for the investigation of polypills for the treatment of cardiovascular diseases: Part 1. Separation of active components and classification of their interaction/degradation products. *Saranjit Singh Journal of Pharmaceutical and Biomedical Analysis*, **47(3)**, 508-515.

[3] Chaudhari, B.G., Patel, N.M., Shah, P.B. and Modi, K.P. (2006) Development and validation of a HPTLC method for the simultaneous estimation of atorvastatin calcium and ezetimibe. *Indian Journal of pharamaceutical Science*, **68(6)**, 793-796.

[4] Jain, N. and Raghuwanshi, R. (2008) Development and validation of RP-HPTLC method for simultaneous estimation of atorvastatin calcium and fenofibrate in tablet

dosage forms. *Deepti Jain Indian Journal of pharmaceutical Science*, **70(2)**, 263-265.

[5] Kova´, L.N. and Atı´nsky´, D.S., (2008) HPLC methods for the determination of simvastatin and atorvastatin. *PetrSolich Trac Trends in Analytical Chemistry*, **27(4)**, 352-367.

[6] Jemal, M., Ouyang, Z. and Powell, M.L.(2000) A strategy for a post-method-validation use of incurred biological samples for establishing the acceptability of a liquid chromatography/tandem mass-spectrometric method for quantitation of drugs in biological samples. *Journal Pharm Biomed Anal*, **16(16)**, 1538-1547.

[7] Zhang, N., Yang, A., Rogers, J.D. and Zhao, J.J. (2004) *Journal Pharm Biomed Anal*, **34**, 175-187.

[8] Nirogi, R., Mudigonda, K. and Kandikere, V. (2004) Chromatography–mass spectrometry methods for the quantitation of statins in biological samples. *Journal of pharmaceutical and Biomedical Analysis*. **44**, 379-387.

[9] Research & Development report, may 2000, Australian Government Analytical Laboratories.

[10] Khor, S.-C. and Tee, E.-S. (1996) Development of a HPLC method for the simultaneous determination of several b-vitamins and ascorbic acid. *Malaysian Journal of Nutrition*, **2(1)**, 49-65.

[11] Euro Fir guidelines for assessment of Methods of Analysis KellieWindahi, V Craige Trenerry and Caroline Ward.

[12] Pfuhl, P., Karcher, U., Haring, N., Baumeister, A., Tawab, M.A. and Schubert-Zsilaveez, M. (2005) Simultaneous Determination of Niacin, Niacinamide and Nicotinuric Acid in Human Plasma. *Journal of Pharmaceutical and Biomedical Analysis*, **36(5)**, 1045-1052.

[13] Todd, P.A. and Goa, K.L., (1990) Simvastatin: A review of its pharmacological properties and therapeutic potential in hyperlipidaemia. *Drugs*, **40(4)**, 583-607.

[14] Pasternak, R.C., Smith, S.C.J., Merz, C.N.B., Grundy, S.M., Cleeman, J.I. and Lenfant, C. (2002) ACC/ AHA/ NHLBI clinical advisory on the use and safety of statins. *Journal Of The American Heart Association*, **40**, 567-572.

[15] Dave, T. and Diab, E. Analysis of Simvastatin Tablets by High Speed LC. *Application Notes* 405, Thermo Fisher Scientific, San Jose, 1-6.

[16] Ashfaq, M., Khan, I.U., Quatab, S.S. and Razz, S.N. (2007) Hplc determination of ezetimibe and simvastatin in pharmaceutical formulations. *Journal of the Chilean Chemical Society*, **52(3)**, 1220-1224.

[17] Ashfaq, M., Khan, I.U. and Asghar, M.N. (2008) Development and Validation of Liquid Chromatographic Method for Gemfibrozil and Simvastatin in Binary Combination. *Journal of the Chilean Chemical Society*, **53(3)**, 1617-1619.

[18] Yang, H., Feng, Y. and Luana, Y. (2003) Determination of Simvastatin in human plasma by liquid chromatography–mass spectrometry. *Journal of Chromatography B*, **785(2)** 369-375.

[19] Basavaiah, K. and Tharpa, K. (2008) The development and validation of visible spectrophotometric methods for simvastatin determination in pure and the tablet dosage forms. *Chemical Industry and Chemical Engineering Quarterly*, **14(3)**, 205-210.

[20] Brown, G.B., Zhao, X.-Q., Chait, A., Fisher, L.D., Cheung, M.C., Morese, J.S., Dowdy, A.A., Marino, E.K., Bolson, E.L., Alaupovic, P., Frohlich, J. and Albers, J.J. (2001) Simvastatin and niacin, antioxidant vitamins, or the combination for the prevention of coronary disease. *The New England Journal of Medicine*, **345(22)**, 1583-1592.

[21] Riordan, M.O. and Waknine, Y. (2008) FDA approves combination niacin and simvastatin. Medical News, Medscape.

[22] I.C.H (Q2A) (1994) Note for guidance on validation of analytical methods, definition and terminology. *International Conference on Harmonization*, Human Medicines Evaluation Unit, the European Agency for the Evaluation of Medicinal Products.

Advances in Bioscience and Biotechnology, 2010, 1, 136-144 **ABB**
doi:10.4236/abb.2010.12019 Published Online June 2010 (http://www.SciRP.org/journal/abb/)

DNA fingerprinting of *Bacillus cereus* from diverse sources by restriction fragment length polymorphism analysis

Swarnakaran Hemalatha, Narasimhan Banu

Department of Biotechnology Vels University, Chennai, India.
Email: hemas81@gmail.com

Received 26 March 2010; revised 10 April 2010; accepted 12 April 2010.

ABSTRACT

***Bacillus cereus* is an opportunistic pathogen causing food poisoning manifested by diarrhoeal or emetic syndrome. It is closely related to animal and human pathogens *Bacillus anthracis* and the insect pathogen *Bacillus thuringiensis*. In the present study, antibiotic resistance, heavy metal tolerance & molecular typing of *Bacillus cereus* from diverse sources such as soil, sewage water, air, fresh water, sea water and milk were studied. *Bacillus cereus* resistant to Penicillin (10 units/ml) and Amoxycillin (10 µg/ml); sensitive to Cobalt and Mercury even at 1 mM concentration were determined. All the isolate had plasmid ranging in number from 3-5 and their molecular weight ranged from 3.0 kb-2.0 kb. Plasmid DNA band specific to 6,557 bp has been found in *Bacillus cereus* isolated from sewage water, air, fresh water, sea water and milk.**

Keywords: *Bacillus Cereus*; Antibiotic Resistance; Heavy Metal Tolerance; RFLP; DNA Finger Printing

1. INTRODUCTION

The members of genus *Bacillus* encompass a great diversity of bacterial species and have a ubiquitous distribution in the environment. Because of their resistant spores and the capacity of vegetative cells to secrete a wide variety of enzymes, this genus is important not only for the production of commercially important bio molecules (insecticides, enzymes, antibiotics, etc.), but also as a source of spoilage or pathogenic organisms transmitted through foods and beverages [1]. *Bacillus anthracis*, *Bacillus cereus*, *Bacillus thuringiensis* are members of the *Bacillus cereus* group of bacteria. They differ widely in their phenotypes and pathological effects. *Bacillus cereus* is probably a ubiquitous soil bacterium. In contrast to their differences in phenotypes, by sequence analysis of nine chromosomal genes, *Bacillus anthracis* can be considered as lineage of *Bacillus cereus*. This is because of potential of horizontal gene transfer within *Bacillus cereus* group [2]. The sequencing and analysis of type strain *Bacillus cereus* ATCC 14579 was reported [3]. The comparative analysis enabled to determine plasmid independent species specific marker. *Bacillus cereus* produces beta-lactamases, unlike *Bacillus anthracis*, and so is resistant to beta-lactum antibiotics; it is usually susceptible to treatment with Clindamycin, Vanomycin, Gentamycin, Chloramphenicol, and Erythromycin [4].

Bacillus cereus which is ubiquitous in the environment and acting as a source of spoilage through air to food samples needs suitable discriminatory typing methods to facilitate epidemiological investigation. It is of paramount importance to establish a more efficient, easily handled and more objective methodology. In recent times various molecular tools are in experimental protocols. The molecular techniques are major tools for the analysis of micro organisms from food and other biological substances. These techniques provide ways to screen for a broad range of agents in a single test [5]. Molecular techniques are used for rapid differentiation of species and strain identification. Among them RFLP fingerprinting technique is regarded as the most sensitive method for strain identification. RFLP can replace AFLP, RAPD in the estimation of genetic diversity [6]. In the current study, the fingerprinting of *Bacillus cereus* from diverse sources such as soil, sewage water, air, fresh water, sea water and milk were studied by molecular analysis in parallel with conventional phenotype based methodologies.

2. MATERIALS AND METHODS

Six different samples *viz*., soil, sewage water, air, fresh water, sea water and milk were collected only once from in and around Chennai. The soil, water and milk samples were serially diluted and spread on nutrient agar medium. The bacteria were isolated from air by open plate method. All the plates were kept for 24 hours incubation at 37˚C. The isolated bacterial colonies were purified to homogeneity by quadrant streaking, stored in nutrient agar slants and sub-cultured periodically. The bacteria

isolated were identified based on physical characterisation and the biochemical tests outlined in Bergey's Manual of Determinative Bacteriology [7].

The sensitivity/resistance of isolates to various antibiotics such as Amoxicillin (10 µg/ml), Chloramphenicol (30 µg/ml), Kanamycin (30 µg/ml), Nalidixic acid (30 µg/ml), Penicillin (10 units/ml) and Streptomycin (25 µg/ml) were studied using microbial sensitivity disc (Hi-Media) by disc diffusion method. 24 hours culture of *Bacillus cereus* was swabbed on Nutrient agar plates under sterile condition in laminar air flow and the antibiotics discs of appropriate concentration were placed on agar plates and incubated at 37˚C. After incubation for 24 hours, the plates were observed for growth. A clear zone around the disc was evidence for antibiotic resistance/susceptibility of the isolate. Diameter of the zones of inhibition was measured in millimetres. Nutrient agar plates without antibiotics served as control.

The tolerance of bacterial isolates to various heavy metals such as Cobalt (Cobalt chloride), Iron (Ferrous sulphate), Mercury (Mercury sulphate), Zinc (Zinc sulphate) and Lead (Lead acetate) was studied by inoculating loopful of overnight grown cultures on Nutrient agar plates amended with 1, 3 and 5 mM concentrations of heavy metals and incubated at 37˚C. After 24 hours of incubation, the plates were observed for growth. Nutrient agar plates without heavy metal served as control.

The plasmid DNA was isolated based on alkali lysis method [8]. The resulting DNA preparation was quantified by UV spectrophotometer and screened by agarose gel electrophoresis and genetic diversity was estimated by restriction endonuclease digestion.

3. RESULTS AND DISCUSSION

Bacillus cereus was isolated from six different samples such as soil, sewage water, air, fresh water, sea water and milk by crowded plate technique. All the isolates were morphologically different in their growth in nutrient agar medium at 37˚C (**Table 1**; **Figures 1** and **2**) but they are biochemically similar. In antibiotic resistance/ sensitivity spectrum, *Bacillus cereus* isolated from different sources such as soil, sewage water, air, fresh water, sea water and milk samples were sensitive to antibiotics such as Chloramphenicol (30 µg/ml), Kanamycin (30 µg/ml), Nalidixic acid (30 µg/ml) and Streptomycin (25 µg/ml). All *Bacillus cereus* isolates were resistant to Penicillin (10 units/ml) and Amoxycillin (10 µg/ml) (**Table 2**; **Figures 3** and **4**). The zone of inhibition of Amoxycillin, Chloramphenicol, Kanamycin, Nalidixic acid, Penicillin and Streptomycin against different isolates of *Bacillus cereus* was measured in millimetres using standard recommendations. The zone of inhibition for Chloramphenicol, Kanamycin, Nalidixic acid and Streptomycin against *Bacillus cereus* obtained from soil was 9 mm, 7 mm, 4 mm and 8 mm respectively. The zone of inhibition for Chloramphenicol, Kanamycin, Nalidixic acid and Streptomycin against *Bacillus cereus* obtained from sewage water was 9 mm, 8 mm, 6 mm and 8 mm respectively. The zone of inhibition for Chloramphenicol, Kanamycin, Nalidixic acid and Streptomycin against *Bacillus cereus* obtained from air was 7 mm, 7 mm, 8 mm and 9 mm respectively. The zone of inhibition for Chloramphenicol, Kanamycin, Nalidixic acid and Streptomycin against *Bacillus cereus* obtained from fresh water was 8 mm, 6 mm,

Table 1. Colonial morphology of *Bacillus cereus* isolates from diverse sources (Jonathan, 2004).

S. No	Cultural characteristics	*Bacillus cereus* Isolate					
		Soil	Sewage Water	Air	Fresh Water	Sea Water	Milk
1.	Medium	Nutrient Agar	Nutrient Agar	Nutrient Agar	Nutrient Agar	Nutrient Agar	Nutrient Agar
2.	Colour	Creamy	Creamy	White	White	Creamy	Creamy
3.	Shape	Spherical	Circular	Circular	Circular	Circular	Spherical
4.	Size	1.6 mm	0.3 mm	0.4 mm	0.3 mm	0.9 mm	1.5 mm
5.	Surface	Dull and dry	Dull	Dull	Dull	Dull	Dull
6.	Edge	Rhizoid	Entire	Entire	Entire	Entire	Undulate
7.	Opacity	Opaque	Opaque	Translucent	Translucent	Opaque	Opaque
8.	Degree of Growth	Profuse	Moderate	Moderate	Moderate	Moderate	Profuse
9.	Elevation	Flat	Low convex	Low convex	Low convex	Low Convex	Low convex
10.	Consistency	Butyrous	Friable	Friable	Friable	Friable	Friable
11.	Emulsifiability	Difficult	Easy	Easy	Easy	Easy	Easy

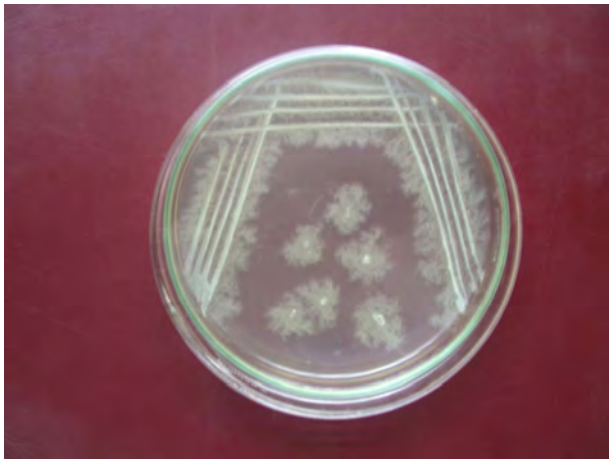

***Bacillus cereus* from Soil**

***Bacillus cereus* from Fresh water**

***Bacillus cereus* from Sewage water**

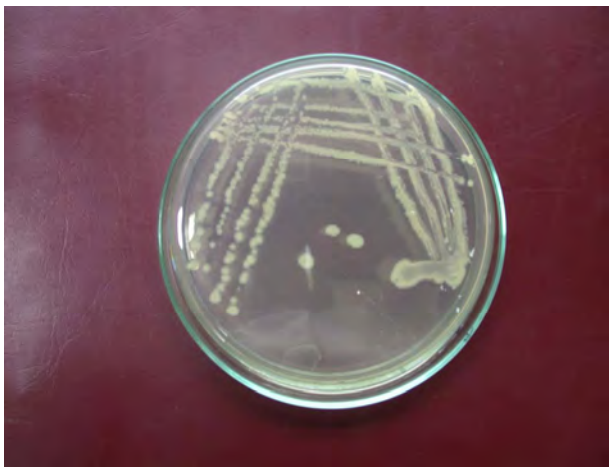

***Bacillus cereus* from Sea water**

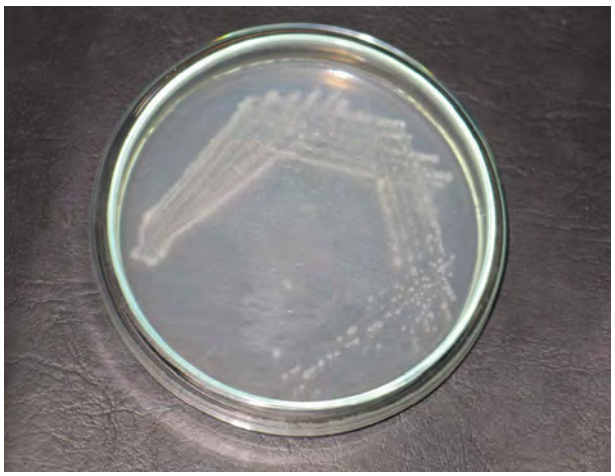

***Bacillus cereus* from Air**

Figure 1. *Bacillus cereus* isolate from diverse sources.

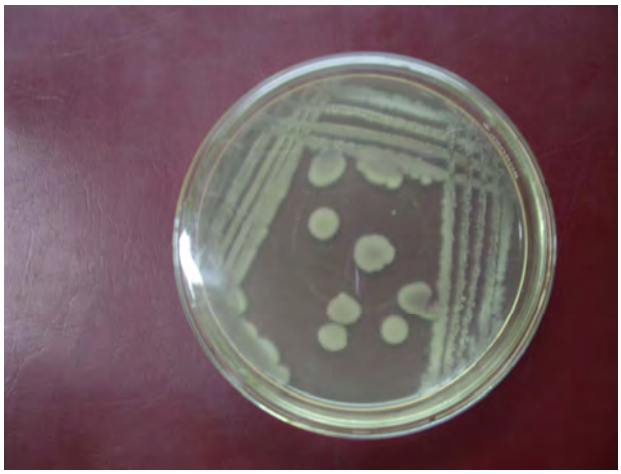

***Bacillus cereus* from Milk**

Figure 2. *Bacillus cereus* isolate from diverse sources.

9 mm and 7 mm respectively. The zone of inhibition for Chloramphenicol, Kanamycin, Nalidixic acid and Streptomycin against *Bacillus cereus* obtained from sea water was 9 mm, 6 mm, 6 mm and 7 mm respectively. The zone of inhibition for Chloramphenicol, Kanamycin, Nalidixic acid and Streptomycin against *Bacillus cereus*

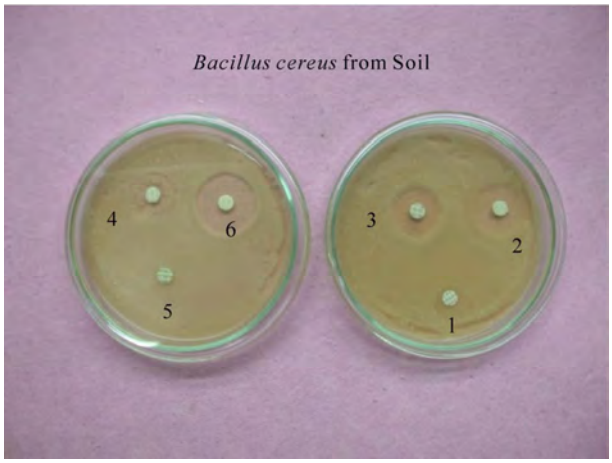

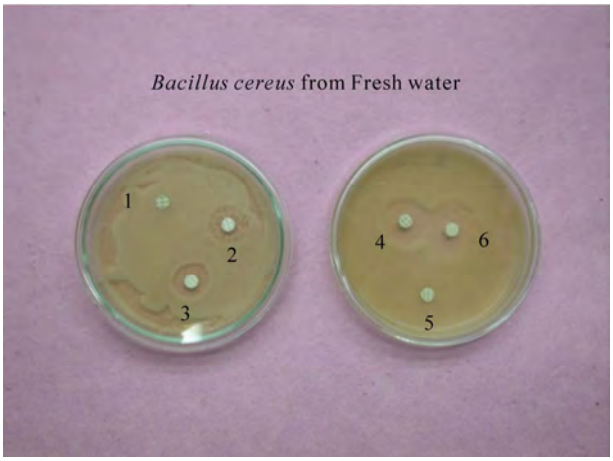

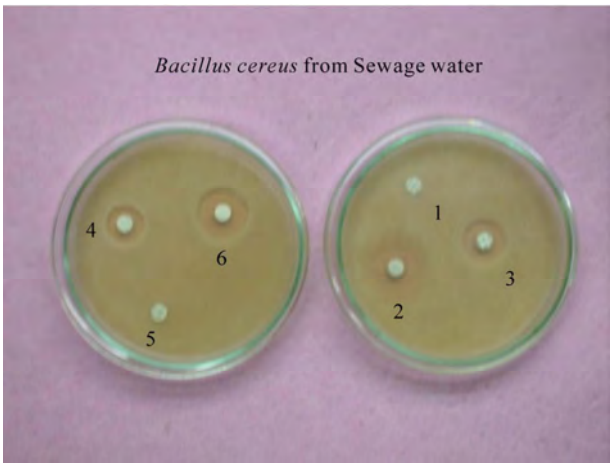

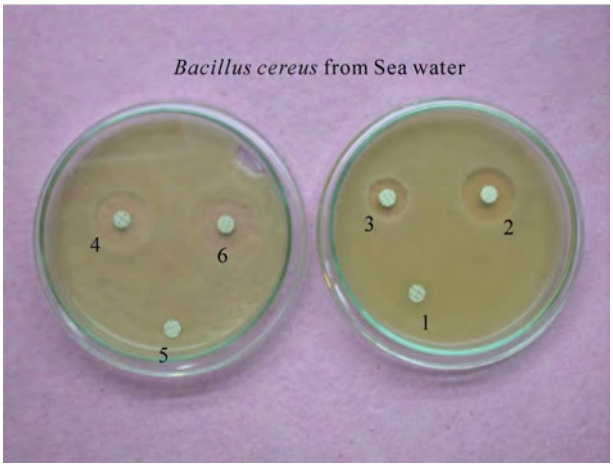

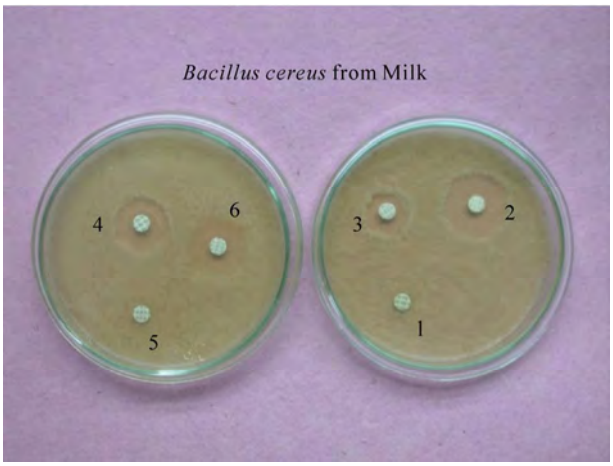

1. Amoxycillin, 2. Chloramphenicol, 3. Kanamycin, 4. Nalidixic acid, 5. Penicillin, 6. Streptomycin

Figure 3. Antibiotic resistance/sensitivity spectrum of *Bacillus cereus* isolate from diverse sources.

1. Amoxycillin, 2. Chloramphenicol, 3. Kanamycin, 4. Nalidixic acid, 5. Penicillin, 6. Streptomycin

Figure 4. Antibiotic resistance/sensitivity spectrum of *Bacillus cereus* isolate from diverse sources.

obtained from milk was 9 mm, 6 mm, 7 mm and 7 mm respectively. Except *Bacillus cereus* from air and fresh water all the other *Bacillus cereus* isolate have shown maximum zone of inhibition (9 mm) for Chloramphenicol (**Table 3**). Therefore Chloramphenicol can be recommended for *Bacillus cereus* infections. Plasmid mediated bacterium will exert resistance towards antimicrobials [9]. Therefore all the *Bacillus cereus* isolate should

Table 2. Antibiotic Resistance /Sensitivity spectrum of *Bacillus cereus* isolate from diverse sources

Antibiotics	Concentration (µg /ml)	*Bacillus cereus* Isolate					
		Soil	Sewage Water	Air	Fresh Water	Sea Water	Milk
Amoxycillin	10	–	–	–	–	–	–
Chloramphenicol	30	+	+	+	+	+	+
Kanamycin	30	+	+	+	+	+	+
Nalidixic acid	30	+	+	+	+	+	+
Penicillin	10	–	–	–	–	–	–
Streptomycin	25	+	+	+	+	+	+

– Sensitive
+ Resistant

Table 3. The measurement of zone of inhibition of antibiotics against *Bacillus cereus* isolate from diverse sources.

Bacillus cereus Isolate	Antibiotics (µg /ml)					
	Amoxycillin	Chloramphenicol	Kanamycin	Nalidixic acid	Penicillin	Streptomycin
Soil	–ve	9 mm	7 mm	4 mm	–ve	8 mm
Sewage Water	–ve	9 mm	8 mm	6 mm	–ve	8mm
Air	–ve	7 mm	7 mm	8 mm	–ve	9 mm
Fresh Water	–ve	8 mm	6 mm	9 mm	–ve	7 mm
Sea Water	–ve	9 mm	6 mm	6 mm	–ve	7 mm
Milk	–ve	9 mm	6 mm	7 mm	–ve	7 mm

– ve Negative

possess plasmid DNA in their genetic makeup.

Bacillus cereus was also tested for their heavy metal tolerance. Five heavy metals namely Cobalt (Cobalt chloride), Iron (Ferrous sulphate), Mercury (Mercury sulphate), Zinc (Zinc sulphate) and Lead (Lead acetate) at a concentration of 1-5 mM were selected to conduct present study. All the isolates were sensitive to Cobalt and Mercury (**Table 4**; **Figures 5, 6** and **7**). *Bacillus cereus* isolated from soil and air was sensitive to Iron at 5 mM concentration. *Bacillus cereus* isolated from fresh water, sewage water and milk were sensitive to zinc at 3 mM concentration. All the isolate were sensitive to Zinc at 5 mM concentration. Being sensitive no growth was observed in their plates. These results revealed that the presence of heavy metal such as Cobalt and Mercury even at 1mM concentration was highly toxic to *Bacillus cereus* which is distributed widely in the environment and food samples and they will pose a serious threat to their metabolism in the natural environment. All the isolates showed resistance to Lead. This could be attributed due to the presence of plasmid. Transferable plasmid encodes resistance to various heavy metals [10]. In the present work, a high frequency of resistance to heavy metal was observed in *Bacillus cereus* isolated from sewage water.

Based on antibiotic resistance/susceptibility spectrum and heavy metal tolerance spectrum of *Bacillus cereus* isolated from different sources, it was not possible to identify whether they belonged to same group or not. Second level information for a bacterial cell other than sequencing of bacterial genome can be obtained only by using any of the molecular techniques. Therefore in the present study Restriction Fragment Length Polymorphism (RFLP) was analysed to estimate genetic diversity of *Bacillus cereus* from different sources and usefulness of RFLP as an identification tool in the genus at sub species level.

The native plasmid profile of all the six *Bacillus cereus* isolates after alkali lysis was observed on 1% agarose gel electrophoresis (**Figure 8**). All the *Bacillus cereus* isolate have shown plasmid number ranging from 3-5. *Bacillus cereus* isolated from sewage water has 5

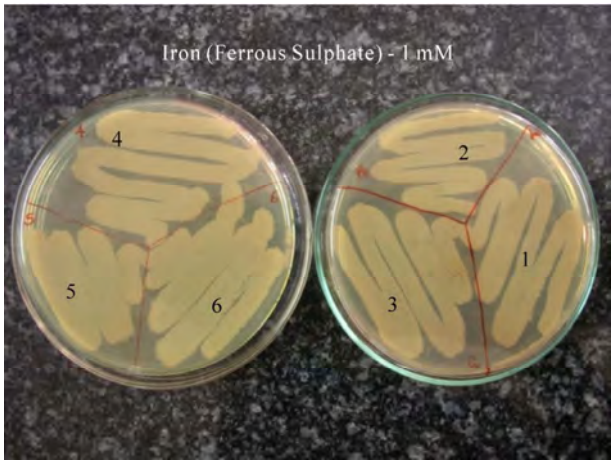

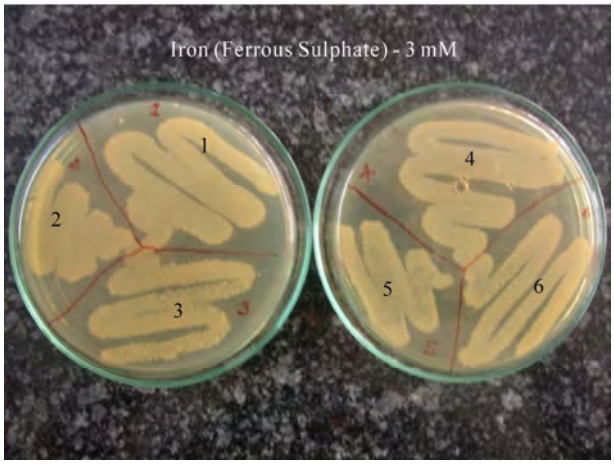

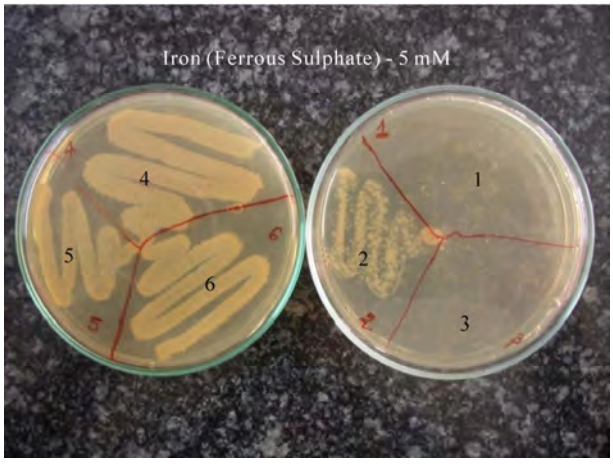

1. *Bacillus cereus* from Soil, 2. *Bacillus cereus* from Sewage water, 3. *Bacillus cereus* from Air, 4. *Bacillus cereus* from Fresh water, 5. *Bacillus cereus* from Sea water, 6. *Bacillus cereus* from Milk

Figure 5. Heavy Metal tolerance spectrum of *Bacillus cereus* isolate from diverse sources.

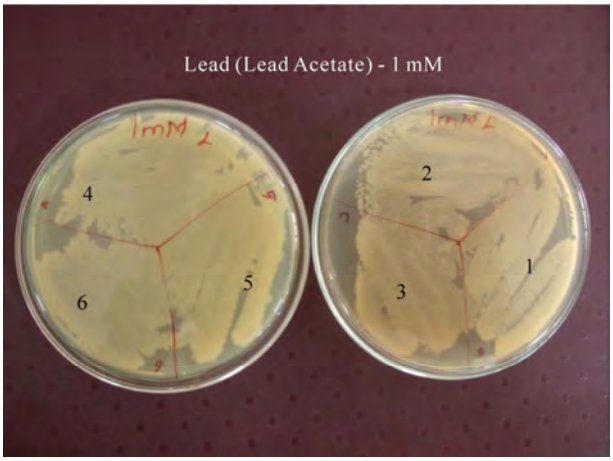

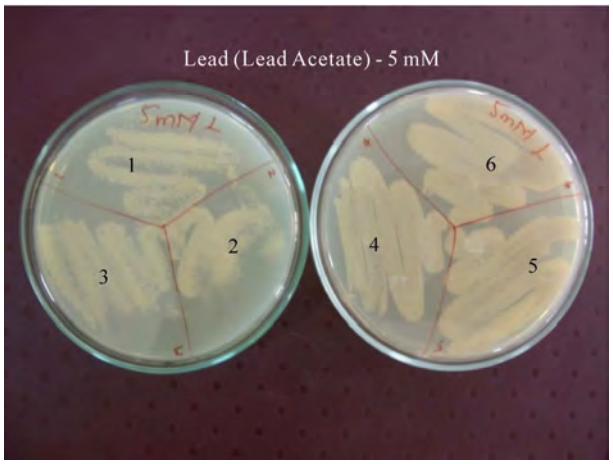

1. *Bacillus cereus* from Soil, 2. *Bacillus cereus* from Sewage water, 3. *Bacillus cereus* from Air, 4. *Bacillus cereus* from Fresh water, 5. *Bacillus cereus* from Sea water, 6. *Bacillus cereus* from Milk

Figure 6. Heavy Metal tolerance spectrum of *Bacillus cereus* isolate from diverse sources.

plasmid in number. The size of the plasmid DNA of different *Bacillus cereus* ranged from 3.0 kb-2.0 kb type as compared with molecular weight marker DNA. Distinct band pattern corresponding to 2.0 kb DNA was seen in *Bacillus cereus* isolated from soil, sewage water and fresh water. Though they are isolated from different

Table 4. Heavy Metal Tolerance Spectrum of *Bacillus cereus* isolate from different sources.

Heavy metals	Concentration (µg /ml)	*Bacillus cereus* Isolate					
		Soil	Sewage water	Air	Fresh water	Sea water	Milk
Cobalt(Cobalt chloride)	1	–	–	–	–	–	–
	3	–	–	–	–	–	–
	5	–	–	–	–	–	–
Iron (Ferrous sulphate)	1	+	+	+	+	+	+
	3	+	+	+	+	+	+
	5	–	+	–	+	+	+
Mercury (Mercury sulphate)	1	–	–	–	–	–	–
	3	–	–	–	–	–	–
	5	–	–	–	–	–	–
Lead (Lead acetate)	1	+	+	+	+	+	+
	3	+	+	+	+	+	+
	5	+	+	+	+	+	+
Zinc (Zinc sulphate)	1	+	+	+	+	+	+
	3	+	+	+	–	–	–
	5	–	–	–	–	–	–

–Sensitive
+ Resistant

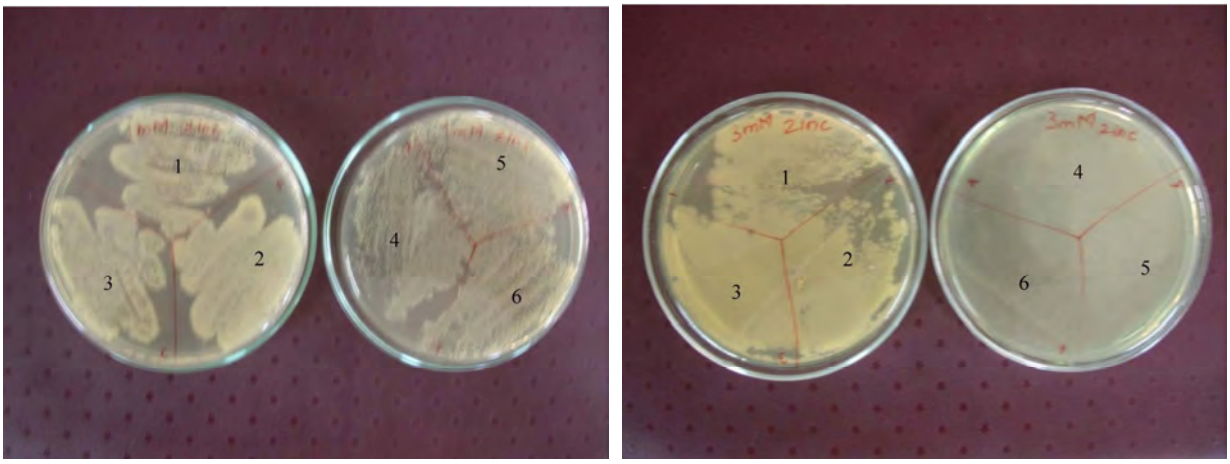

Zinc (Zinc Sulphate)—1 mM Zinc (Zinc Sulphate)—3 mM

1. *Bacillus cereus* from Soil, 2. *Bacillus cereus* from Sewage water, 3. *Bacillus cereus* from Air, 4. *Bacillus cereus* from Fresh water, 5. *Bacillus cereus* from Sea water, 6. *Bacillus cereus* from Milk

Figure 7. Heavy Metal tolerance spectrum of *Bacillus cereus* isolate from diverse sources.

sources, all the isolates have shown similar molecular weight plasmid DNA. The DNA was quantified using UV spectrophotometry. All the isolates had DNA concentration ranging from 0.372 µg/ml–0.79 µg/ml (**Table 5**). *Bacillus cereus* isolated from air had the highest plasmid DNA concentration (0.802 µg/ml) followed by

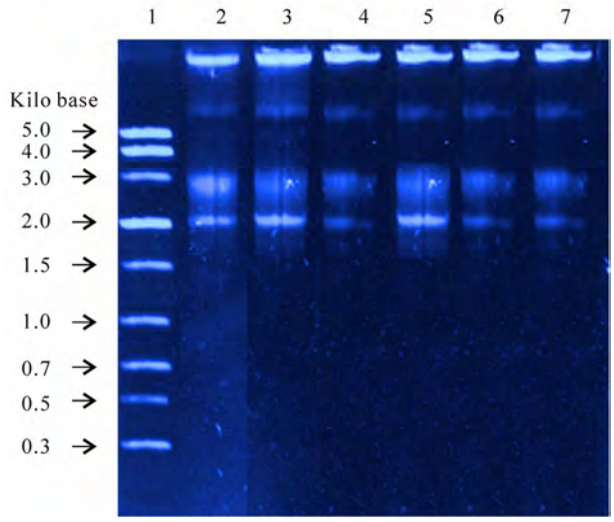

Lane 1—1 Kb DNA ladder, Lane 2—*Bacillus cereus* from Soil, Lane 3—*Bacillus cereus* from Sewage water, Lane 4—*Bacillus cereus* from Air, Lane 5—*Bacillus cereus* from Fresh water, Lane 6—*Bacillus cereus* from Sea water, Lane 7—*Bacillus cereus* from Milk

Figure 8. Gel photograph showing plasmid DNA profile of *Bacillus cereus.*

Table 5. Determining concentration and purity of DNA.

Bacillus cereus isolate	Absorbance at OD 260 nm	Absorbance at OD 280 nm	A260/280	Concentration of DNA (µg/ml)
Soil	0.217	0.122	1.7	0.5425
Sewage water	0.176	0.093	1.8	0.44
Air	0.321	0.182	1.76	0.802
Fresh water	0.149	0.082	1.8	0.372
Sea water	0.316	0.175	1.8	0.79
Milk	0.170	0.090	1.8	0.425

Bacillus cereus from sea water (0.79 µg/ml) and *Bacillus cereus* from soil (0.54 µg/ml). The DNA obtained by alkali lysis was sufficient to carry out restriction digestion since only nanogram quantity is required to carry out RFLP. The DNA obtained was free of protein contaminants and RNA since absorbance ratio between 260 and 280 nm was 1.8 which determines pure DNA.

Type II restriction endonucleases are most important tools in gene manipulation techniques. Hind III are very useful in modern science particularly in DNA sequencing and mapping. Hind III restriction endonuclease performs very specific cleavage of DNA and they cleave only at their specific recognition site. Hind III utilizes a common mechanism of recognition and catalyses of DNA found in other type II enzymes such as Eco RI, Bam HI and Bgl II. Hind III restriction enzyme is sufficient to generate unique fragment of DNA molecule.

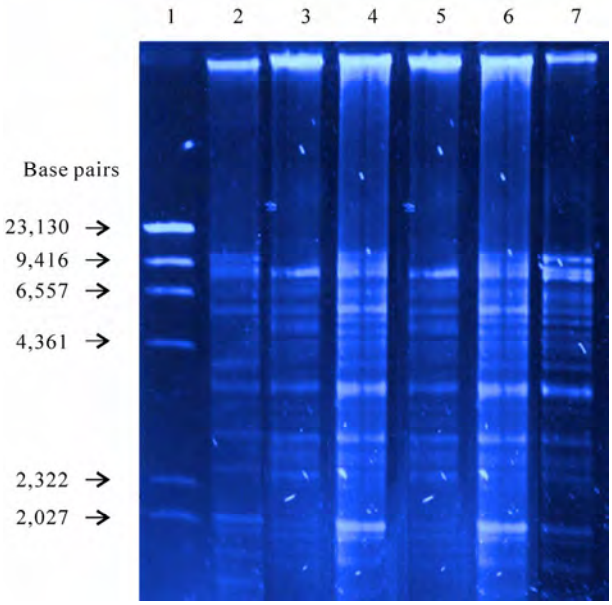

Lane 1—λ / Hind III digest, Lane 2—*Bacillus cereus* from Soil, Lane 3—*Bacillus cereus* from Sewage water, Lane 4—*Bacillus cereus* from Air, Lane 5—*Bacillus cereus* from Fresh water, Lane 6—*Bacillus cereus* from Sea water, Lane 7—*Bacillus cereus* from Milk

Figure 9. RFLP analysis of *Bacillus cereus* isolates.

Therefore in the present study, plasmid DNA was digested with Hind III restriction enzyme to analyse the Restriction Fragment Length Polymorphism. The Hind III restriction of total plasmid resulted into 12-17 bands in each isolate (**Figure 9**). Fragment length of all the isolate lies between 23,130 bp and 2,027 bp. *Bacillus cereus* isolate from soil, air, sea water and milk have shown bands corresponding to 9,416 bp. Plasmid DNA band specific to 6,557 bp has been found in *Bacillus cereus* isolated from sewage water, air, fresh water, sea water and milk. A clear distinct band corresponding to 2,027 bp has been observed in *Bacillus cereus* from air and sea water. *Bacillus cereus* from soil and milk have shown different restriction pattern to *Bacillus cereus* from air, sea water, sewage water and fresh water. *Bacillus cereus* from air and sea water belonged to the same group whereas *Bacillus cereus* from sewage water and freshwater are of same group. RFLP analysis has shown variations among the different isolates but the level of RFLP diversity among different *Bacillus cereus* isolate was low. This may be due to non specificity of restriction endonuclease.

4. CONCLUSIONS

The molecular approach in present study is complementary to traditional methods. RFLP based molecular approach has provided ways to screen whether the same isolate from diverse origin belong to same group or not in a single test rather than time consuming conventional

phenotype based methodologies. The knowledge of genetic diversity based on molecular approach will facilitate the study of relationship between them. Therefore, the approach provided here is applicable to DNA fingerprinting of micro organisms. But in future, amplification of any specific gene and their restriction digestion can be carried out which could enable to detect polymorphism in same isolate from diverse origin to a high frequency level.

REFERENCES

[1] Kramer, J.M. and Gilbert, R.J. (1992) *Bacillus cereus* gastroenteritis. In: Tu, A.T. Ed., Food poisoining, Handbook of Natural toxins, **7**, 119-153.

[2] Helgason, E., Okstad, O.A., Caugant, D.A., Johansen, H.A., Fouet, A., Mock M. and Hegna, I. (2000) *Bacillus anthracis*, *Bacillus cereus* and *Bacillus thuringiensis* – one species on the basis of genetic evidence. *Applied and Environmental Microbiology*, **66(6)**, 2627-2630.

[3] Ivanova, N., Sorokin, A., Galleron, I.A., Candelon, B., Bhattacharya, A. K., Reznik, G., Mikhailova, N., Lapidus, A., Chu, L., Mazur, M., Goltsman, E., Walnus, T.L., Grechkin, G., Pusch, M., Haselkorn, M., Fonstein, S., Ehrlich, Y., Overbeek, R. and Kyrpides, N. (2003) Genome sequence of *Bacillus cereus* and comparative analysis with *Bacillus anthracis*. *Nature*, **423**, 87-91.

[4] Drobniewski, F.A. (1998) *Bacillus cereus* and related species. *Clinical Microbiology Reviews*, **6(4)**, 324-328.

[5] Field, D. and Wills, C. (1998) Abundant micro satellite polymorphism in *Saccharomyces cerevisiae*, and the different distributions of micro satellite in eight prokaryotes and *S.cerevisiae*, results from strong mutation pressures and a variety of selective forces. *Proceedings of National Academy of Sciences*, USA, **95(4)**, 1647-1652.

[6] Lu, J., Knox, M.R., Ambrose, M.J., Brown J.K.M. and Ellis, T.H.N. (1996) Comparative analysis of genetic diversity in pea assessed by RFLP and PCR based methods. *Theoritical and Applied Genetics*, **93(7)**, 1103-1111.

[7] Williams and Wilkins. (1994) Bergy's Manual of Determinative Bacteriology. In: Williams and Wilkins, 9th Edition.

[8] Sambrook, J. and David, W.R. (2001) Molecular cloning: A laboratory manual. Cold spring Harbor Laboratory Press, Newyork.

[9] Forster, T.J. (1983) Plasmid mediated resistance to antimicrobial and toxic metal in bacteria. *Microbiology Review*, **47(3)**, 361-409.

[10] Ghosh, A., Singh, A., Ramteke, P. and Singh, V. (2000) Characterisation of large plasmid encoding resistance to toxic heavy metals in *Salmonella* abortus equi. *Biochemical and Biophysical Research Communications*, **272(1)**, 6-11.

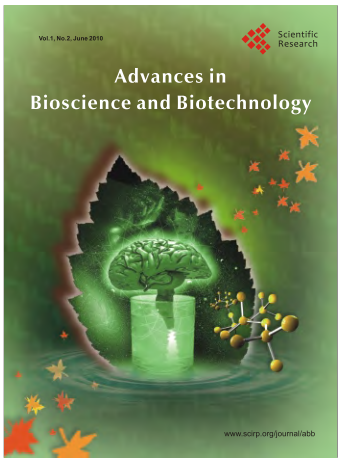

Call for Papers

Advances in Bioscience and Biotechnology

http://www.scirp.org/journal/abb

Advances in Bioscience and Biotechnology (ABB) is an international journal dedicated to the latest advancement of biosciences. The goal of this journal is to provide a platform for scientists and academicians all over the world to promote, share, and discuss various new issues and developments in different areas of biosciences. All manuscripts must be prepared in English, and are subject to a rigorous and fair peer-review process. Accepted papers will immediately appear online followed by printed hard copy.

Editor-in-Chief

Prof. Jinfu Wang Zhejiang University, China

Editorial Board

Subject Coverage

This journal invites original research and review papers that address the following issues in bioscience and biotechnology. Topics of interest include, but are not limited to:

- Biochemistry
- Botany
- Cytobiology
- Developmental Biology
- Ecology
- Genetics
- Inorganic and Analytic Chemistry
- Microbiology
- Molecular Biology
- Neurobiology
- Organic Chemistry
- Physics
- Zoology

We are also interested in short papers (letters) that clearly address a specific problem, and short survey or position papers that sketch the results or problems on a specific topic. Authors of selected short papers would be invited to write a regular paper on the same topic for future issues of the ***ABB***.

Notes for Intending Authors

Submitted papers should not have been previously published nor be currently under consideration for publication elsewhere. Paper submission will be handle electronically through the website. All papers are refereed through a peer review process. Authors are responsible for having their papers checked for style and grammar prior to submission to ABB. For more details about the submissions, please access the website.

Website and E-Mail

http://www.scirp.org/journal/abb **E-mail: abb@scirp.org**

Advances in Bioscience and Biotechnology, 2010, 1, 64-144
Published Online June 2010 in SciRP (http://www.SciRP.org/journal/abb/).

TABLE OF CONTENTS

Volume 1 Number 2 **June 2010**

